8-18-2016 12:00 AM

Studying Both Direct and Indirect Effects in Predator-Prey Interaction

Xiaoying Wang
The University of Western Ontario

Supervisor
Zou, Xingfu
The University of Western Ontario

Graduate Program in Applied Mathematics
A thesis submitted in partial fulfillment of the requirements for the degree in Doctor of Philosophy

Abstract

Studying and modelling the interaction between predators and prey have been one of the central topics in ecology and evolutionary biology. In this thesis, we study two different aspects of predator-prey interaction: direct effect and indirect effect.

Firstly, we study the direct predation between predators and prey in a patchy landscape. A model where prey reside in two isolated patches and predators move between two patches to forage prey with the strategy that maximizes their fitness is proposed. Analytical conditions of persistence and extinction of predators are obtained. Moreover, numerical simulations indicate that either weak or strong adaptation of predators has a stabilizing effect in predator-prey system for certain cases. Torus bifurcation is also observed, which implies complex dynamic behaviors.

Secondly, we study indirect effects between predators and prey. Without being directly killed by predators, prey reproduction success is largely reduced by avoidance behaviors. We propose a model which incorporates the impact of fear effect in prey reproduction. Our model shows that high levels of anti-predator behaviors may stabilize predator-prey system by excluding periodic solutions while relatively low levels of anti-predator behaviors may induce Hopf bifurcation. Moreover, the direction of Hopf bifurcation can be either supercritical or subcritical, in contrast to the model without fear effect.

Thirdly, we extend our previous model by incorporating a stage-structure into prey. We also assume that adult prey avoid direct predation adaptively to maximize instant growth rate of both adults and juveniles. Mathematical analyses show that fear effect can interplay with maturation delay between juvenile and adult prey in determining the long-term population dynamics. The positive equilibrium may lose stability with an intermediate value of delay and regain stability if the delay is large.

Finally, we further extend our previous model by incorporating spatial structures into modeling. Pattern formation is studied for the model with avoidance behaviors of prey and the cost on prey reproduction. Mathematical and numerical analyses show that either small or large predator-taxis may induce pattern formation, depending on the form of functional response.

Keywords: Predator-prey, adaptive behavior, uniform persistence, anti-predator response, fear effect, stability, bifurcation, delay, pattern formation.

Co-Authorship Statement

Chapter 2: X. Wang and X. Zou (2016), On a two-patch predator-prey model with adaptive habitancy of predators, *Discrete and Continuous Dynamical Systems-Series B*, 21(2), 677-697.

Chapter 3: X. Wang, L. Y. Zanette, and X. Zou (2016), Modelling the fear effect in predator-prey interactions, *Journal of Mathematical Biology*, DOI 10.1007/s00285-016-0989-1, in press.

Chapter 4 is based on the paper: X. Wang and X. Zou, Modelling the fear effect in predator-prey interactions with adaptive avoidance of predators, preprint.

Chapter 5 is based on the paper: X. Wang and X. Zou, Pattern formation of a predator-prey model with the cost of anti-predator behaviors, preprint.

The model in Chapter 2 is formulated by X. Wang and X. Zou. The models in Chapter 3, Chapter 4, and Chapter 5 are formulated by X. Wang and X. Zou, according to discussion with L. Y. Zanette. The mathematical analyses and numerical simulations in each of the above chapters are performed by X. Wang under the supervision of X. Zou.

The draft of the paper in Chapter 2 is prepared by X. Wang and then revised by X. Zou.

The draft of the paper in Chapter 3 is prepared by X. Wang and then revised by L. Y. Zanette and X. Zou.

The draft of the paper in Chapter 4 is prepared by X. Wang and then revised by X. Zou.

The draft of the paper in Chapter 5 is prepared by X. Wang and then revised by X. Zou.

Acknowledgements

At this point, firstly, I would like to express my sincere gratitude to my supervisor Dr. Xingfu Zou. His enthusiasm for research and rigorous attitude of academics highly inspire me. Without his helpful guidance during the past five years, countless discussions and timely responses about research, I couldn't make it this far on the way to pursue an academic career.

Secondly, I would like to thank all the professors and staff in the applied math department. I have learned a lot of valuable knowledge of math and have acquired essential skills such as programming from taking courses within the department. I have also received continuous help from administrative staff since I initially arrived at Western.

Thirdly, I am thankful for the companion of all my friends here, especially members in Dr. Zou's group, which makes my stay at Western a very enjoyable experience.

Last but not least, I thank the unconditional support and tremendous encouragement from both my parents and my husband. I am very lucky to have such family members who respect my decisions and support my pursuit of academic goals.

Contents

List of Figures

List of Tables

Chapter 1

Introduction

1.1 Overview of predator-prey interaction

Understanding predator-prey interaction has been one of the central topics in ecology and conservation biology. In an ecological community, most species depend on successful predation to survive because prey serve as food resources which provide predators with energy. Consequences of converting prey biomass into predator biomass through direct predation are referred to as a direct effect between predators and prey, and have been the focus of modelling predator-prey interactions ([5, 33]).

Among direct effects between predator-prey interactions, successful hunting is essential for predators to survive as a species. Although for an individual predator, the hunting mode may vary instantly according to changes of the surrounding environment, most species have adopted particular hunting strategy via long-term evolution ([38]). There are two main but completely different types of hunting strategy: one is called ambush strategy and the other one is called active strategy ([38]). Species in an ecological community can be classified into two categories of predators depending on their hunting mode when they forage prey. Species such as snakes or spiders are ambush predators because their hunting strategy is "sit and wait" ([43]). When prey approach, ambush predators trap the prey or take the opportunity to pounce on it. On the contrary, species such as African wild dogs forage prey actively in a habitat and usually catch prey after a relatively long-distance chase ([10]). Hence, wild dogs can be classified as active foragers due to their active movement when foraging prey.

Because active foragers move widely in habitats when searching for prey, one natural question is that how will the difference in landscape impact the predator-prey interaction? Habitat fragmentation disconnects landscape and separates habitats for prey or predators into different patches. Naturally, different patches represent unbalanced living conditions and uneven

abundance of prey. When migration or dispersal of a predator is incorporated, one interesting question is that what is the optimal dispersal strategy for a predator? Moreover, dispersal of a predator between patches may change the pattern of predator-prey dynamics in a single isolated patch. For example, without dispersal of a predator, the prey and predators may tend to a steady state in an isolated patch. However, dispersal of predators may destroy the steady state and induce oscillations in predator or prey demography. Extensive research has been conducted concerning patches and dispersals of predators or prey (see references [7, 8, 28, 29, 42] for example).

Earlier research about predation behaviors and dispersal of either prey or predators assume random dispersal of species (see e.g. [28, 29] for example). However, it has been argued that almost all species have the ability to learn and adapt to changes of the nearby environment ([6, 40]). The adaptive behaviors of a species play an important role in determining the species' survival and evolution by maximizing individual payoff ([6, 40]). In recent years, there have been some studies that combined the spatial dispersal of species and adaptive behaviors of species together ([7, 8, 12, 13, 14, 27]).

Because direct effects such as direct killing of prey or migration of a species can be easily observed in an ecological community, and have been the central topic in research by far, indirect effects may play an even more important role in determining the demography of species. Indirect effects between predators and prey are mainly induced by anti-predator behaviors of prey. It has been argued by theoretical biologists that prey can perceive predation risk at least to some extent and avoid direct killing by predators through a variety of anti-predator behaviors ([15, 35, 36, 37, 41]). The fear of predators drives prey to show anti-predators responses, which include habitat switch, foraging behaviors change, and increased vigilance ([9]). Specifically, when prey are in breeding season, any change of the above anti-predator responses may lead to a loss on prey reproduction success even though no direct killing has been involved ([9, 15, 30, 31]). Because of such decay on prey reproduction, anti-predator behaviors may increase short-term survival rate of prey but in the long-term, there is a cost in the fitness of prey as a species ([9]). Recently, a field study on song sparrow populations confirms the theoretical argument that even rare presence of predators can exert a large impact on prey demography ([45]).

In [45], a field study on song sparrows has been conducted by Zanette *et al.* during the whole breeding season. The authors in [45] eliminated all direct predation of both juvenile and adult song sparrows by effectively using netting and electrical fences to protect nests. Without direct predation, however, the authors used sounds of predators to manipulate predation risk. Two groups of breeding song sparrows were monitored, within which one was exposed to sounds of predators and the other was exposed to sounds of non-predators. By comparing the

reproduction success of the two tested groups, the authors concluded that the group exposed to predation risk reproduced 40% less offspring than the other group. In fact, the impact of adult song sparrow's anti-predator behaviors exist in every stage of breeding process. When exposed to predation risk, adult song sparrows laid fewer eggs, fewer eggs were successfully hatched and fewer nestlings survived, which all contributed to the eventual 40% loss of offspring. Moreover, various anti-predator behaviors of adult song sparrows were observed in [45], such as change of habitat. As indicated in [45], adult song sparrows were more willing to locate nests in habitats with sub-optimal quality if a predation risk is persisted. On one hand, relocating to habitats with less predation risk increases the surviving probability of adult song sparrows, but on the other hand, it decreases the survival rate of newborn song sparrows due to less suitable living conditions. In addition, the authors also documented that adult song sparrows in the group exposed to predator's sounds feed their offspring less and stayed less on brood to protect juveniles. As a consequence, lower survival rate of nestlings was found for the group with predation risk compared to the one without predation risk. In recent years, similar results have also been obtained from field experiments of other vertebraes, such as birds ([17, 18, 19, 20, 24, 25, 26, 34]), elk ([11]), snowshoe hares ([39]) ,and dugongs ([44]). All the aforementioned experiments offered evidence that the mere presence of predators could be strong enough to impact the interaction between predators and prey. Indirect effects may play a more important role in determining the demography of both prey and predators than direct predation.

1.2 Mathematical modelling of direct effects

1.2.1 Functional responses

As mentioned in the previous section, direct effects measure the conversion of prey biomass to predator biomass through predation. Extensive and intensive research has been done about modelling direct predation between prey and predators. One of the earliest work that modeled direct effects between predator-prey interaction is the Lotka-Volterra predator-prey model

$$\begin{aligned} \frac{dx}{dt} &= \alpha\, x - \beta\, x\, y, \\ \frac{dy}{dt} &= c\,\beta\, x\, y - \gamma\, y, \end{aligned} \tag{1.1}$$

where x and y represents the biomass of prey and predators respectively, β is the attacking rate of prey by predators, c is the conversion rate from prey biomass to predator biomass. One of the characteristics of (1.1) is that the predation term $\beta\, x\, y$ is linear with respect to x and therefore is

called a linear functional response of the predator ([5, 33]). After the classic work of Lotka and Volterra, Holling ([22, 23]) proposed the well-known Holling type II functional response

$$f(x) = \frac{\beta x}{1 + \beta h x} \tag{1.2}$$

and the Holling type III functional response ([22, 23])

$$f(x) = \frac{\beta x^{\theta}}{1 + \beta h x^{\theta}}. \tag{1.3}$$

Derived from a more realistic assumption, Holling improved the linear functional response by incorporating a predator handling time of prey besides attacking. In (1.2) and (1.3), h represents predator handling time of prey, and in (1.3), $\theta > 1$ is a constant. Obviously, the Holling type III functional response can be viewed as a generalization of the type II functional response. The common feature of the Holling type II and type III functional responses lies in that they are both saturating functions when the density of prey becomes large. However, the Holling type III functional response differs from the type II functional response when prey density is at lower level. A possible explanation is that it is more difficult for the predators to learn searching for prey effectively if the density of prey itself is low ([22, 23]).

Although assumptions and detailed mechanisms are different for each of Holling's functional responses, all of the Holling type functional responses are predator-independent functional responses. Prey-dependent functional response assumes that the predator per capita consumption rate of prey is influenced by prey density alone. However, it is argued that the conversion of prey biomass to predator biomass does not only depend on prey density but also depends on predator density ([2, 3]). A well-known functional response which depends on both prey and predator density is the Beddington-DeAngelis functional response ([4, 16])

$$f(x, y) = \frac{\beta x}{1 + a x + b y}. \tag{1.4}$$

The Beddington-DeAngelis functional response (1.4) can be regarded as a generalization of the Holling type II functional response (1.2) by incorporating an extra term $b y$ in the denominator. Here, in fact, the term $b y$ models the interference between predators when searching for prey. In prey dependent only functional responses (e.g. Holling type functional responses), the encounter between predators and prey is assumed to be random and unbiased. However, the competition of prey or resources increases if the density of predators becomes larger. Hence, the successful predation rate of prey by a predator decreases with increasing density of predators. Another functional response that depends on both prey and predator densities and has been studied extensively is the ratio dependent functional response

$$f(x, y) = \frac{\beta \frac{x}{y}}{a \frac{x}{y} + b} = \frac{\beta x}{a x + b y}. \tag{1.5}$$

The ratio-dependent functional response (1.5) is suitable when the predator is active foragers since the predation success is an increasing function of the rate x/y, which accounts for the average number of prey per predator can have. The function (1.5) can also be derived from separating different time scales between behavioral change and demographical change of prey and predators ([2, 3]). The authors of [2, 3] found empirical evidence that the ratio-dependent functional response fitted experimental data of certain species better than prey-dependent functional response.

Debate about whether prey dependent only functional responses or functional responses that depend on both prey and predator densities could describe a more realistic predation behavior has lasted for more than a decade ([1]). Due to the complexity of food webs, no explicit and general conclusions have been recognized commonly by either theoretical or experimental ecologists. Each type of the aforementioned functional responses has its merits and drawbacks, and fits different situations.

1.2.2 Paradox of enrichment

Paradox of enrichment describes a phenomenon which arises from predator-prey model with the Holling type II functional response

$$\begin{aligned} \frac{dx}{dt} &= r_0\, x\left(1-\frac{x}{K}\right)-\frac{\beta\, x}{1+\beta\, h\, x}, \\ \frac{dy}{dt} &= \frac{c\beta\, x}{1+\beta\, h\, x}-\gamma\, y. \end{aligned} \tag{1.6}$$

Gilpin *et al.* studied the stability of the positive equilibrium of (1.6) ([21]). By regarding the carrying capacity K as a bifurcation parameter, Gilpin *et al.* find that prey and predator densities tend to a steady state if K is small but oscillate periodically if K is large enough to pass a critical value. By plotting the phase portrait of prey/predator density, it is observed that a limit cycle exists and stays very close to both axes for a large portion of time. Therefore, a small perturbation or stochasticity would drive prey/predator species to extinction. It is counter intuitive because the coexistence of prey and predator should be enhanced if the carrying capacity is large (equivalently better environment).

1.3 Mathematical theories and methodologies

This thesis uses dynamical system approach to explore the population dynamics of predator-prey system. The main notions are the following two.

1.3.1 Stability analysis of equilibria

In dynamical system theory, equilibrium solutions are solutions which do not change with time ([32]). Studying equilibrium solutions is important in mathematical biology because it predicts long-term behaviors of a system. An equilibrium solution can be asymptotically stable, which means that the equilibrium attracts trajectories in some neighborhood of the equilibrium or unstable, meaning it repels trajectories. The stability of an equilibrium may be local or global, depending on the basin of attraction of the equilibrium. To determine the local stability of an equilibrium, linearization of a system at the equilibrium is an useful tool. The equilibrium is locally asyptotically stable if all eigenvalues of the Jacbian matrix evaluated at this point have negative real parts and is unstable if at least one eigenvalue has a positive real part ([32]). If one of the eigenvalues has zero real part, then the linearized system is not enough to capture dynamical behaviors nearby the equilibrium and therefore, higher order approximation is required.

1.3.2 Hopf bifurcation

Bifurcation describes an abrupt change from one state to the other when some parameters pass the critical values. For example, water start to froze instead of keeping flowing when temperature goes to zero. Bifurcation study is a powerful tool in understanding an ecological community because bifurcation implies an abrupt change from one state to the other. For predator-prey systems, the population of prey and predators may stay at a steady state or oscillate periodically. Hopf bifurcation may be the mathematical mechanism for the change of demography of prey and predators.

Hopf bifurcation occurs when the Jacobian matrix evaluated at an equilibrium has a pair of pure imaginary roots crossing the imaginary axis in the complex plane, and no other eigenvalues have zero real parts. If the pair of pure imaginary roots cross the imaginary axis with non-zero speed, and the nondegeneracy condition is satisfied, Hopf bifurcation gives rise to a periodic solution. A periodic solution can be stable or unstable. Typically, for Hopf bifurcation, the stability of a bifurcated limit cycle depends on the direction of Hopf bifurcation.

1.4 Thesis motivation and outline

In this thesis, we study both direct and indirect effects in predator-prey interactions. For direct effect, we particularly consider a case where prey reside in two isolated patches while predators are mobile and hence can forage on prey between patches. As mentioned above,

spatial models including patch models which incorporate dispersal of either prey or predators have been studied extensively (see ([7, 8, 12, 13, 14, 27]) for example). The key point in our modelling is that we consider adaptive dispersal of predators instead of random dispersal or density-independent dispersal. In addition, by studying the combined system of both population dynamics and adaptive dynamics, we obtain some interesting results which are induced by dispersal of predators. More importantly, we also study indirect effects systematically, including an ODE (ordinary differential equation) model, a DDE (delay differential equation) model, and a PDE (partial differential equation) model, depending on the focus of modelling. By mathematical analysis and numerical simulations, we find that indirect effects play an important role in determining prey or/and predator demography. Under certain constraints, indirect effects induce new dynamical behaviors of predator-prey system and may stabilize or destabilize an equilibrium depending on the strength of anti-predator behaviors of the prey.

In Chapter **2**, we propose a two-patch predator-prey model where prey reside in two isolated patches but predators move between patches to forage prey. Predators are assumed to move adaptively between patches to maximize individual fitness. Analytical conditions of persistence and extinction of predators are obtained. Moreover, numerical simulations show that either weak or strong adaptation of predators stabilizes the system if the population of prey and predators tend to a steady state in one patch but oscillate in the other. When the population of prey and predators oscillate in both patches, torus bifurcation is identified, which implies more complicated behaviors.

In Chapter **3**, we propose a model which incorporates the cost of anti-predator behaviors of prey in the birth rate of prey. As discussed above, indirect effects induced by fear of predators (or equivalently anti-predator behaviors of prey) play an even more important role in predator-prey interaction and thus should be modeled explicitly. Mathematical analyses show that high levels of anti-predator responses may exclude the appearance of periodic oscillations in the predator-prey system and thus eliminate the 'paradox of enrichment'. However, periodic oscillations of prey and predator demography are still possible due to Hopf bifurcation, if the level of anti-predator response is relatively low. Different from classical model without fear effect where Hopf bifurcation is typically supercritical, Hopf bifurcation in our model can be both supercritical and subcritical. Subcritical Hopf bifurcation implies a case where bi-stability exists, which shows rich dynamical behaviors. Moreover, numerical simulations show that prey demonstrate weaker anti-predator behaviors if the birth rate of prey increases or the death rate of predators increases, but avoid predation more strongly if the attack rate of predators increases.

In Chapter **4**, we extend the model in Chapter **3** by incorporating a stage structure of prey into modelling. As indicated in [45], the cost of anti-predator behaviors exists through all stages of prey, and thus can be modeled more accurately by explicitly dividing prey into different

stages. Based on the experimental findings, we propose a predator-prey model with the cost of fear and adaptive avoidance of predators. Mathematical analyses show that the fear effect can interplay with maturation delay between juvenile prey and adult prey in determining the long term population dynamics. A positive equilibrium may lose stability with an intermediate value of delay and regain stability if the delay is large. Numerical simulations show that both strong adaptation of adult prey and the large cost of fear have destabilizing effects while large population of predators has a stabilizing effect on the predator-prey interactions. Numerical simulations also imply that adult prey demonstrate stronger anti-predator behaviours if the population of predators is larger and show weaker anti-predator behaviours if the cost of fear is larger.

In Chapter **5**, we extend the model in Chapter **3** by incorporating spatial structures explicitly into modelling. Anti-predator behaviors of prey that cause change of spatial locations such as switch of habitat usage have been observed in experiments ([45]) and therefore should be examined in detail. We propose and analyse a reaction-diffusion-advection predator-prey model in which it is assumed that predators move randomly but prey avoid predation by perceiving repulsion along predator density gradient. Based on recent experimental evidence that anti-predator behaviors alone lead to a 40% reduction on prey reproduction rate, we also incorporate the cost of anti-predators responses into the local reaction terms in the model. Sufficient and necessary conditions of spatial pattern formation are obtained for various functional responses between predators and prey. By mathematical and numerical analyses, we find that small prey sensitivity to predation risk may lead to pattern formation if the functional response is the Holling type II functional response or the Beddington-DeAngelis functional response but large cost of anti-predator behaviors homogenises the system by excluding pattern formation. However, the ratio-dependent functional response gives an opposite result where large predator-taxis may lead to pattern formation but small cost of anti-predator behaviors inhibits the emergence of spatial heterogeneous steady states.

We end the thesis by conclusions and discussions in Chapter **6**, in which a brief summary of main results is given. We also discuss possible future extensions in this chapter.

Bibliography

[1] P. A. Abrams and L. R. Ginzburg. The nature of predation: prey dependent, ratio dependent or neither? *Trends in Ecology & Evolution*, 15:337–341, 2000.

[2] H. R. Akçakaya, R. Arditi, and L. R. Ginzburg. Ratio-dependent predation: an abstraction that works. *Ecology*, 76:995–1004, 1995.

[3] R. Arditi and L. R. Ginzburg. Coupling in predator-prey dynamics: ratio-dependence. *Journal of Theoretical Biology*, 139:311–326, 1989.

[4] J. R. Beddington. Mutual interference between parasites or predators and its effect on searching efficiency. *Journal of Animal Ecology*, 44:331–340, 1975.

[5] F. N. Britton. *Essential Mathematical Biology*. Springer, 2012.

[6] D. M. Buss and H. Greiling. Adaptive individual differences. *Journal of Personality*, 67: 209–243, 1999.

[7] R. S. Cantrell, C. Cosner, D. L. Deangelis, and V. Padron. The ideal free distribution as an evolutionarily stable strategy. *Journal of Biological Dynamics*, 1:249–271, 2007.

[8] R. S. Cantrell, C. Cosner, and Y. Lou. Evolutionary stability of ideal free dispersal strategies in patchy environments. *Journal of Mathematical Biology*, 65:943–965, 2012.

[9] S. Creel and D. Christianson. Relationships between direct predation and risk effects. *Trends in Ecology & Evolution*, 23:194–201, 2008.

[10] S. Creel and N. M. Creel. *The African wild dog: behavior, ecology, and conservation*. Princeton University Press, 2002.

[11] S. Creel, D. Christianson, S. Liley, and J. A. Winnie. Predation risk affects reproductive physiology and demography of elk. *Science*, 315:960–960, 2007.

[12] R. Cressman and V. Křivan. Migration dynamics for the ideal free distribution. *The American Naturalist*, 168:384–397, 2006.

[13] R. Cressman and V. Křivan. Two-patch population models with adaptive dispersal: the effects of varying dispersal speeds. *Journal of Mathematical Biology*, 67:329–358, 2013.

[14] R. Cressman, V. Křivan, and J. Garay. Ideal free distributions, evolutionary games, and population dynamics in multiple-species environments. *The American Naturalist*, 164: 473–489, 2004.

[15] W. Cresswell. Predation in bird populations. *Journal of Ornithology*, 152:251–263, 2011.

[16] D. L. DeAngelis, R. A. Goldstein, and R. V. O'neill. A model for tropic interaction. *Ecology*, 56:881–892, 1975.

[17] S. Eggers, M. Griesser, and J. Ekman. Predator-induced plasticity in nest visitation rates in the Siberian jay (*perisoreus infaustus). Behavioral Ecology*, 16:309–315, 2005.

[18] S. Eggers, M. Griesser, M. Nystrand, and J. Ekman. Predation risk induces changes in nest-site selection and clutch size in the siberian jay. *Proceedings of the Royal Society of London B: Biological Sciences*, 273:701–706, 2006.

[19] J. J. Fontaine and T. E. Martin. Parent birds assess nest predation risk and adjust their reproductive strategies. *Ecology letters*, 9:428–434, 2006.

[20] C. K. Ghalambor, S. I. Peluc, and T. E. Martin. Plasticity of parental care under the risk of predation: how much should parents reduce care? *Biology Letters*, 9:20130154, 2013.

[21] M. E. Gilpin and M. L. Rosenzweig. Enriched predator-prey systems: theoretical stability. *Science*, 177:902–904, 1972.

[22] C. S. Holling. The components of predation as revealed by a study of small-mammal predation of the European pine sawfly. *The Canadian Entomologist*, 91:293–320, 1959.

[23] C. S. Holling. Some characteristics of simple types of predation and parasitism. *The Canadian Entomologist*, 91:385–398, 1959.

[24] F. Hua, R. J. Fletcher, K. E. Sieving, and R. M. Dorazio. Too risky to settle: avian community structure changes in response to perceived predation risk on adults and offspring. *Proceedings of the Royal Society of London B: Biological Sciences*, 280:20130762, 2013.

[25] F. Hua, K. E. Sieving, R. J. Fletcher, and C. A. Wright. Increased perception of predation risk to adults and offspring alters avian reproductive strategy and performance. *Behavioral Ecology*, 25:509–519, 2014.

[26] J. D. Ibáñez-Álamo and M. Soler. Predator-induced female behavior in the absence of male incubation feeding: an experimental study. *Behavioral Ecology and Sociobiology*, 66:1067–1073, 2012.

[27] V. Křivan. The lotka-volterra predator-prey model with foraging–predation risk trade-offs. *The American Naturalist*, 170:771–782, 2007.

[28] Y. Kuang and Y. Takeuchi. Predator-prey dynamics in models of prey dispersal in two-patch environments. *Mathematical Biosciences*, 120:77–98, 1994.

[29] S. A. Levin. Dispersion and population interactions. *The American Naturalist*, 108: 207–228, 1974.

[30] S. L. Lima. Nonlethal effects in the ecology of predator-prey interactions. *Bioscience*, 48: 25–34, 1998.

[31] S. L. Lima. Predators and the breeding bird: behavioral and reproductive flexibility under the risk of predation. *Biological Reviews*, 84:485–513, 2009.

[32] J. D. Meiss. *Differential dynamical systems*, volume 14. SIAM, 2007.

[33] J. D. Murray. *Mathematical Biology, I, An Introduction*. Springer, 2002.

[34] J. L. Orrock and R. J. Fletcher. An island-wide predator manipulation reveals immediate and long-lasting matching of risk by prey. *Proceedings of the Royal Society of London B: Biological Sciences*, 281:20140391, 2014.

[35] S. D. Peacor, B. L. Peckarsky, G. C. Trussell, and J. R. Vonesh. Costs of predator-induced phenotypic plasticity: a graphical model for predicting the contribution of nonconsumptive and consumptive effects of predators on prey. *Oecologia*, 171:1–10, 2013.

[36] N. Pettorelli, T. Coulson, S. M. Durant, and J-M Gaillard. Predation, individual variability and vertebrate population dynamics. *Oecologia*, 167:305–314, 2011.

[37] E. L. Preisser and D. I. Bolnick. The many faces of fear: comparing the pathways and impacts of nonconsumptive predator effects on prey populations. *PloS One*, 3:e2465, 2008.

[38] I. Scharf, E. Nulman, O. Ovadia, and A. Bouskila. Efficiency evaluation of two competing foraging modes under different conditions. *The American Naturalist*, 168:350–357, 2006.

[39] M. J. Sheriff, C. J. Krebs, and R. Boonstra. The sensitive hare: sublethal effects of predator stress on reproduction in snowshoe hares. *Journal of Animal Ecology*, 78:1249–1258, 2009.

[40] J. E. R. Staddon. *Adaptive behavior and learning*. CUP Archive, 1983.

[41] T. O. Svennungsen, Ø. H. Holen, and O. Leimar. Inducible defenses: continuous reaction norms or threshold traits? *The American Naturalist*, 178:397–410, 2011.

[42] W. Wang and Y. Takeuchi. Adaptation of prey and predators between patches. *Journal of Theoretical Biology*, 258:603–613, 2009.

[43] D. K. Wasko and M. Sasa. Food resources influence spatial ecology, habitat selection, and foraging behavior in an ambush-hunting snake (Viperidae: Bothrops asper): an experimental study. *Zoology*, 115:179–187, 2012.

[44] A. J. Wirsing and W. J. Ripple. A comparison of shark and wolf research reveals similar behavioral responses by prey. *Frontiers in Ecology and the Environment*, 9:335–341, 2011.

[45] L. Y. Zanette, A. F. White, M. C. Allen, and M. Clinchy. Perceived predation risk reduces the number of offspring songbirds produce per year. *Science*, 334:1398–1401, 2011.

Chapter 2

On a two-patch predator-prey model with adaptive habitancy of predators

2.1 Introduction

Foraging behaviour is a common phenomenon in nature. As indicated in [19], foraging behaviour varies from ambush to active, in response to changes in environment and other circumstances. Although the foraging mode for a certain individual may change from time to time, many species have adopted the most advantageous foraging strategy through long-term evolution, either ambush or active, to maximize their survival probability. Species like spiders, or snakes, as indicated in [25], are classified as ambush predators because they "sit and wait" and then pounce when the opportunity arises. In contrast, other species, like wild dogs, as described in [6], move actively to forage prey.

Active foragers move back and forth searching for prey. Foraging behaviour of predators does not depend only on intra-species competition, but also depends on spatial abundance of resources and interspecies interaction in different patches. It has been widely observed in nature that many species migrate between different patches to search for resources because of apparent differences of resources, landscapes, or other environmental factors that affect the predators' survival probability in different patches. Consequently, patch models have been introduced to simulate predator-prey dynamics with active foraging behaviour and dispersal of predators, as indicated in [3, 4, 16, 17].

Patch models with dispersal of certain species have been studied extensively, see, e.g., [3, 4, 16, 17, 24] and the references therein. The common point in [16] and [17] is the assumption of density-independent dispersal rates. However, more and more experimental results and field observations in nature seem to suggest that predators have the ability to choose

a better patch in which they can gain more fitness. Predators are more likely to move between different patches adaptively.

In behavioural ecology, an adaptive behaviour is a behaviour which contributes directly or indirectly to an individual's survival or reproductive success and is thus subject to the forces of natural selection ([22]). Adaptations are commonly defined as evolved solutions to recurrent environmental problems of survival and reproduction ([2]). Ecological species have the ability to adapt through learning ([21]). An individual will adjust its behaviour or strategy by learning in response to a change of the environment in order to survive and acquire the highest payoff. In evolutionary biology, analyzing an evolutionary stable strategy (ESS) under adaptation is one of the central topics. Another important concern is how species distribute themselves among different patches under adaptive dispersal. Based on the assumption that each individual has the ability to assess the condition of different patches and can move freely to maximize the individual fitness, the ideal free distribution (IFD) is proposed to illustrate the ecological equilibrium under adaptive dynamics ([3, 10]). It is natural to analyze the relationship between the ecological equilibrium and the evolutionary stable strategy. Several papers of [3, 4, 7, 9, 14] studied a variety of models including a single-species model, a two-patch competition model, a two-patch predator-prey model and an interacting-species model within finitely-many patches. They conclude that under certain conditions and assumptions, the evolutionary stable strategies are those which lead to the ideal free distribution.

In addition to the evolutionary and ecological aspects, predation behaviour can also produce a significant effect on predator-prey systems. As indicated in [1], different behaviour mechanisms can result in surprisingly different outcomes. Behavioural dynamics exerts significant effect on ecological and evolutionary dynamics. Functional responses are used to connect different behavioural dynamics of prey and predators. One important functional response which connects prey density and prey catch-per-predator is the Holling type II functional response, which was proposed by Holling ([13]). In contrast to the classical linear functional response, the Holling type II functional response assumes that the encounter rate of prey by predators is density-dependent. This matches experimental data for many species very well, as indicated in [5, 20]. Seitz *et al.* ([20]) conducted a series of experiments to study predator-prey dynamics of thin-shelled clams and their predators, the blue crabs, which inhabit the Chesapeake Bay. As indicated in [20], the predation on *Mya arenaria* (soft-shell clam) in mud and *M. mercenaria* (hard clam) in sand by their major predators, the blue crabs, obeys the Holling type II functional response. Clark *et al.* ([5]) conducted another experiment about foraging behaviour of the blue crabs in the Chesapeake Bay, but focused on studying the mechanism of foraging behaviour of the blue crabs between patches. In addition to predation of clams by the blue crabs in the Chesapeake Bay, there are other species in the ecological system which have similar predation mode, such

as predation behaviour of rotifers on sessile planktonic species, and grazing behaviour of large herbivores. The above biological instances share one feature in common: all predators are mobile and migrate between different patches to forage prey or resources while prey or resources are sessile. In addition, as mentioned above, foraging behaviour of predators is adaptive because predators try to maximize individual fitness.

Křivan and Cressman ([15]) studied fast behaviour of predators moving between patches and showed that there exists a complicated relationship involving behavioural, population and evolutionary dynamics by studying three different predator-prey models. Their study is based on the assumption that the behavioural dynamics runs on a much faster time scale than the demographical time scale and thus simplifies the original system. Křivan and Cressman ([15]) also explored the effect of adaptive dispersal exerting on population dynamics by using computer simulations. Based on [15], we consider a two-patch predator-prey model where predators move between two patches foraging on prey freely but each individual of the prey resides only within one patch. We combine population dynamics and behavioural dynamics together and investigate detailed dynamics of the whole system under the effect of adaptive dispersal.

The rest of the paper is organized as follows. In Section 2, we present the two-patch predator-prey model with the Holling type II functional response and adaptive dispersal of predators. In Section 3, mathematical analysis of the model is carried out to provide analytical conditions for persistence and extinction of the predators. Section 4 contains some numerical simulations. One interesting observation from these simulations is that if under isolation, the populations of the prey and predators in one patch tend to an equilibrium but those in the other patch tend to a limit cycle, then either weak or strong adaptation of the predators may stabilize the system in the sense that populations in both patches will tend to an equilibrium. Moreover, the strength of adaption has influences on the average biomass of predators. When the populations of the prey and predators tend to limit cycles in both patches under isolation, adaptive dispersal of predators may results in torus bifurcation. In Section 5, we summarize our findings and discuss some possible future projects along this line.

2.2 Model formulation

Our model will be built upon a two-patch predator-prey model with the Holling type II functional response, which is also known as the Rosenzweig-MacArthur model. This model is based on the assumptions that (i) prey and predators inhabit two patches which are totally separated; (ii) an individual of the prey does not disperse between the two patches and only predators move between two patches to forage on prey; (iii) the predators, they have the complete knowledge on the patch qualities and always tend to move to the better patch to gain more payoff which

is measured by the per capita growth rate of predators. Under these assumptions, the two-patch Rosenzweig-MacArthur model is given by the following system of ordinary differential equations

$$\begin{aligned}
\frac{dx_1}{dt} &= x_1\,(r_1 - a_1\,x_1) - \frac{s_1\,x_1\,v\,y}{1 + h_1\,s_1\,x_1},\\
\frac{dx_2}{dt} &= x_2\,(r_2 - a_2\,x_2) - \frac{s_2\,x_2\,(1-v)\,y}{1 + h_2\,s_2\,x_2},\\
\frac{dy}{dt} &= y\left(-m_1\,v - m_2\,(1-v) + \frac{s_1\,x_1\,e_1\,v}{1 + h_1\,s_1\,x_1} + \frac{s_2\,x_2\,e_2\,(1-v)}{1 + h_2\,s_2\,x_2}\right),
\end{aligned} \tag{2.1}$$

where x_1 denotes the density of prey in patch 1, x_2 denotes the density of prey in patch 2, y represents the density of predators, v is the proportion of time that predators stay in patch 1 on average, r_i for $i = 1, 2$, is the intrinsic growth rate of prey in patch i, r_i/a_i is the carrying capacity of prey in patch i, s_i is the attacking rate of the predators in patch i, e_i is the expected biomass of prey converted to predators in patch i, m_i is the per capita mortality rate of predators in patch i, and h_i is the handling time of the predation in patch i respectively.

In model (2.1), the proportional time v that predators spend in patch 1 is assumed to be constant. However, predators seem to choose their habitat intelligently according to resource abundance in patches. In other words, they migrate between patches adaptively with the change of surrounding environment. If v increases, prey in patch 1 will be reduced due to the high predation risk and meanwhile, intra-specific competition of predators will be increased. As a consequence, predators tend to migrate to the second patch in order to maximize energy intake. Consequently, aggregation of predators in the second patch will again cause prey reduction in this patch, and this in turn impels predators to migrate to the first patch. Through adaptation of predators, v in model (2.1) should change with time rather than remain as a constant. Thus v can be viewed as the strategy of predators.

We now derive the strategy equation based on [10] and the idea of the replicator dynamics. As indicated in [10], the assumption that predators have the complete knowledge about patch qualities and always tend to move to a better patch to gain more fitness is valid. Let

$$f_1 = -m_1 + \frac{e_1\,s_1\,x_1}{1 + h_1\,s_1\,x_1}, \qquad f_2 = -m_2 + \frac{e_2\,s_2\,x_2}{1 + h_2\,s_2\,x_2},$$

which measures the fitness of predators in patches 1 and 2 respectively. Because the proportion of time that predators forage in patch 1 is v and the corresponding proportion of time that predators stay in patch 2 is $1 - v$, the *average fitness* of predators switching over the two patches is

$$\overline{f} = v\,f_1 + (1-v)f_2. \tag{2.2}$$

By the theory of adaptive dynamics ([12]), we have

$$\frac{dv}{dt} = k\,v\left(f_1 - \overline{f}\right). \tag{2.3}$$

By plain language, this means that the relative change rate of v is proportional to the difference of the fitness in patch 1 and the mean fitness over the two patches. In equation (2.3), k is a positive constant, with large k accounting for strong (fast) adaptation of predators in response to a change of prey abundance in the local patch, while small k explaining weak (slow) adaptation of predators.

Plugging (2.2) into (2.3), we obtain

$$\begin{aligned}\frac{dv}{dt} &= k\,v\,(1-v)\,(f_1 - f_2)\\ &= k\,v\,(1-v)\left(-m_1 + m_2 + \frac{e_1\,s_1\,x_1}{1+h_1\,s_1\,x_1} - \frac{e_2\,s_2\,x_2}{1+h_2\,s_2\,x_2}\right).\end{aligned} \tag{2.4}$$

Combining (2.1) and (2.4), we obtain our model system which describes both population dynamics and adaptive dynamics:

$$\begin{aligned}\frac{dx_1}{dt} &= x_1\,(r_1 - a_1\,x_1) - \frac{s_1\,x_1\,v\,y}{1+h_1\,s_1\,x_1},\\ \frac{dx_2}{dt} &= x_2\,(r_2 - a_2\,x_2) - \frac{s_2\,x_2\,(1-v)\,y}{1+h_2\,s_2\,x_2},\\ \frac{dy}{dt} &= y\left(-m_1\,v - m_2\,(1-v) + \frac{s_1\,x_1\,e_1\,v}{1+h_1\,s_1\,x_1} + \frac{s_2\,x_2\,e_2\,(1-v)}{1+h_2\,s_2\,x_2}\right),\\ \frac{dv}{dt} &= k\,v\,(1-v)\left(-m_1 + m_2 + \frac{e_1\,s_1\,x_1}{1+h_1\,s_1\,x_1} - \frac{e_2\,s_2\,x_2}{1+h_2\,s_2\,x_2}\right).\end{aligned} \tag{2.5}$$

In the next section, we will analyze this model system.

2.3 Mathematical analysis

We first address the well-posedness of the model (2.5), including non-negativity and boundedness of solutions. Since (2.5) is of Gauss type, the solution with any set of non-negative initial values for the four unknowns will remain non-negative for all t at which the solution exists. Moreover, if $x_1(0) = 0$, then $x_1(t) = 0$ for all $t \geq 0$. The same conclusion also holds for all other unknowns. For the strategy variable $v(t)$, writing the last equation in (2.5) as the following integral form

$$v(t) = 1 - 1/\left(1 + v(0)/(1-v(0))\exp\left\{\int_0^t \psi(\xi)d\xi\right\}\right), \tag{2.6}$$

where

$$\begin{aligned}\psi(\xi) =& k\Big(- m_1 + m_2 + (e_1\, s_1\, x_1(\xi))/(1 + h_1\, s_1\, x_1(\xi)) \\ & - (e_2\, s_2\, x_2(\xi))/(1 + h_2\, s_2\, x_2(\xi))\Big).\end{aligned} \tag{2.7}$$

From (2.6), we know that $v(t) \in [0, 1]$ for $t \geq 0$, as long as $v(0) \in [0, 1]$; if the case $v(0) = 0$ then $v(t) = 0$ for all $t \geq 0$; if $v(0) = 1$ then $v(t) = 1$ for $t \geq 0$; and if $v(0) \in (0, 1)$ then so is $v(t)$ for all $t \geq 0$. Although the dedicated cases $v(0) = 0$ and $v(0) = 1$ will be addressed for mathematical purpose, we are mainly interested in the case of $v(0) \in (0, 1)$. This can be justified by assuming that initially there are predators in both patches. Next, we address boundedness of solutions. To this end, let $(x_1(t), x_2(t), y(t), v(t))$ be any non-negative solution with $x_1(0) \geq 0,\ \ x_2(0) \geq 0,\ \ y(0) \geq 0$ and $v(0) \in [0, 1]$. We have seen from the above that $v(t) \in [0, 1]$ for all $t \geq 0$ where the solution exists. We only need to confirm the boundedness of $x_1(t),\ \ x_2(t)$ and $y(t)$. To this end, let $G = e_1\, x_1 + e_2\, x_2 + y$. By direct calculation, we obtain

$$\begin{aligned}\frac{dG}{dt} =& - m_1\, v\, G - m_2\, (1 - v)\, G + [e_1\, r_1 + m_1\, v\, e_1 + m_2\, (1 - v)\, e_1]\, x_1 \\ & + [e_2\, r_2 + m_1\, v\, e_2 + m_2\, (1 - v)\, e_2]\, x_2 - e_1\, a_1\, x_1^2 - e_2\, a_2\, x_2^2 \\ & \leq -m_1\, v\, G - m_2\, (1 - v)\, G + \frac{[e_1\, r_1 + m_1\, v\, e_1 + m_2\, (1 - v)\, e_1]^2}{4\, e_1\, a_1} \\ & + \frac{[e_2\, r_2 + m_1\, v\, e_2 + m_2\, (1 - v)\, e_2]^2}{4\, e_2\, a_2}.\end{aligned} \tag{2.8}$$

Because we have shown that v is bounded between 0 and 1, we obtain

$$\frac{dG}{dt} \leq -m_0 G + \eta_0, \tag{2.9}$$

where $m_0 = \min\{m_1, m_2\}$ and η_0 is a positive constant. By the comparison principle, we conclude that

$$\limsup_{t\to\infty} G(t) = \frac{\eta_0}{m_0},$$

implying that G is bounded. This also indicates that $\eta_0/m_0e_1,\ \ \eta_0/m_0e_2$ and η_0/m_0 are also *a priori* bounds of $x_1(t),\ \ x_2(t)$ and $y(t)$ respectively. The boundedness of the solution also implies that it exists globally, that it, it exists for all $t \in (0, \infty)$.

The above analysis also show that the set

$$X = \mathcal{R}_+^4 = \{(x_1, x_2, y, v) : x_1 \geq 0, x_2 \geq 0, y \geq 0, 0 \leq v \leq 1\},$$

is positively invariant, and we will only need to consider the dynamics of the model in this set.

In order to analyze the long-term behaviour of system (2.5), we first discuss the structure of all possible equilibria for this system. For convenience of notations, we let

$$\begin{aligned} &A_1 = \frac{e_1\, s_1\, r_1}{a_1 + h_1\, s_1\, r_1} - m_1,\ A_2 = \frac{e_2\, s_2\, r_2}{a_2 + h_2\, s_2\, r_2} - m_2,\\ &A_3 = e_2,\ A_4 = e_2 - m_2\, h_2,\ \ A_5 = r_2\, s_2,\ \ A_6 = a_2\, m_2,\\ &A_7 = e_1,\ A_8 = e_1 - m_1\, h_1,\ \ A_9 = r_1\, s_1,\ \ A_{10} = a_1\, m_1. \end{aligned} \tag{2.10}$$

Denote

$$\begin{aligned} x_1^* &= \frac{m_1}{s_1(e_1 - m_1\, h_1)},\ y_1^* = \frac{e_1(r_1\, s_1\, e_1 - r_1\, s_1\, h_1\, m_1 - a_1\, m_1)}{s_1^2(e_1 - m_1\, h_1)^2},\\ x_2^* &= \frac{m_2}{s_2(e_2 - m_2\, h_2)},\ y_2^* = \frac{e_2(r_2\, s_2\, e_2 - r_2\, s_2\, h_2\, m_2 - a_2\, m_2)}{s_2^2(e_2 - m_2\, h_2)^2}. \end{aligned} \tag{2.11}$$

Then, direct calculations show that there are always eight equilibria for the biologically meaningful parameters:

$$\begin{aligned} &E_0^2 = (0,0,0,0),\ E_1^2 = \left(\frac{r_1}{a_1}, 0, 0, 0\right),\ E_2^2 = \left(0, \frac{r_2}{a_2}, 0, 0\right),\ E_3^2 = \left(\frac{r_1}{a_1}, \frac{r_2}{a_2}, 0, 0\right),\\ &E_0^1 = (0,0,0,1),\ E_1^1 = \left(\frac{r_1}{a_1}, 0, 0, 1\right),\ E_2^1 = \left(0, \frac{r_2}{a_2}, 0, 1\right),\ E_3^1 = \left(\frac{r_1}{a_1}, \frac{r_2}{a_2}, 0, 1\right). \end{aligned}$$

In addition, five other equilibria including a unique positive equilibrium may come into existence under certain conditions on the model parameters:

$$\begin{aligned} &E_4^1 = (x_1^*, 0, y_1^*, 1), \quad E_5^1\left(x_1^*, \frac{r_2}{a_2}, y_1^*, 1\right),\\ &E_4^2 = (0, x_2^*, y_2^*, 0), \quad E_5^2 = \left(\frac{r_1}{a_1}, x_2^*, y_2^*, 0\right),\\ &E^* = (\tilde{x}_1^*, \tilde{x}_2^*, \tilde{y}^*, \tilde{v}^*) \ \text{ with } \ \tilde{x}_1^* > 0,\ \ \tilde{x}_2^* > 0,\ \ \tilde{y}^* > 0,\ \ \tilde{v}^* \in (0,1). \end{aligned}$$

Obviously, $y_1^* > 0$ if and only if $A_1 > 0$ which implies $A_8 > 0$ (hence $x_1^* > 0$). Similarly, $y_2^* > 0$ if and only if $A_2 > 0$ which implies $A_4 > 0$ (hence $x_2^* > 0$). Here, all equilibria, except for E^*, have explicit formulas and each represents one situation of the specialist strategies ($v = 0$ or $v = 1$) meaning that all predators choose to inhabit in one patch. However, E^* with $\tilde{v}^* \in (0,1)$ represents a generalist strategy, which can not be obtained explicitly; indeed, its existence will be established by an argument using abstract persistence theory.

The stability/instability of these equilibria can be analyzed by the standard method of investigating the characteristic equation at each of them, except for E^*. Below, we showcase the analysis on E_5^2.

Theorem 2.3.1 *Assume that $A_2 > 0$ so that E_5^2 exists. Then, it is locally asymptotically stable if and only if*

$$A_1 < 0 \ \text{ and } \ A_4\, A_5\, (A_3 - A_4) < A_6\, (2\, A_3 - A_4)\,. \tag{2.12}$$

Proof The Jacobian matrix of (2.5) is

$$\begin{bmatrix} J_{11} & 0 & -\frac{s_1\,x_1\,v}{1+h_1\,s_1\,x_1} & -\frac{s_1\,x_1\,y}{1+h_1\,s_1\,x_1} \\ 0 & J_{22} & -\frac{s_2\,x_2\,(1-v)}{1+h_2\,s_2\,x_2} & \frac{s_2\,x_2\,y}{1+h_2\,s_2\,x_2} \\ \frac{e_1\,v\,s_1\,y}{(1+h_1\,s_1\,x_1)^2} & \frac{e_2\,(1-v)\,s_2\,y}{(1+h_2\,s_2\,x_2)^2} & J_{33} & J_{34} \\ \frac{k\,v\,(1-v)\,e_1\,s_1}{(1+h_1\,s_1\,x_1)^2} & -\frac{k\,v\,(1-v)\,e_2\,s_2}{(1+h_2\,s_2\,x_2)^2} & 0 & J_{44} \end{bmatrix}, \tag{2.13}$$

where

$$\begin{aligned} J_{11} &= r_1 - 2\,a_1\,x_1 - \frac{s_1\,v\,y}{(1+h_1\,s_1\,x_1)^2}, \\ J_{22} &= r_2 - 2\,a_2\,x_2 - \frac{s_2\,(1-v)\,y}{(1+h_2\,s_2\,x_2)^2}, \\ J_{33} &= -m_1\,v - m_2\,(1-v) + e_1\,v\frac{s_1\,x_1}{1+h_1\,s_1\,x_1} + e_2\,(1-v)\,\frac{s_2\,x_2}{1+h_2\,s_2\,x_2}, \\ J_{34} &= y\Big(-m_1 + m_2 + \frac{e_1\,s_1\,x_1}{1+h_1\,s_1\,x_1} - \frac{e_2\,s_2\,x_2}{1+h_2\,s_2\,x_2}\Big), \\ J_{44} &= k\,(1-2\,v)\Big(-m_1 + m_2 + \frac{e_1\,s_1\,x_1}{1+h_1\,s_1\,x_1} - \frac{e_2\,s_2\,x_2}{1+h_2\,s_2\,x_2}\Big). \end{aligned}$$

Substituting equilibrium E_5^2 into the Jacobian matrix (3.26) gives the characteristic equation at E_5^2 :

$$(\lambda + r_1)\left(\lambda - \overline{J}_{44}\right)\left(\lambda^2 - \overline{J}_{22}\lambda - \overline{J}_{23}\,\overline{J}_{32}\right) = 0, \tag{2.14}$$

where

$$\begin{aligned} \overline{J}_{44} &= k\left(-m_1 + m_2 + \frac{e_1\,s_1\,r_1}{a_1 + h_1\,s_1\,r_1} - \frac{e_2\,s_2\,x_2^*}{1+h_2\,s_2\,x_2^*}\right), \\ \overline{J}_{22} &= r_2 - \frac{2\,a_2\,m_2}{s_2\,(-m_2\,h_2 + e_2)} - \frac{s_2\,y_2^*}{\left(1+h_2\,s_2\,x_2^*\right)^2}, \\ \overline{J}_{23} &= -\frac{s_2\,x_2^*}{1+h_2\,s_2\,x_2^*}, \quad \overline{J}_{32} = \frac{e_2\,s_2\,y_2^*}{\left(1+h_2\,s_2\,x_2^*\right)^2}. \end{aligned}$$

Obviously, $\lambda_1 = -r$ and $\lambda_2 = \overline{J}_{44}$ are real roots of (2.14), and the other two roots of (2.14) are determined by the quadratic equation:

$$\lambda^2 - \overline{J}_{22}\lambda - \overline{J}_{23}\,\overline{J}_{32} = 0. \tag{2.15}$$

Note that $\overline{J}_{23}\,\overline{J}_{32} < 0$. Thus, the two roots of (2.15) have negative real parts if and only if $\overline{J}_{22} < 0$. Therefore, all roots of (2.14) have negative real parts if and only if

$$\overline{J}_{22} < 0 \quad \text{and} \quad \overline{J}_{44} < 0,$$

which are, by the notations defined in (2.11), equivalent to the two conditions in (2.12). This completes the proof.

Equilibrium	**Existence**	**Stability**	**Condition for stability**
$E_0^2(0,0,0,0)$	always exists	unstable	
$E_1^2\left(\frac{r_1}{a_1},0,0,0\right)$	always exists	unstable	
$E_2^2\left(0,\frac{r_2}{a_2},0,0\right)$	always exists	unstable	
$E_3^2\left(\frac{r_1}{a_1},\frac{r_2}{a_2},0,0\right)$	always exists	Locally Stable	$A_2<0,\ A_1<A_2$
$E_4^2(0,x_0^*,y_0^*,0)$	$0<A_2$	unstable	
$E_5^2\left(\frac{r_1}{a_1},x_0^*,y_0^*,0\right)$	$0<A_2$	Locally Stable	$A_1<0, A_4A_5(A_3-A_4)<A_6(2A_3-A_4)$
$E_0^1(0,0,0,1)$	always exists	unstable	
$E_1^1\left(\frac{r_1}{a_1},0,0,1\right)$	always exists	unstable	
$E_2^1\left(0,\frac{r_2}{a_2},0,1\right)$	always exists	unstable	
$E_3^1\left(\frac{r_1}{a_1},\frac{r_2}{a_2},0,1\right)$	always exists	Locally Stable	$A_1<0,\ A_2<A_1$
$E_4^1(x_1^*,0,y_1^*,1)$	$0<A_1$	unstable	
$E_5^1\left(x_1^*,\frac{r_2}{a_2},y_1^*,1\right)$	$0<A_1$	Locally Stable	$A_2<0, A_8A_9(A_7-A_8)<A_{10}(2A_7-A_8)$
$E(\tilde{x}_1^*,\tilde{x}_2^*,\tilde{y}^*,\tilde{v}^*)$	$0<A_1,\ 0<A_2$		

Table 2.1: The upper index i ($i=1,2$) indicates that predators forage only in patch i without migrating to the other patch. $E(\tilde{x}_1^*,\tilde{x}_2^*,\tilde{y}^*,\tilde{v}^*)$ is the unique positive equilibrium.

The analysis of stability/instability of other equilibria, except for E^*, can be similarly done and will be omitted here since it would cost too much space. Table 2.1 summarizes such results.

As mentioned before, the existence of E^* can not established through solving the equations for equilibria. Instead it is established as a result of uniform persistence of the model. To this end, we will first establish the uniform persistence of the population with a generalist strategy ($v\in(0,1)$) under the conditions $A_1>0$ and $A_2>0$. For this purpose, we need to obtain some information about the patch-wise dynamics, that is, the population dynamics when the predator only stays in one patch, by considering the following system (obtained by taking taking $v=0$ or

$v = 1$ in (2.5)):

$$\begin{cases} \dfrac{dx_i}{dt} = x_i\,(r_i - a_i\,x_i) - \dfrac{s_i\,x_i\,y}{1 + h_i\,s_i\,x_i}, \\ \dfrac{dy}{dt} = y\left(-m_i + e_i\,\dfrac{s_i\,x_i}{1 + h_i\,s_i\,x_i}\right). \end{cases} \tag{2.16}$$

For such a classic prey-predator model, generally, when the carrying capacity of the prey is not too large, the populations of prey and predator tend to a unique positive steady state; while when the carrying capacity of the prey is sufficiently large, oscillations will occur and the populations of prey and predators tend to a globally stable limit cycle. To state this more precisely, we first note that for $i = 1, 2$, $A_i > 0$ is equivalent to

$$\frac{m_i\,h_i}{s_i\,h_i(e_i - m_i\,h_i)} < \frac{r_i}{a_i},$$

which is also the condition for x_i^* and y_i^* to be positive (hence existence of positive equilibrium (x_i^*, y_i^*) for (2.16)). Thus, if both A_1 and A_2 are negative, regardless of whether choosing to stay in patch 1 ($v(t) = 1$) or patch 2 ($v(t) = 0$), the predator will go to extinction. Indeed, in such a case, this conclusion remains true for any general strategies in (2.5), as is confirmed in the following theorem.

Theorem 2.3.2 *The predators go to extinction if $A_1 < 0$ and $A_2 < 0$.*

Proof Applying the comparison principle to the first and the second equation in (2.5), we have the estimates:

$$\limsup_{t\to\infty} x_i(t) \le \frac{r_i}{a_i}, \quad i = 1, 2.$$

Thus, for any $\epsilon > 0$, there exists $t^* > 0$ such that

$$x_i(t) \le \frac{r_1}{a_1} + \epsilon \quad \text{for} \quad t \ge t^*. \tag{2.17}$$

This together with the third equation in (2.5) lead to

$$\frac{dy}{dt} \le By, \tag{2.18}$$

where

$$B = -m_1\,v - m_2\,(1 - v) + \frac{e_1\,v\,s_1(r_1 + a_1\,\epsilon)}{a_1 + h_1\,s_1(r_1 + a_1\,\epsilon)} + \frac{e_2\,(1 - v)\,s_2(r_2 + a_2\,\epsilon)}{a_2 + h_2\,s_2(r_2 + a_2\,\epsilon)}.$$

Noting that

$$\begin{aligned} &\lim_{\epsilon\to 0}\left(-m_1\,v - m_2\,(1 - v) + \frac{e_1\,v\,s_1(r_1 + a_1\,\epsilon)}{a_1 + h_1\,s_1(r_1 + a_1\,\epsilon)} + \frac{e_2\,(1 - v)\,s_2(r_2 + a_2\,\epsilon)}{a_2 + h_2\,s_2(r_2 + a_2\,\epsilon)}\right) \\ &= v(A_1 - A_2) + A_2 = vA_1 + (1 - v)A_2 < 0. \end{aligned} \tag{2.19}$$

One can choose $\epsilon > 0$ sufficiently small such that $B < 0$. This together with (2.18) implies that $y(t) \to 0$ as $\to \infty$, that is, the predator goes to extinction.

By this theorem, in order for the predators to be persistent, at least one of the two quantities A_1 and A_2 must be positive. To proceed further, we need the following lemma, which can be easily proved by standard methods (see, e.g., [18]), on the prey-predator model (2.16).

Lemma 2.3.3 *Assume that $A_i > 0$. If*

$$(H_i) \qquad \frac{r_i}{a_i} < \frac{e_i + m_i h_i}{s_i h_i (e_i - m_i h_i)},$$

then, every positive solution of (2.16) *approaches to a positive equilibrium; and if*

$$(H_i^-) \qquad \frac{e_i + m_i h_i}{s_i h_i (e_i - m_i h_i)} < \frac{r_i}{a_i},$$

then, every positive solution of (2.16) *tends to a positive limit cycle, except for those solutions starting from unstable equilibria.*

In the remainder of this section, we consider the case when both A_1 and A_2 are positive, and will leave the case that $A_1 A_2 < 0$ to the next section for discussion where we will present some numerical simulation results.

Now we are in the position to establish the persistence of the predators, as well as of the strategy functions $v(t)$ and $1 - v(t)$ for the case when both A_1 and A_2 are positive.

Theorem 2.3.4 *Assume that $A_1 > 0$ and $A_2 > 0$. Then the predator population in system* (2.5) *is uniformly persistent.*

Proof We apply the theory in [11, 23] to complete the proof. To this end, we distinguish four cases:

(I) (H_1) and (H_2) hold; (II) (H_1) and (H_2^-) hold;

(III) (H_1^-) and (H_2) hold; (IV) (H_1^-) and (H_2^-) hold.

We only give the proof for Case (I), since the proofs for the other three cases are similar and are thus omitted to save space.

Define

$$\begin{aligned} X &= \{(x_1, x_2, y, v) : x_1 \geq 0, x_2 \geq 0, y \geq 0, 0 \leq v \leq 1\}, \\ X_0 &= \{(x_1, x_2, y, v) : x_1 \geq 0, x_2 \geq 0, y > 0, 0 \leq v \leq 1\}, \\ Y &= X/X_0 = \{(x_1, x_2, y, v) : x_1 \geq 0, x_2 \geq 0, y = 0, 0 \leq v \leq 1\}. \end{aligned} \tag{2.20}$$

There are eight equilibria in set Y:

$$E_0^2(0,0,0,0),\ E_1^2\left(\frac{r_1}{a_1},0,0,0\right),\ E_2^2\left(0,\frac{r_2}{a_2},0,0\right),\ E_3^2\left(\frac{r_1}{a_1},\frac{r_2}{a_2},0,0\right),$$
$$E_0^1(0,0,0,1),\ E_1^1\left(\frac{r_1}{a_1},0,0,1\right),\ E_2^1\left(0,\frac{r_2}{a_2},0,1\right),\ E_3^1\left(\frac{r_1}{a_1},\frac{r_2}{a_2},0,1\right).$$

Following notations in [11], A_∂ being the global attractor in the boundary set Y, we have

$$\begin{aligned}\widetilde{A}_\partial &= \bigcup_{x\in A_\partial} \omega(x) \\ &= \cup E_i^j, \qquad i = 0,1,2,3, \quad j = 1,2.\end{aligned}$$

In order to show $\widetilde{A}_\partial$ is isolated and has an acyclic covering, first, we consider the system restricted on Y:

$$\begin{aligned}\frac{dx_1}{dt} &= x_1(r_1 - a_1x_1), \\ \frac{dx_2}{dt} &= x_2(r_2 - a_2x_2), \\ \frac{dv}{dt} &= kv(1-v)\left(-m_1 + m_2 + \frac{e_1\, s_1\, x_1}{1 + h_1\, s_1\, x_1} - \frac{e_2\, s_2\, x_2}{1 + h_2\, s_2\, x_2}\right).\end{aligned} \tag{2.21}$$

Note that among equilibria E_i^j for $i = 0,1,2,3$; $j = 1,2$, the sequence E_i^2, $i = 0,1,2,3$ correspond to $v = 0$ and the sequence E_i^1, $i = 0,1,2,3$ correspond to $v = 1$. First, we show the analysis for the former case. When $v = 0$, the three-dimensional system (2.21) reduces to a two-dimensional system. Because equilibrium E_3^2 is globally asymptotically stable for the two-dimensional system, it is clear that $E_0^2, E_1^2, E_2^2, E_3^2$ are isolated and acyclic in set Y. By checking eigenvalues of each equilibrium, it can be shown that $E_0^2, E_1^2, E_2^2, E_3^2$ are also isolated in set X.

Next, we show that $W^s(E_3^2) \cap X_0 = \emptyset$. Suppose this is not true. Then there exists a solution of (2.5) with $y(t)$ positive such that

$$\lim_{t\to\infty}(x_1(t), x_2(t), y(t), v(t)) = \left(\frac{r_1}{a_1}, \frac{r_2}{a_2}, 0, 0\right). \tag{2.22}$$

Denote

$$R(t) = -m_1\, v - m_2\,(1-v) + \frac{e_1\, v\, s_1\, x_1}{1 + h_1\, s_1\, x_1} + \frac{e_2\,(1-v)\, s_2\, x_2}{1 + h_2\, s_2\, x_2}.$$

Then (2.22) implies that $R(t) \to A_2 > 0$ as $\to \infty$. Thus, for $\epsilon \in (0, A_2)$, there exists $T > 0$ such that $R(t) > A_2 - \epsilon > 0$ for $t \geq T$. Therefore,

$$\frac{dy}{dt} = R(t)y \geq (A_2 - \epsilon)y, \quad \text{for } t \geq T, \tag{2.23}$$

which implies that y grows unboundedly by the comparison principle. This contradicts the boundedness of $y(t)$. Therefore, $W^s(E_3^2) \cap X_0 = \emptyset$ if $A_2 > 0$. Similarly, we can prove $W^s(E_i^2) \cap X_0 = \emptyset$ for $i = 0,1,2$ when condition $A_2 > 0$ holds.

For the case corresponding to $v = 1$, we can prove that $A_1 > 0$ implies $W^s(E_i^1) \cap X_0 = \emptyset$ for $i = 0,1,2,3$. The proof here is similar to the proof for the case $v = 0$ (it is actually a result of the conjugacy of v and $1 - v$) and is thus omitted.

Now, by the theoretical results in persistence theory (see, e.g., [11] or [23]), we have proved that the predator's population in system (2.5) is uniformly persistent.

Next, we show that strategy variable $v(t)$ is also persistent if both A_1 and A_2 are positive. We also distinguish the local case (H_i) (convergence to equilibrium) from the local case (H_i^-) (convergence to limit cycle).

Theorem 2.3.5 *Assume that $A_1 > 0$ and $A_2 > 0$. Then the strategy functions $v(t)$ and $1 - v(t)$ are uniformly persistent in the sense that there exists a $\eta > 0$ such that*

$$\liminf_{t\to\infty} v(t) > \eta, \quad \textit{and} \quad \liminf_{t\to\infty} [1 - v(t)] > \eta.$$

In order to prove the strategy's persistence, we need to prove that $v = 0$ and $v = 1$ are both uniform repellers. To this end, we define the same set X as in the proof of Theorem 2.3.4 but define the interior set and the boundary set with respect to v and $1 - v$ by

$$\hat{X}_0 = \{(x_1, x_2, y, v) : x_1 \geq 0, x_2 \geq 0, y \geq 0, 0 < v < 1\},$$
$$\hat{Y} = X/\hat{X}_0 = Y_1 \cup Y_2,$$

where, $Y_1 = \{(x_1, x_2, y, v) : x_1 \geq 0, x_2 \geq 0, y \geq 0, v = 0\}$ and $Y_2 = \{(x_1, x_2, y, v) : x_1 \geq 0, x_2 \geq 0, y \geq 0, v = 1\}$.

As in the proof of Theorem 2.3.4, we also distinguish four local cases as in the proof of Theorem 2.3.5, depending on whether the local dynamics is convergence to equilibrium (i.e., under (H_i)), or convergence to limit cycle (i.e., under (H_i^-)).

Proof of Case (I). (H_1) and (H_2) hold. First, we prove that $v = 0$ (i.e. Y_1) is a uniform repeller. When $v = 0$, six equilibria, namely

$$E_0^2(0,0,0,0), E_1^2\left(\frac{r_1}{a_1}, 0, 0, 0\right), E_2^2\left(0, \frac{r_2}{a_2}, 0, 0\right),$$
$$E_3^2\left(\frac{r_1}{a_1}, \frac{r_2}{a_2}, 0, 0\right), E_4^2\left(0, x_2^*, y_2^*, 0\right), E_5^2\left(\frac{r_1}{a_1}, x_2^*, y_2^*, 0\right),$$

exist in set Y_1. Let us consider the system restricted in Y_1:

$$\begin{aligned} \frac{dx_1}{dt} &= x_1(r_1 - a_1\, x_1), \\ \frac{dx_2}{dt} &= x_2(r_2 - a_2\, x_2) - \frac{s_2\, x_2\, y}{1 + h_2\, s_2\, x_2}, \\ \frac{dy}{dt} &= y\left(-m_2 + \frac{e_2\, s_2\, x_2}{1 + h_2\, s_2\, x_2}\right). \end{aligned} \tag{2.24}$$

For system (2.24), equilibrium E_5^2 is globally asymptotically stable when $A_2 > 0$, i.e. when equilibrium E_5^2 exists. Therefore, equilibria E_0^2, E_1^2, E_2^2, E_3^2, E_4^2, E_5^2 are isolated and acyclic

in the set Y. By checking the eigenvalues of each equilibrium, we can see that E_i^2 for $i = 0, 1, 2, 3, 4, 5$ are also isolated in set X.

Next, we prove that $W^s(E_5^2) \cap X_0 = \emptyset$. Suppose that is not the case. Then there exists a solution of (2.5) in X_0, such that

$$\lim_{t\to\infty}(x_1(t), x_2(t), y(t), v(t)) = \left(\frac{r_1}{a_1}, x_2^*, y_2^*, 0\right). \tag{2.25}$$

Denote

$$r(t) = -m_1 + m_2 + \frac{e_1\, s_1\, x_1}{1 + h_1\, s_1\, x_1} - \frac{e_2\, s_2\, x_2}{1 + h_2\, s_2\, x_2}.$$

Then (2.25) implies that $r(t) \to A_1 > 0$ as $t \to \infty$. Thus for any $\epsilon \in (0, A_1)$, there exists $T > 0$ such that $r(t) > A_1 - \epsilon$ for $t \geq T$. Therefore,

$$\frac{dv}{dt} \;=\; k\, v(1-v)r(t) \geq k\, v(1-v)(A_1 - \epsilon), \quad \text{for } t \geq T, \tag{2.26}$$

which implies that v is increasing in t. This contradicts the fact that $v \to 0$ when $t \to \infty$. Therefore, $W^s(E_5^2) \cap X_0 = \emptyset$ if condition $A_1 > 0$ is satisfied. Similarly, we can prove that $W^s(E_i^2) \cap X_0 = \emptyset$, for $i = 0, 1, 2, 3, 4$.

For the case where $v = 1$, we can prove that $W^s(E_i^1) \cap X_0 = \emptyset$ for $i = 0, 1, 2, 3, 4, 5$ if $A_2 > 0$ by the conjugacy of v and $1 - v$.

Based on persistence theory (e.g.,[11] or [23]), we have proved that the strategy is uniformly persistent. ∎

Proof of Case (II). (H_1^-) and (H_2^-) hold. We assume the period in patch 1 is T_1 and the period in patch 2 is T_2, and $T_2 > T_1$ for convenience. First, we show that $v = 0$, i.e. Y_1 is a uniform repeller. Let $(\overline{x}_2(t), \overline{y}(t))$ denote points of the limit cycle. It is sufficient to prove $W^s\left(\frac{r_1}{a_1}, \overline{x}_2, \overline{y}, 0\right) \cap X_0 = \emptyset$ in order to prove that $v = 0$ is a uniform repeller. Suppose this is not the case. Then there exists a solution of (2.5) such that

$$\lim_{t\to\infty}(x_1(t), x_2(t), y(t), v(t)) = \left(\frac{r_1}{a_1}, \overline{x}_2, \overline{y}, 0\right). \tag{2.27}$$

As indicated in (2.6), we have obtained the solution of v as

$$v(t) = 1 - 1/\left(1 + v(0)/(1 - v(0)) \exp\left\{\int_0^t \psi(\xi)d\xi\right\}\right).$$

We rewrite $\exp\left\{\int_0^t \psi(\xi)d\xi\right\}$ as

$$\exp\left\{\int_0^t \psi(\xi)d\xi\right\} = \exp\left\{\frac{\left(\int_0^t \psi(\xi)d\xi\right)}{t}\, t\right\}. \tag{2.28}$$

Substituting (2.7) into $\int_0^t \psi(\xi)d\xi/t$, we obtain

$$\begin{aligned}
&- k(m_2 + \epsilon\, e_2\, s_2\, L_1) + \frac{k\, e_1\, s_1(r_1/a_1 - \epsilon)}{1 + h_1\, s_1(r_1/a_1 - \epsilon)} \\
&\leq \frac{k\int_0^{nT_2}(e_1\, s_1\, x_1)/(1 + h_1\, s_1\, x_1)ds}{n\, T_2} - \frac{k\int_0^{nT_2}(e_2\, s_2\, x_2)/(1 + h_2\, s_2\, x_2)ds}{n\, T_2} \\
&\leq \frac{k\, e_1\, s_1(r_1/a_1 + \epsilon)}{1 + h_1\, s_1(r_1/a_1 + \epsilon)} - k(m_2 - \epsilon\, e_2\, s_2\, L_2).
\end{aligned} \tag{2.29}$$

Substituting $t = n\, T_2$ into (2.29), we obtain

$$\begin{aligned}
&\frac{\int_0^{nT_2} k\left((e_1\, s_1\, x_1)/(1 + h_1\, s_1\, x_1) - (e_2\, s_2\, x_2)/(1 + h_2\, s_2\, x_2)\right) d\xi}{n\, T_2} \\
&= \frac{k\int_0^{nT_2}(e_1\, s_1\, x_1)/(1 + h_1\, s_1\, x_1)d\xi}{n\, T_2} - \frac{k\int_0^{nT_2}(e_2\, s_2\, x_2)/(1 + h_2\, s_2\, x_2)d\xi}{n\, T_2}.
\end{aligned} \tag{2.30}$$

The predator's equation in system (2.5) shows

$$\frac{dy}{y} = \left(-m_2 + \frac{e_2\, s_2\, x_2}{1 + h_2\, s_2\, x_2}\right)dt. \tag{2.31}$$

Substituting $(\overline{x}_2, \overline{y})$ into (2.31) and integrating both sides of (2.31) from 0 to $n\, T_2$ gives

$$\int_0^{nT_2} \frac{d\,\overline{y}}{\overline{y}} = \int_0^{nT_2}\left(-m_2 + \frac{e_2\, s_2\, \overline{x}_2}{1 + h_2\, s_2\, \overline{x}_2}\right)dt. \tag{2.32}$$

Direct calculations indicate that $\int_0^{nT_2} \frac{d\,\overline{y}}{\overline{y}} = 0$. Further calculations show that the right-hand side of (2.32) equals $-m_2\, n\, T_2 + \int_0^{nT_2}(e_2\, s_2\, \overline{x}_2)/(1 + h_2\, s_2\, \overline{x}_2)dt$. Therefore, we obtain

$$\int_0^{nT_2} \frac{e_2\, s_2\, \overline{x}_2}{1 + h_2\, s_2\, \overline{x}_2}dt = n\, m_2\, T_2. \tag{2.33}$$

Let

$$f(x) = \frac{e_2\, s_2\, x}{1 + h_2\, s_2\, x}.$$

The function $f(x)$ is increasing. In addition, from (2.27), for ϵ small enough, there exists $n^* > 0$ such that $\overline{x}_2 - \epsilon < x_2 < \overline{x}_2 + \epsilon$. Using the above two properties, when $n > n^*$, we obtain,

$$\begin{aligned}
\frac{e_2\, s_2\,(\overline{x}_2 - \epsilon)}{1 + h_2\, s_2\, \overline{x}_2} &< \frac{e_2\, s_2\,(\overline{x}_2 - \epsilon)}{1 + h_2\, s_2\,(\overline{x}_2 - \epsilon)} < \frac{e_2\, s_2\, x_2}{1 + h_2\, s_2\, x_2} \\
&< \frac{e_2\, s_2\,(\overline{x}_2 + \epsilon)}{1 + h_2\, s_2\,(\overline{x}_2 + \epsilon)} < \frac{e_2\, s_2\,(\overline{x}_2 + \epsilon)}{1 + h_2\, s_2\, \overline{x}_2}.
\end{aligned}$$

By using (2.33),when $n > n^*$, we have

$$\begin{aligned}
&\frac{\int_0^{nT_2} (e_2\, s_2\, (\overline{x}_2 + \epsilon)) \,/\, (1 + h_2\, s_2\, \overline{x}_2)\, d\xi}{nT_2} \\
&= \frac{\int_0^{nT_2} (e_2\, s_2\, \overline{x}_2) \,/\, (1 + h_2\, s_2\, \overline{x}_2)\, d\xi}{n\, T_2} + \frac{\int_0^{nT_2} (e_2\, s_2\, \epsilon) \,/\, (1 + h_2\, s_2\, \overline{x}_2)\, d\xi}{nT_2} \\
&= \frac{n\, m_2\, T_2}{n\, T_2} + \frac{\int_0^{nT_2} (e_2\, s_2\, \epsilon) \,/\, (1 + h_2\, s_2\, \overline{x}_2)\, d\xi}{n\, T_2} \\
&= m_2 + \frac{\epsilon\, e_2\, s_2 \int_0^{nT_2} 1/\,(1 + h_2\, s_2\, \overline{x}_2)\, d\xi}{n\, T_2}.
\end{aligned} \tag{2.34}$$

Because $\overline{x}_2$ is bounded, we assume

$$L_2 \le 1/(1 + h_2\, s_2\, \overline{x}_2) \le L_1, \tag{2.35}$$

where L_1 and L_2 are positive constants. By using (2.35), we obtain

$$\epsilon\, e_2\, s_2\, L_2 \le \frac{\epsilon\, e_2\, s_2 \int_0^{nT_2} 1/(1 + h_2\, s_2\, \overline{x}_2) d\xi}{nT_2} \le \epsilon\, e_2\, s_2\, L_1, \quad \text{when} \quad n > n^*.$$

From the above analysis, when $n > n^*$, we have

$$\begin{aligned}
m_2 - \epsilon\, e_2\, s_2\, L_2 &\le \frac{\int_0^{nT_2} (e_2\, s_2\, (\overline{x}_2 - \epsilon)) \,/\, (1 + h_2\, s_2\, \overline{x}_2)\, d\xi}{nT_2} \\
&\le \frac{\int_0^{nT_2} (e_2\, s_2\, x_2)/(1 + h_2\, s_2\, x_2) d\xi}{nT_2} \\
&\le \frac{\int_0^{nT_2} (e_2\, s_2\, (\overline{x}_2 + \epsilon))/(1 + h_2\, s_2 \overline{x}_2) d\xi}{nT_2} \le m_2 + \epsilon\, e_2\, s_2\, L_1.
\end{aligned} \tag{2.36}$$

Again from (2.27), when $n > n^*$, we have

$$\frac{r_1}{a_1} - \epsilon < x_1(t) < \frac{r_1}{a_1} + \epsilon.$$

By using the above inequality, we obtain

$$\frac{e_1\, s_1\, (r_1/a_1 - \epsilon)}{1 + h_1\, s_1\, (r_1/a_1 - \epsilon)} < \frac{e_1\, s_1\, x_1}{1 + h_1\, s_1\, x_1} < \frac{e_1\, s_1\, (r_1/a_1 + \epsilon)}{1 + h_1\, s_1\, (r_1/a_1 + \epsilon)}. \tag{2.37}$$

Integrating (2.37) from 0 to $n\, T_2$, we obtain

$$\begin{aligned}
\frac{n\, T_2\, e_1\, s_1\, (r_1/a_1 - \epsilon)}{1 + h_1\, s_1\, (r_1/a_1 - \epsilon)} &< \int_0^{nT_2} (e_1\, s_1\, x_1)/(1 + h_1\, s_1\, x_1) d\xi \\
&< \frac{n\, T_2\, e_1\, s_1\, (r_1/a_1 + \epsilon)}{1 + h_1\, s_1\, (r_1/a_1 + \epsilon)}.
\end{aligned} \tag{2.38}$$

It is obvious that (2.38) is equivalent to

$$\begin{aligned}\frac{k\,e_1\,s_1\,(r_1/a_1-\epsilon)}{1+h_1\,s_1\,(r_1/a_1-\epsilon)} <& \frac{k\int_0^{nT_2}(e_1\,s_1\,x_1)/(1+h_1\,s_1\,x_1)d\xi}{n\,T_2}\\ <& \frac{k\,e_1\,s_1\,(r_1/a_1+\epsilon)}{1+h_1\,s_1\,(r_1/a_1+\epsilon)}.\end{aligned} \tag{2.39}$$

Comparing (2.36), (2.39) with (2.30), when $n > n^*$, we obtain

$$\begin{aligned}&-k(m_2+\epsilon\,e_2\,s_2\,L_1)+\frac{k\,e_1\,s_1(r_1/a_1-\epsilon)}{1+h_1\,s_1(r_1/a_1-\epsilon)}\\ &\le \frac{k\int_0^{nT_2}(e_1\,s_1\,x_1)/(1+h_1\,s_1\,x_1)ds}{n\,T_2}-\frac{k\int_0^{nT_2}(e_2\,s_2\,x_2)/(1+h_2\,s_2\,x_2)ds}{n\,T_2}\\ &\le \frac{k\,e_1\,s_1(r_1/a_1+\epsilon)}{1+h_1\,s_1(r_1/a_1+\epsilon)}-k(m_2-\epsilon\,e_2\,s_2\,L_2).\end{aligned} \tag{2.40}$$

From (2.40), we have

$$\begin{aligned}&\limsup_{n\to\infty}\frac{k\int_0^{nT_2}(e_1\,s_1\,x_1)/(1+h_1\,s_1\,x_1)ds}{n\,T_2}-\frac{k\int_0^{nT_2}(e_2\,s_2\,x_2)/(1+h_2\,s_2\,x_2)ds}{n\,T_2}\\ &=\frac{k\,e_1\,s_1\,r_1}{a_1+h_1\,s_1\,r_1}-k\,m_2,\\ &\liminf_{n\to\infty}\frac{k\int_0^{nT_2}(e_1\,s_1\,x_1)/(1+h_1\,s_1\,x_1)ds}{n\,T_2}-\frac{k\int_0^{nT_2}(e_2\,s_2\,x_2)/(1+h_2\,s_2\,x_2)ds}{n\,T_2}\\ &=\frac{k\,e_1\,s_1\,r_1}{a_1+h_1\,s_1\,r_1}-k\,m_2.\end{aligned} \tag{2.41}$$

By comparing (2.41) and (2.29), we obtain

$$\frac{\int_0^t\psi(\xi)d\xi}{t}\to -k\,m_1+\frac{w\,e_1\,s_1\,r_1}{a_1+h_1\,s_1\,r_1},\qquad \text{when}\ \ t\to\infty. \tag{2.42}$$

Let $\alpha = k\,((e_1\,s_1\,r_1)/(a_1+h_1\,s_1\,r_1)-m_1) = k\,A_1$. From (2.6) and (2.42), we obtain

$$\begin{aligned}v(t) &= 1-1/\left(1+(v(0)/(1-v(0)))\exp\left\{\int_0^t\psi(\xi)d\xi\right\}\right)\\ &\to 1,\qquad \text{when}\ \ t\to\infty.\end{aligned} \tag{2.43}$$

This contradicts the fact that $v\to 0$, when $t\to\infty$. Therefore, we can conclude that $v=0$ is a uniform repeller.

The proof of $v=1$ being a uniform repeller is similar to the proof above. The only difference lies in choosing $t = n\,T_1$ instead of $t = n\,T_2$. Here we omit this part.

When $t\neq n\,T_1$ or $t\neq n\,T_2$, from (2.41), we see that

$$\int_0^{nT_2}(e_i\,s_i\,x_i)/(1+h_i\,s_i\,x_i)ds,\quad i=1,2$$

are bounded because $x_1,\ x_2$ are bounded. When n is sufficiently large, (2.41) is still valid. Taking all the above into consideration, we can conclude that if $A_1 > 0, A_2 > 0$, the strategies $v(t)$ and $1 - v(t)$ are uniformly persistent. ∎

Proof of Case (III). (H_1) and (H_2^-) hold. When (H_1) and (H_2^-) hold, we assume the period of the limit cycle of (2.5) in patch 2 is T. First, we prove that $v = 0$ is a uniform repeller. When $v = 0$, predators forage only in patch 2. Let $(\overline{x}_{20}(t), \overline{y}_0(t))$ denote points of the limit cycle in patch 2. It is sufficient to prove $W^s\left(\frac{r_1}{a_1}, \overline{x}_{20}, \overline{y}_0, 0\right) \cap X_0 = \emptyset$ in order to prove that v is a uniform repeller. The remaining proof is similar to the proof of Case (II) except that we choose $t = n\,T$ here instead of $t = n\,T_1$ or $t = n\,T_2$. Following the same procedure as in the proof of Case (II), we can prove that $v = 0$ is a uniform repeller when conditions $A_1 > 0, A_2 > 0$ are satisfied. The proof of $v = 1$ being a uniform repeller is similar to the proof of $v = 0$ being a uniform repeller of Case (II), and is thus omitted.

The proof of the theorem is completed. ∎

2.4 Numerical simulations

We now discuss the mixed scenario of either "$A_1 > 0$ and $A_2 < 0$" or "$A_1 < 0$ and $A_2 > 0$". In such a case, if the two patches are fully isolated, then the results on the dynamics of the patch-wise model (2.16) show that the predators will persist in the advantageous patch (i.e., with $A_i > 0$) but go to extinction in the disadvantageous patch (i.e., with $A_i < 0$). When the two patches are not isolated, $v(t)$ evolves in $(0, 1)$. Unfortunately we are unable to obtain any theoretical results at this moment for such a case. However, our numerical explorations seem to suggest that the above conclusion remains true. For example, if we take the parameter values $r_1 = 2.0, r_2 = 0.3, a_1 = 2, a_2 = 1.3, s_1 = 1.2, s_2 = 1, m_1 = 0.2, m_2 = 0.1, e_1 = 0.4, e_2 = 0.3, h_1 = 0.3, h_2 = 0.2, k = 1.0$, we have $A_1 > 0$ and $A_2 < 0$. Numerical simulation shows that $v(t) \to 1$ as $t \to \infty$ (see Fig. 2.1(a)), implying that the predators will eventually stay in patch 1 (the advantageous patch). Then by the theory of asymptotically autonomous systems, we obtain the above conclusion. Similarly, by choosing the parameter values $r_1 = 0.8, r_2 = 2.0, a_1 = 2, a_2 = 1.3, s_1 = 1.2, s_2 = 1, m_1 = 0.2, m_2 = 0.1, e_1 = 0.4, e_2 = 0.3, h_1 = 0.3, h_2 = 0.2, k = 1.0$, we have $A_1 < 0$ and $A_2 > 0$, and simulation shows that $v(t) \to 0$ as $t \to \infty$ (see Fig. 2.1(b)), leading to the above conclusion again.

Mathematical results in Section 3 show that the dispersal rate of predators or the strength of adaptation (i.e., k) does not affect the persistence or extinction of the predators. However, numerical simulations indicate that k may induce rich patterns and have an effect on average biomass of the predators. Figures 2.2, 2.3, 2.4 are obtained under the case where the carrying

capacity of prey in patch 1 is small and the carrying capacity of prey in patch 2 is large enough to support oscillations, reflected by the conditions "$A_1 > 0$ and $A_2 > 0$" together with "(H_1) and (H_2^-)".

Figure 2.2 indicates that when k is large or small, i.e. when the adaptation strength of predators is strong or weak, the dispersal of predators stabilizes the system; while when the adaptation strength is mediate, there will be Hopf bifurcation. Figures 2.3 and 2.4 show that in the interval of Hopf bifurcation, prey, predators and the strategy behave periodically. Figure 2.5 shows that there is a complicated relationship between predator's average biomass and the dispersal rate k in the interval of Hopf bifurcation.

When the carrying capacity of prey in each isolated patch is large enough to support oscillations, i.e. conditions (H_1^-) and (H_2^-)in Lemma 2.3.3 are satisfied, a torus bifurcation may occur. Figures 2.6(a) and 2.6(b) are produced under conditions (H_1^-) and (H_2^-) in Lemma 2.3.3. Figure 2.6(a) shows modulated oscillation. Figure 2.6(b) shows a torus surface. As indicated in [8], a torus bifurcation may be due to the aperiodic behavior of predators. Making use of the simulations in Figures 2.3, 2.4, or 2.5, we increase the local recruitment rate of prey in patch 1 such that prey and predators in both patches exhibit periodic behaviour. Because the amplitude of the periodic solutions in two patches are different, the aperiodic behaviour of the predators occurs, which leads to the torus bifurcation.

2.5 Conclusion and discussions

In this paper, we have studied the dynamics of a two-patch predator-prey model with the Holling type II functional response and allowing the predators to move adaptively between the two patches to gain fitness. We have analyzed the persistence and extinction of predators and the corresponding mixed strategy, in terms of the combined parameters $A_i,\ i = 1, 2$ which determine whether patch i is advantageous or disadvantageous to the predators. When patches are isolated, in an advantageous patch, by Lemma 2.3.3, prey and predators can persist in two different modes: (i) convergence to a positive equilibrium; (ii) convergence to a positive periodic solution, depending on whether (H_i) or its opposite (H_i^-) holds.

With the adaptive dispersal, we have proved that predators will go to extinction on both patches when $A_1 < 0$ and $A_2 < 0$; and when $A_1 > 0, A_2 > 0$, the predators will persist in both patches, and so will be the dispersion strategy function $v(t)$. Interestingly, the strength of adaptation (i.e. k) does not affect the above conclusion. However, numerical simulations indicate that it does have an impact on the patterns of persistence and affect the average population of the predators. When prey and predators tend to an equilibrium in one patch and tend to a limit cycle in the other patch, numerical simulations show that the adaptive movement of predators

can stabilize the system when the adaptation of predators is either weak or strong, and there is an intermediate window for the adaptation strength in which Hopf bifurcation occurs, causing periodic fluctuations for prey and predator populations in both patches. Also found by numerical simulations is that the average biomass of predators has a complicated relationship with the dispersal rate of the predators. Moreover when prey and predators tend to limit cycles in each isolated patch, a torus bifurcation is numerically observed.

For the case of $A_1A_2 < 0$ (i.e., one patch is advantageous and the other is disadvantageous), we are unable to obtain theoretical results. In such situation, our numerical investigations seem to show that adaptive dispersal also does not affect the global outcome in the sense that the predators will persist in the advantageous patch and go extinct in the disadvantageous patch. In plain language, the adaptive dispersal is always in favor of the advantageous patch, if any.

We point out that recently Cressman and Křivan ([8]) studied a two-patch predator-prey model focusing on adaptive dispersals of both prey and predators. In contrast to their work, we consider a system including both population dynamics and adaptive dynamics. By studying the combined system, we can gain more biological and mathematical insights.

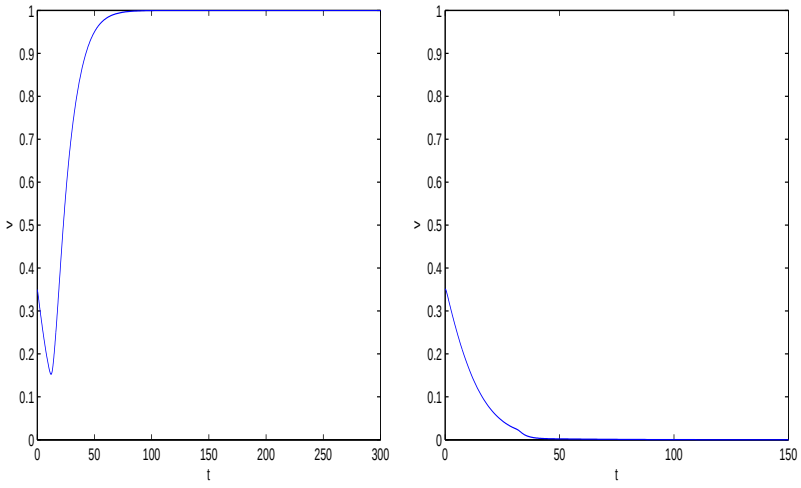

(a) Adaptive dispersion is in favor of patch 1

(b) Adaptive dispersion is in favor of patch 2

Figure 2.1: Adaptive dispersion. (a) The initial values are $(0.2, 0.1, 12, 0.35)$, and the parameter values are $r_1 = 2.0, r_2 = 0.3, a_1 = 2, a_2 = 1.3, s_1 = 1.2, s_2 = 1, m_1 = 0.2, m_2 = 0.1, e_1 = 0.4, e_2 = 0.3, h_1 = 0.3, h_2 = 0.2, k = 1.0$ leading to $A_1 > 0$ and $A_2 < 0$; (b) The initial values are $(0.5, 0.2, 12, 0.35)$, and the parameter values are $r_1 = 0.8, r_2 = 2.0, a_1 = 2, a_2 = 1.3, s_1 = 1.2, s_2 = 1, m_1 = 0.2, m_2 = 0.1, e_1 = 0.4, e_2 = 0.3, h_1 = 0.3, h_2 = 0.2, k = 1.0$ leading to $A_1 < 0$ and $A_2 > 0$.

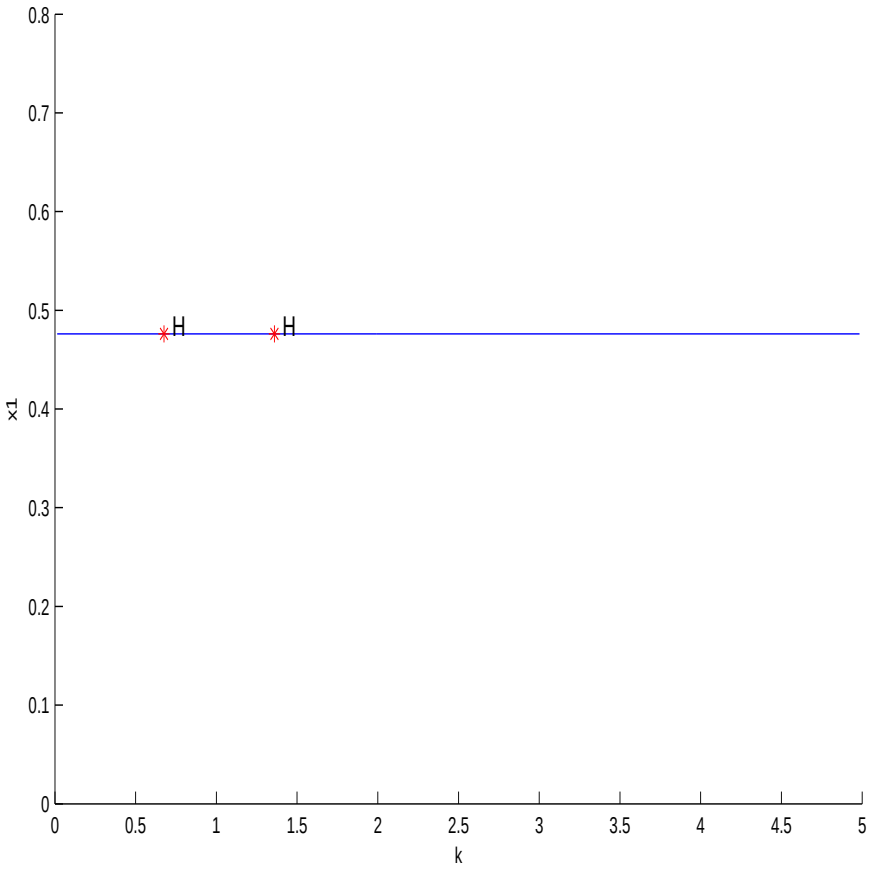

Figure 2.2: There exists Hopf bifurcation for the case where $A_1 > 0, A_2 > 0, H_1, H_2^-$. Between the two Hopf bifurcation point, periodic solutions exist. Parameters are $r_1 = 5, r_2 = 8, a_1 = 2, a_2 = 1.3, s_1 = 1.2, s_2 = 1, m_1 = 0.2, m_2 = 0.1, e_1 = 0.4, e_2 = 0.3, h_1 = 0.3, h_2 = 0.2$.

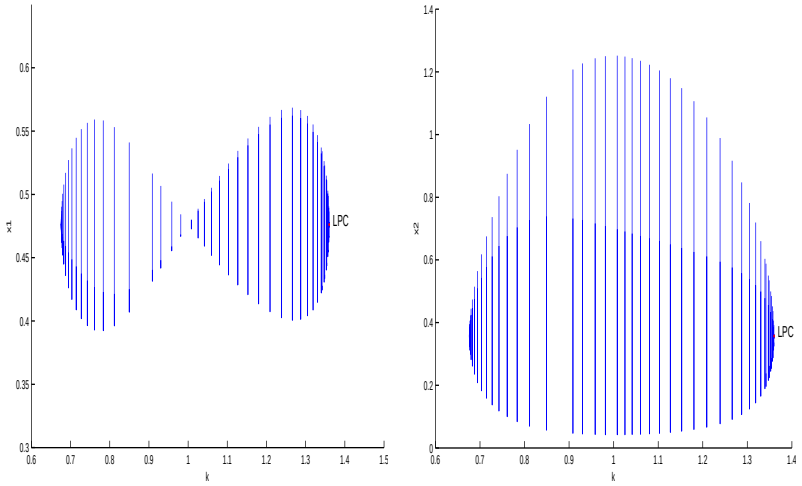

(a) Prey 1 (b) Prey 2

Figure 2.3: Prey populations in both patches oscillate periodically with varying k in the interval of Hopf bifurcation, when $A_1 > 0, A_2 > 0, H_1, H_2^-$. Parameters are $r_1 = 5, r_2 = 8, a_1 = 2, a_2 = 1.3, s_1 = 1.2, s_2 = 1, m_1 = 0.2, m_2 = 0.1, e_1 = 0.4, e_2 = 0.3, h_1 = 0.3, h_2 = 0.2$.

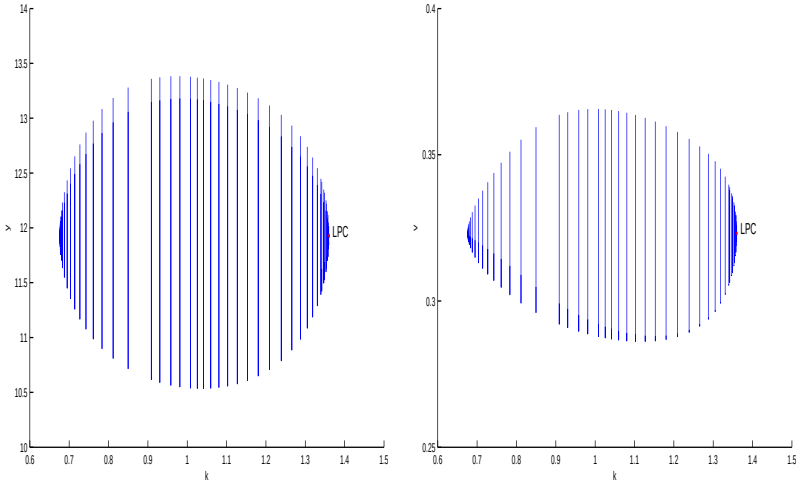

(a) Predator (b) Strategy

Figure 2.4: Predators population and strategy oscillate periodically with varying k in the interval of Hopf bifurcation, when $A_1 > 0, A_2 > 0, H_1, H_2^-$. Parameters are $r_1 = 5, r_2 = 8, a_1 = 2, a_2 = 1.3, s_1 = 1.2, s_2 = 1, m_1 = 0.2, m_2 = 0.1, e_1 = 0.4, e_2 = 0.3, h_1 = 0.3, h_2 = 0.2$.

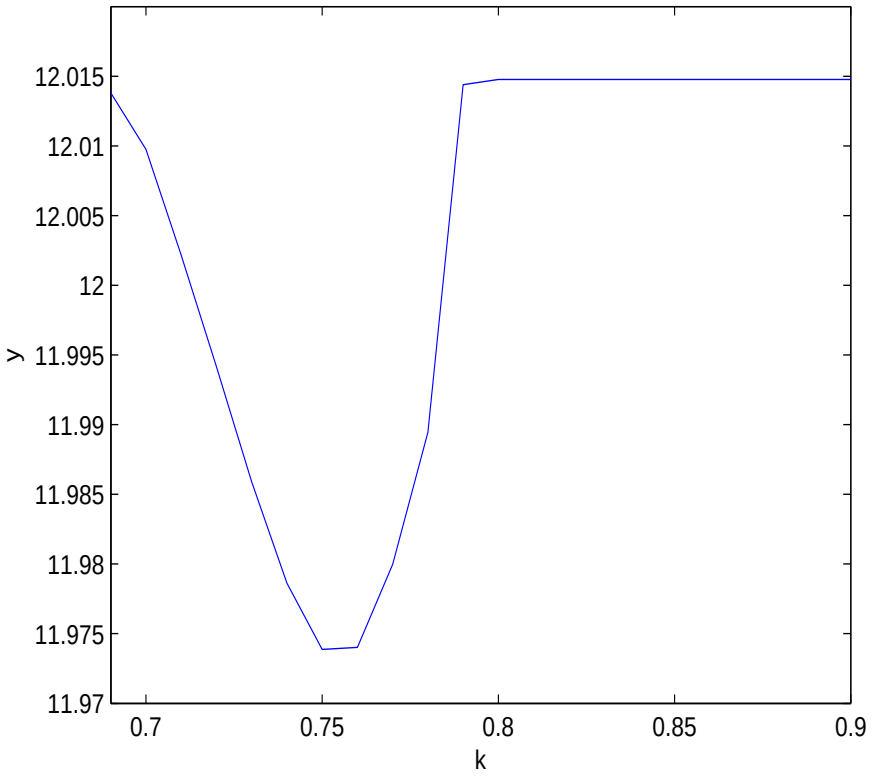

Figure 2.5: The average biomass of predators has a complicated relationship with the strength of adaptation of predators in the interval of Hopf bifurcation, when $A_1 > 0, A_2 > 0, H_1, H_2^-$. Parameters are $r_1 = 5, r_2 = 8, a_1 = 2, a_2 = 1.3, s_1 = 1.2, s_2 = 1, m_1 = 0.2, m_2 = 0.1, e_1 = 0.4, e_2 = 0.3, h_1 = 0.3, h_2 = 0.2$.

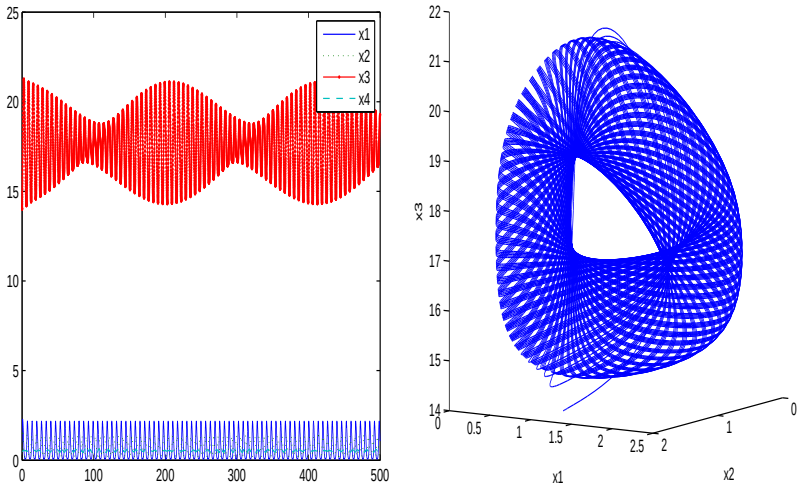

(a) Modulated oscillation (b) Torus surface

Figure 2.6: A torus surface exists when $A_1 > 0, A_2 > 0, H_1^-, H_2^-$, which indicates a torus bifurcation. Parameters are $r_1 = 9, r_2 = 8, a_1 = 2, a_2 = 2, s_1 = 1, s_2 = 1, m_1 = 0.2, m_2 = 0.2, e_1 = 0.4, e_2 = 0.4, h_1 = 0.4, h_2 = 0.4, w = 1.0$.

Bibliography

[1] P. A. Abrams, R. Cressman, and V. Křivan. The role of behavioral dynamics in determining the patch distributions of interacting species. *The American Naturalist*, 169:505–518, 2007.

[2] D. M. Buss and H. Greiling. Adaptive individual differences. *Journal of Personality*, 67: 209–243, 1999.

[3] R. S. Cantrell, C. Cosner, D. L. Deangelis, and V. Padron. The ideal free distribution as an evolutionarily stable strategy. *Journal of Biological Dynamics*, 1:249–271, 2007.

[4] R. S. Cantrell, C. Cosner, and Y. Lou. Evolutionary stability of ideal free dispersal strategies in patchy environments. *Journal of Mathematical Biology*, 65:943–965, 2012.

[5] M. E. Clark, T. G. Wolcott, D. L. Wolcott, and A. H. Hines. Foraging behavior of an estuarine predator, the blue crab Callinectes sapidus in a patchy environment. *Ecography*, 23:21–31, 2000.

[6] S. Creel and N. M. Creel. *The African wild dog: behavior, ecology, and conservation*. Princeton University Press, 2002.

[7] R. Cressman and V. Křivan. Migration dynamics for the ideal free distribution. *The American Naturalist*, 168:384–397, 2006.

[8] R. Cressman and V. Křivan. Two-patch population models with adaptive dispersal: the effects of varying dispersal speeds. *Journal of Mathematical Biology*, 67:329–358, 2013.

[9] R. Cressman, V. Křivan, and J. Garay. Ideal free distributions, evolutionary games, and population dynamics in multiple-species environments. *The American Naturalist*, 164: 473–489, 2004.

[10] S. D. Fretwell and J. S. Calver. On territorial behavior and other factors influencing habitat distribution in birds. *Acta Biotheoretica*, 19:37–44, 1969.

[11] J. K. Hale and P. Waltman. Persistence in infinite-dimensional systems. *SIAM Journal on Mathematical Analysis*, 20:388–395, 1989.

[12] J. Hofbauer and K. Sigmund. *Evolutionary games and population dynamics*. Cambridge University Press, 1998.

[13] C. S. Holling. The functional response of predators to prey density and its role in mimicry and population regulation. *Memoirs of the Entomological Society of Canada*, 97:5–60, 1965.

[14] V. Křivan. The lotka-volterra predator-prey model with foraging–predation risk trade-offs. *The American Naturalist*, 170:771–782, 2007.

[15] V. Křivan and R. Cressman. On evolutionary stability in predator-prey models with fast behavioral dynamics. *Evolutionary Ecology Research*, 11:227–251, 2009.

[16] Y. Kuang and Y. Takeuchi. Predator-prey dynamics in models of prey dispersal in two-patch environments. *Mathematical Biosciences*, 120:77–98, 1994.

[17] S. A. Levin. Dispersion and population interactions. *The American Naturalist*, 108: 207–228, 1974.

[18] J. D. Murray. *Mathematical Biology, I, An Introduction*. Springer, 2002.

[19] I. Scharf, E. Nulman, O. Ovadia, and A. Bouskila. Efficiency evaluation of two competing foraging modes under different conditions. *The American Naturalist*, 168:350–357, 2006.

[20] R. D. Seitz, R. N. Lipcius, A. H. Hines, and D. B. Eggleston. Density-dependent predation, habitat variation, and the persistence of marine bivalve prey. *Ecology*, 82:2435–2451, 2001.

[21] J. E. R. Staddon. *Adaptive behavior and learning*. CUP Archive, 1983.

[22] C. Starr, R. Taggart, C. Evers, and L. Starr. *Biology: The Unity and Diversity of Life*. Nelson Education, 2015.

[23] H. R. Thieme. Persistence under relaxed point-dissipativity (with application to an endemic model). *SIAM Journal on Mathematical Analysis*, 24:407–435, 1993.

[24] W. Wang and Y. Takeuchi. Adaptation of prey and predators between patches. *Journal of Theoretical Biology*, 258:603–613, 2009.

[25] D. K. Wasko and M. Sasa. Food resources influence spatial ecology, habitat selection, and foraging behavior in an ambush-hunting snake (Viperidae: Bothrops asper): an experimental study. *Zoology*, 115:179–187, 2012.

Chapter 3

Modelling the fear effect in predator-prey interactions

3.1 Introduction

Studying the mechanisms driving predator-prey systems is a central topic in ecology and evolutionary biology. The long-standing view, is that predators can impact prey populations only through direct killing. Predation events are relatively easy to observe in the field and by removing individuals from the population, it stands to reason that direct killing would be involved ([5, 7, 26, 27]). An emerging view, however, is that the mere presence of a predator may alter the behaviour and physiology of prey to such an extent that it can exert an effect on prey populations even more powerful than direct predation ([5, 7, 26, 27]).

All animals in every taxa respond to perceived predation risk and show a variety of anti-predator responses including changes in habitat usage, foraging behaviours, vigilance and physiological changes ([7, 32, 34, 35, 43]). For example, when prey assess predation risk, they may choose to abandon the original high-risk habitat and relocate to low-risk habitats, which can carry an energetic cost especially if the low-risk habitats are of suboptimal quality ([7]). Similarly, scared prey are well-known to forage less, which could reduce the birth rate and survival through mechanisms like starvation ([5, 7]). High levels of acute predation risk can cause prey to leave habitats or foraging sites temporarily, returning only when the acute risk has passed and the prey are relatively safe ([7]). Moreover, fear may affect the physiological condition of juvenile prey and leave harmful impacts on their survival as adults ([4, 5]). Birds, for example, respond to the sounds of predators with anti-predator defences ([5, 7]), and when nesting, will flee from their nests at the first sign of danger ([7]). Such an anti-predator behaviour may be beneficial in increasing the probability of survival, but can carry some long-term costs

on reproduction that may affect population numbers ([7]).

Although some theoretical ecologists and evolutionary biologists have realized that the interactions between prey and predators should not be simply described by direct predation alone and that the cost of fear should be considered ([32, 34, 35]), no mathematical models have been proposed to quantitatively investigate whether or the extent to which fear can affect prey populations. This is mainly due to lack of direct experimental evidence demonstrating that fear can affect the populations of terrestrial vertebrates.

Recently, however, Zanette *et al.* ([48]) conducted a manipulation on song sparrows during an entire breeding season to determine whether perceived predation risk could affect reproduction even in the absence of direct killing. The authors manipulated predation risk by broadcasting predator sounds to some populations of song sparrows while others heard non-predator sounds. At the same time, all nests in the manipulation were protected from direct killing ensuring that any effects on reproduction could only be ascribed to fear. Zanette *et al.* ([48]) found that the fear of predators alone led to a 40% reduction in the number of offspring of the song sparrows parents could produce. The reason this effect was so dramatic, is because predation risk had effects on both the birth rate and survival of offspring because song sparrow females laid fewer eggs (the birth rate), fewer of those eggs hatched (survival) and more nestlings died in the nest (survival). Moreover, the authors showed that a variety of anti-predator responses led to these effects on demography. For example, scared parents fed their nestlings less, their nestlings were lighter and much more likely to die. Correlational evidence in birds ([11, 12, 13, 15, 18, 19, 23, 31]), elk ([6]), snowshoe hares ([39]) and dugongs ([44]) also provide some evidence that fear can affect populations.

Predator-prey models have been studied extensively, but no models to date have incorporated the plastic anti-predator behaviour of prey in addition to the behaviour of the predator. Following the classic Lotka-Volterra model, Holling ([17]) proposed the well-known Holling type II functional response of predators. The population dynamics of predator-prey systems with the Holling type II functional response have been studied by many scholars and the existence of a unique stable limit cycle for such a model has been confirmed ([24, 25, 42]). There have been many other predator-prey systems that have modelled more complicated functional responses. For example, within the prey dependent functional responses, [20, 28, 38] considered some monotone response functions and [14, 45, 46, 47] studied some non-monotone response functions. In addition to functional responses dependent on prey numbers only, there are also studies considering functional responses dependent on *both prey and predators* numbers, among which are the Beddington-DeAngelis functional responses ([1, 2, 8, 21, 22]) and ratio dependent functional response ([40, 41]).

No matter how sophisticated functional responses may be when incorporated into predator-

prey models, they still only reflect what can happen regarding direct killing. In this paper, we propose and analyze a predator-prey model incorporating the cost of fear (indirect effects) to explore the impact that fear can have on population dynamics in predator-prey systems. In Section 2, we formulate the model incorporating the cost of fear generated by anti-predator behaviors. In Section 3, we analyze the model for the case when the functional response is a linear function of the prey population. In Section 4, we consider the Holling type II functional response for the model, and present some results on the stability of equilibria, existence of Hopf bifurcation and direction of Hopf bifurcation. Our mathematical results show that while incorporating fear (i.e. predation risk) effects into predator-prey models do not affect the structure of the equilibria, it may change the stability of the equilibria. Moreover, the existence of Hopf bifurcation and its direction in our model will be different from the classic model ignoring fear effects. In Section 5, we provide some numerical simulation results which reveal some potential roles that the fear effect may play in predator-prey interactions. We end the paper by Section 6, consisting of some conclusions and we also, discuss the biological implications of our mathematical results and possible future projects.

3.2 Model Formulation

Assume that the prey obey a logistic growth in the absence of predation and the cost of fear. The logistic growth of prey can be separated into three parts: a birth rate, a natural death rate and a density dependent death rate due to intra-species competition. This leads to the following ODE

$$\frac{du}{dt} = r_0 u - d\,u - a\,u^2, \tag{3.1}$$

where u represents the population of the prey, r_0 is the birth rate of prey, d is the natural death rate of prey, a represents the death rate due to intra-species competition.

Let v represent the population of the predator. Since fields experiments show that the fear effect will reduce the production, we modify (3.1) by multiplying the production term by a factor $f(k, v)$ which accounts for the cost of anti-predator defence due to fear, leading to

$$\frac{du}{dt} = [f(k, v)\, r_0]\, u - d\,u - a\,u^2. \tag{3.2}$$

Here, the parameter k reflects the level of fear which drives anti-predator behaviours of the prey. By the biological meanings of k, v and $f(k, v)$, it is reasonable to assume that

$$\begin{cases} f(0, v) = 1, \quad f(k, 0) = 1, \quad \lim\limits_{k\to\infty} f(k, v) = 0, \quad \lim\limits_{v\to\infty} f(k, v) = 0, \\ \dfrac{\partial f(k, v)}{\partial k} < 0, \quad \dfrac{\partial f(k, v)}{\partial v} < 0. \end{cases} \tag{3.3}$$

Although there are arguments and beliefs (e.g., [4]) that fear may lead to lower survival rate of adults due to physiological impacts when they are young, by far there are no direct experimental evidences showing such an impact. As such, we do not incorporate this factor into modelling in this work, meaning that we regard d and a as constants.

Next, we incorporate a predation term $g(u)v$ into (3.2) to obtain the following general prey-predator model with cost of fear reflected:

$$\begin{cases} \dfrac{du}{dt} = u\, r_0\, f(k,v) - d\, u - a\, u^2 - g(u)\, v, \\ \dfrac{dv}{dt} = v\,(-m + c\, g(u)). \end{cases} \tag{3.4}$$

Here $g : \mathbb{R}_+ \to \mathbb{R}_+$ is the functional response of predators, v represents the density of predators, c is the conversion rate of prey's biomass to predators' biomass, m is the death rate of predators. Typically, $g(u)$ is of the form $up(u)$ with $p : \mathbb{R}_+ \to \mathbb{R}_+$. When $p(u) = p$ is a constant, $g(u)$ gives a linear functional response, and when $p(u) = p/(1 + qu)$, $g(u)$ represents the Holling type II functional response.

By the standard basic theory of ODE systems, one can easily show that for any initial value $(u_0, v_0) \in \mathbb{R}^2_+$, (3.4) has a unique solution, and with the form $g(u) = p(u)u$, it is easily seen that the solution remains positive and bounded, and hence it exists globally.

From the first equation in (3.4), we have $u'(t) \le (r_0 - d)u$ which establishes a linear comparison equation from the above for the first equation. By a comparison argument, we conclude that if $r_0 < d$, then $u(t) \to 0$ as $t \to \infty$, and applying the theory of asymptotically autonomous systems (see, e.g. [3]) to the second equation in (3.4), we also obtain $v(t) \to 0$ as $t \to \infty$. This means that when $r_0 < d$, both prey and predator species will go to extinction, regardless of the fear effect and particular predation mechanism. Therefore, we only need to consider the case when $r_0 > d$ which will be assumed in the rest of the paper.

3.3 Model with the linear functional response

For the case of linear functional response $g(u) = pu$, we consider general function $f(k, v)$ that satisfies conditions (3.3), reducing the model (3.4) to

$$\begin{cases} \dfrac{du}{dt} = r_0\, u\, f(k,v) - d\, u - a\, u^2 - p\, u\, v, \\ \dfrac{dv}{dt} = c\, p\, u\, v - m\, v. \end{cases} \tag{3.5}$$

In addition to the trivial equilibrium $E_0 = (0, 0)$, this system also has a boundary equilibrium $E_1 = ((r_0 - d)/a, 0)$ under the condition $r_0 > d$. In addition, there exists a unique positive

(co-existence) equilibrium for system (3.5) given by $E_2 = (\overline{u}, \overline{v})$ if

$$r_0 > d + \frac{am}{cp} \tag{3.6}$$

holds, where $\overline{u} = m/(c\,p)$ and $\overline{v}$ satisfies

$$r_0\, f(k, \overline{v}) - d - a\,\overline{u} - p\,\overline{v} = 0. \tag{3.7}$$

If (3.6) is reversed, (3.7) has no positive solution and hence system (3.5) has no positive (coexistence) equilibrium.

The following theorem describes the local stability of all three equilibria.

Theorem 3.3.1 *The following statements hold:*

(i) The semi-trivial equilibrium E_1 is locally asymptotically stable if (3.6) *is reversed and is unstable if* (3.6) *holds.*

(ii) The positive equilibrium E_2, as long as it exists (i.e., when (3.6) *is satisfied), is locally asymptotically stable.*

Proof We only show the proof of the local stability of E_2 because the proof for the local stability of E_1 is similar. The Jacobian matrix of system (3.5) at E_2 is

$$J = \begin{bmatrix} J_{11} & J_{12} \\ J_{21} & J_{22} \end{bmatrix}, \tag{3.8}$$

where

$$\begin{aligned} &J_{11} = r_0\, f(k, \overline{v}) - d - 2\,a\,\overline{u} - p\,\overline{v} = -a\bar{u} < 0, \quad J_{12} = r_0\,\overline{u}\,\frac{\partial f(k, v)}{\partial v}\Big|_{v=\overline{v}} - p\,\overline{u} < 0, \\ &J_{21} = c\,p\,\overline{v} > 0, \quad J_{22} = c\,p\,\overline{u} - m = 0. \end{aligned} \tag{3.9}$$

Obviously, $\mathrm{tr}(J) = -a\bar{u} < 0$, and by (3.3), $\det(J) = -J_{12}J_{21} > 0$. Thus, E_2 is locally asymptotically stable.

The above theorem shows that, as the parameter r_0 increases, the model experiences two bifurcations of equilibrium: when $r_0 \in (0, d)$, E_0 is the only equilibrium which is globally asymptotically stable; when r_0 passes d to enter the interval $(d, d + am/cp)$, E_0 loses its stability to a new equilibrium E_1; and when r_0 further passes $d + am/cp$, E_1 loses its stability to another new equilibrium E_2. The next theorem further confirms that the stability claimed in Theorem 3.3.1 is actually global for both E_1 and E_2.

Theorem 3.3.2 *The boundary equilibrium E_1 is globally asymptotically stable if $r_0 \in (d, d + am/cp)$, and the unique positive equilibrium E_2 is globally asymptotically stable if $r_0 > d + am/cp$.*

Proof Assume $r_0 > d + am/cp$ and let $P(u, v),\ Q(u, v)$ represent the two functions on the right hand side of system (3.5). Choose the Dulac function $B(u, v) = 1/(u\,v)$. After calculations, we obtain

$$D = \frac{\partial(P\,B)}{\partial u} + \frac{\partial(Q\,B)}{\partial v} = -\frac{a}{v} < 0 \tag{3.10}$$

for $(u, v) \in (0, \infty) \times (0, \infty)$. Therefore, by the Dulac-Bendixson theorem (Theorem 2, p265, [33]), there is no periodic orbit in $(0, \infty) \times (0, \infty)$ for system (3.5). Moreover, E_2 is the unique positive equilibrium in $(0, \infty) \times (0, \infty)$ if (3.6) holds; hence, every positive solution will tend to E_2. This together with the local stability confirmed in Theorem 3.3.1 implies that E_2 is indeed globally asymptotically stable, if (3.6) holds.

When $r_0 \in (d, d + am/cp)$, there is no other equilibrium other than E_0 and E_1 in $\mathbb{R}^2_+$, and hence, there can not be any periodic orbit in $\mathbb{R}^2_+$, implying that every positive solution will either approach E_0 or E_1. It can be easily seen that E_0 is repelling (under $r_0 > d$), and thus, every positive solution actually approaches E_1. This together with Theorem 3.3.1 again implies that E_1 is indeed globally asymptotically stable if $r_0 \in (d, d + am/cp)$.

3.4 Model with the Holling Type II functional response

In this section, we consider the Holling type II functional response $g(u) = pu/(1 + qu)$, and in the mean time, for convenience of analysis, we adopt the following particular form for the fear effect term $f(k, v)$:

$$f(k, v) = \frac{1}{1 + k\,v}. \tag{3.11}$$

With $g(u)$ and $f(k, v)$ specified as above, the model (3.4) becomes

$$\begin{aligned} \frac{du}{dt} &= \frac{r_0\,u}{1 + k\,v} - d\,u - a\,u^2 - \frac{p\,u\,v}{1 + q\,u}, \\ \frac{dv}{dt} &= \frac{c\,p\,u\,v}{1 + q\,u} - m\,v. \end{aligned} \tag{3.12}$$

3.4.1 Existence of equilibria and dynamical behaviours in boundary

In addition to the trivial equilibrium $E_0 = (0, 0)$, system (3.12) has one semi-trivial equilibrium $E_1 = ((r_0 - d)/a, 0)$ if $r_0 > d$, which is assumed in the rest of the paper. We address the local stability of E_1 in the following theorem.

Theorem 3.4.1 *Semi-trivial equilibrium E_1 is locally asymptotically stable if*

$$(r_0 - d)(c\,p - m\,q) < a\,m \tag{3.13}$$

is satisfied and is unstable if

$$(r_0 - d)(c\,p - m\,q) > a\,m \tag{3.14}$$

holds.

The proof for Theorem 3.4.1 is similar to the proof in Theorem 3.3.1 and is thus omitted. Note that E_0 is unstable, E_1 is locally asymptotically stable and there is no other equilibrium provided that

$$c\,p \leq m\,q. \tag{3.15}$$

This implies that E_1 is indeed globally asymptotically stable if (3.15) holds. Thus, we have the following theorem.

Theorem 3.4.2 *The boundary equilibrium E_1 is globally asymptotically stable if* (3.15) *is satisfied.*

By Theorem 3.4.2, the dynamical behaviour of system (3.12) is clear when (3.15) holds. In the sequel, we only need to study the case when

$$c\,p > m\,q. \tag{3.16}$$

In order to simplify the analysis, we make the following transformations for system (3.12) by

$$\begin{aligned} dt &= \frac{(1 + q\,u)(1 + k\,v)}{m}\,d\bar{t}, \\ \bar{u} &= \frac{c\,p - m\,q}{m}\,u, \bar{v} = k\,v. \end{aligned} \tag{3.17}$$

Dropping the bars system (3.12) is transformed to the following equivalent system

$$\begin{aligned} \frac{du}{dt} &= u\left(a_1 + a_2\,u - a_3\,v - a_4\,u\,v - a_5\,u^2 - a_6\,v^2 - a_5\,u^2\,v\right), \\ \frac{dv}{dt} &= v\,(u - 1)(1 + v), \end{aligned} \tag{3.18}$$

where

$$\begin{aligned} a_1 &= \frac{r_0 - d}{m},\ a_2 = \frac{(r_0 - d)\,q - a}{c\,p - m\,q},\ a_3 = \frac{d\,k + p}{m\,k}, \\ a_4 &= \frac{d\,q + a}{c\,p - m\,q},\ a_5 = \frac{a\,m\,q}{(c\,p - m\,q)^2},\ a_6 = \frac{p}{m\,k}. \end{aligned} \tag{3.19}$$

By (3.16), we have $a_i > 0$ where $i = 1, 3, 4, 5, 6$. Thus, there exists a positive equilibrium $E_2 = (1, \overline{v}_2)$ for system (3.18) if

$$a_1 + a_2 > a_5 \ \ (\Longleftrightarrow a_5 - a_1 < a_2), \tag{3.20}$$

where $\overline{v}_2$

$$a_6\,\overline{v}_2^2 + (a_3 + a_4 + a_5)\,\overline{v}_2 - (a_1 + a_2 - a_5) = 0. \tag{3.21}$$

By (3.21), we actually obtain

$$\overline{v}_2 = \frac{-(a_3 + a_4 + a_5) + \sqrt{(a_3 + a_4 + a_5)^2 + 4\,a_6(a_1 + a_2 - a_5)}}{2\,a_6}. \tag{3.22}$$

The local stability of E_2 is addressed in the following theorem.

Theorem 3.4.3 *The positive equilibrium E_2 is locally asymptotically stable if*

$$a_5 - a_1 < a_2 \le 2\,a_5, \tag{3.23}$$

or

$$a_2 > 2\,a_5 \ \ \textit{and} \ \ \overline{v}_2 > \frac{a_2 - 2\,a_5}{a_4 + 2\,a_5}; \tag{3.24}$$

it is unstable if

$$a_2 > 2\,a_5 \ \ \textit{and} \ \ \overline{v}_2 < \frac{a_2 - 2\,a_5}{a_4 + 2\,a_5}. \tag{3.25}$$

Proof Jacobian matrix of system (3.18) at $E_2(1, \overline{v}_2)$ is

$$J^* = \begin{bmatrix} J_{11} & J_{12} \\ \\ J_{21} & J_{22} \end{bmatrix}, \tag{3.26}$$

where

$$\begin{aligned} &J_{11} = a_1 + 2\,a_2 - a_3\,\overline{v}_2 - 2\,a_4\,\overline{v}_2 - 3\,a_5 - a_6\,\overline{v}_2^2 - 3\,a_5\,\overline{v}_2, \\ &J_{12} = -a_3 - a_4 - 2\,a_6\,\overline{v}_2 - a_5 < 0,\ J_{21} = \overline{v}_2\,(1 + \overline{v}_2) > 0,\ J_{22} = 0. \end{aligned} \tag{3.27}$$

Obviously, $\det(J) = -J_{12}J_{21} > 0$ by (3.20) and then the stability of E_2 is determined by $\mathrm{tr}(J^*) = J_{11}$. Direct calculations show that $\mathrm{tr}(J^*) < 0$ is equivalent to

$$(a_2 - 2\,a_5) < (a_4 + 2\,a_5)\,\overline{v}_2. \tag{3.28}$$

Because $\overline{v}_2$, a_4, a_5 are all positive, (3.28) is satisfied if (3.23) holds. Furthermore, if $a_2 > 2\,a_5$, the local stability of E_2 further requires $\overline{v}_2 > (a_2 - 2\,a_5)/(a_4 + 2\,a_5)$, as presented in (3.24). Equilibrium E_2 loses stability when (3.25) holds.

Note that (3.23) is equivalent to

$$\begin{cases} r_0 > \dfrac{a\,m}{c\,p - m\,q} + d, \\ r_0 \leq d + \dfrac{a\,(c\,p + m\,q)}{q\,(c\,p - m\,q)}, \end{cases} \tag{3.29}$$

and (3.24) is equivalent to

$$\begin{cases} r_0 > d + \dfrac{a\,(c\,p + m\,q)}{q\,(c\,p - m\,q)}, \\ k > \dfrac{q\,(c\,p - m\,q)^2\,((r_0 - d)\,q\,(c\,p - m\,q) - a\,(c\,p + m\,q))}{c^2\,p\,a\;(q\,d(c\,p - m\,q) + a\,(c\,p + m\,q))}. \end{cases} \tag{3.30}$$

Then, by Theorem 3.4.3, we obtain that prey and predators will tend to a steady state if (3.29) holds. In this case, the stability of E_2 is not affected by the cost of fear, which is similar to the results we obtained from the previous Section 3. In other words, the stability of the co-existence equilibrium will not change if the birth rate of prey is not large enough to support oscillations no matter how sensitive prey are to predation risks. However, in contrast to the results of model with linear functional response (3.5), for the model with the Holling type II functional response (3.12), conditions in (3.30) imply that the stability of E_2 is affected by the level of anti-predator defence. Conditions in (3.30) indicate that when the birth rate of prey is large enough, prey and predators still tend to a steady state if prey are sensitive enough to perceive potential attacking by predators and show anti-predation behaviours accordingly but lose stability if not. It is well-known that the classic predator-prey model without the cost of fear but with the Holling type II functional response admits the occurrence of Hopf bifurcation when the carrying capacity of prey is large enough. The phenomenon 'paradox of enrichment' ([16, 29, 36, 37]) appears as a consequence. However, as discussed above, incorporating the cost of fear into predator-prey models can rule out such phenomenon 'paradox of enrichment' by choosing large enough k.

3.4.2 Global stability of positive equilibrium

In the above section, we have shown that E_2 is locally asymptotically stable if (3.23) or (3.24) holds. The following theorem confirms that E_2 is globally symptomatically stable under (3.23) and another condition.

Theorem 3.4.4 *The positive equilibrium E_2 is globally asymptotically stable if*

$$a_5 - a_1 < a_2 \leq 2\,a_5 \;\; \textit{and} \;\; 1 \leq a_2 + a_4. \tag{3.31}$$

Proof Denote the right-hand sides of system (3.18) by $P(u,v)$, $Q(u,v)$ respectively. Take the following function as a Dulac function: $B(u,v) = u^{-1}\,v^{\beta}$ where β is to be specified later. Then the divergence of the vector is

$$\begin{aligned} D &= \frac{\partial(P(u,v)\,B(u,v))}{\partial u} + \frac{\partial(Q(u,v)\,B(u,v))}{\partial v} \\ &= u^{-1}\,v^{\beta}\,(f_1(u)\,v + f_2(u))\,, \end{aligned} \tag{3.32}$$

where

$$\begin{aligned} f_1(u,\beta) &= -2\,a_5\,u^2 + u\,(2+\beta-a_4) - (\beta+2), \\ f_2(u,\beta) &= -2\,a_5\,u^2 + u\,(a_2+\beta+1) - (\beta+1). \end{aligned} \tag{3.33}$$

By (3.33) and (3.31), we have

$$f_1(u,\beta) = f_2(u,\beta) + (u(1-a_4-a_2) - 1) \le f_2(u,\beta) \tag{3.34}$$

for u in $[0,\infty)$. Thus, we have $D \le 0$ for $(u,v) \in \mathbb{R}^2_+$ if

$$f_2(u,\beta) \le 0, \quad \text{for} \quad u \quad \in [0,\infty). \tag{3.35}$$

Therefore, it suffices to find a β such that (3.35) holds. Because $a_5 > 0$, (3.35) is satisfied if

$$\Delta(\beta) = (a_2+\beta+1)^2 - 8\,a_5\,(\beta+1) \le 0 \tag{3.36}$$

holds. For convenience, let $\beta + 1 = \overline{\beta}$. Then (3.36) becomes

$$\overline{\Delta}(\overline{\beta}) = \overline{\beta}^2 + 2\,(a_2 - 4\,a_5)\overline{\beta} + a_2^2 \le 0. \tag{3.37}$$

The existence of $\overline{\beta}$ satisfying (3.37) is implied by $\overline{\Delta}(4a_5 - a_2) \le 0$ which is equivalent to

$$a_5\,(2\,a_5 - a_2) \ge 0. \tag{3.38}$$

But this is ensured by the first inequality in (3.31). Thus, under (3.31), there exists β such that $D \le 0$ for $(u,v) \in \mathbb{R}^2_+$, and by the well-known Dulac-Bendixson theorem (Theorem 2, p265, [33]), E_2 is globally asymptotically stable.

3.4.3 Existence of limit cycles and Hopf bifurcation

In the above section, we have shown that there is no limit cycle if (3.31) holds. Now we show that there exists a limit cycle if (3.25) is satisfied.

Theorem 3.4.5 *There exists a limit cycle if* (3.25) *holds.*

Proof By (3.25) and Theorem 3.4.3, $E_2 = (1, \overline{v}_2)$ is unstable and $E_1 = (\overline{u}_1, 0)$ is a saddle point. Note that by (3.25) we have

$$\bar{u}_1 = \frac{a_2 + \sqrt{a_2^2 + 4a_1a_5}}{2a_5} > 1.$$

Let $L_1 = u - \overline{u}_1$. Then

$$\frac{du}{dt}\Big|_{L_1=0} = \overline{u}_1 \left(-a_3\, v - a_4\, \overline{u}_1\, v - a_6\, v^2 - a_5\, \overline{u}_1^2\, v\right) < 0, \tag{3.39}$$

since a_3, a_4, a_5, a_6 are all positive.

Next, let $L_2 = v - \lambda$ with $\lambda > 0$ to be specified later. By calculations, we obtain

$$\begin{aligned} \frac{dL_2}{dt}\Big|_{L_2=0} &= \frac{dv}{dt}\Big|_{v=\lambda} \\ &= \lambda\,(u-1)\,(1+\lambda) < 0, \quad \text{for } u \in (0,1). \end{aligned} \tag{3.40}$$

Moreover, let

$$L_3 = 2\,(\overline{u}_1 - 1)(v - \lambda) + \lambda\,(u-1). \tag{3.41}$$

Calculations give

$$\begin{aligned} \frac{dL_3}{dt}\Big|_{L_3=0} &= 2\,(\overline{u}_1 - 1)\frac{dv}{dt} + \lambda\,\frac{du}{dt} \\ &= 2\,(\overline{u}_1 - 1)v\,(u-1)\,(1+v) \\ &\quad + \lambda\, u\left(a_1 + a_2\, u - a_3\, v - a_4\, u\, v - a_5\, u^2 - a_6\, v^2 - a_5\, u^2\, v\right) \\ &\le -\frac{a_6\, u}{4}\,\lambda^3 + \lambda^2\left(2\,(\overline{u}_1 - 1)^2 - \frac{u}{2}\left(a_3 + a_4\, u + a_5\, u^2\right)\right) \\ &\quad + \lambda\left(\left(a_1 + a_2\, u - a_5\, u^2\right)u + 2\,(\overline{u}_1 - 1)^2\right). \end{aligned} \tag{3.42}$$

Because $a_6 > 0$ and $0 < u < \overline{u}_1$, it follows from (3.42) that $dL_3/dt < 0$ for sufficiently large $\lambda > 0$.

By Poincaré-Bendixson theorem (Theorem 6.12, [30]), there exists a limit cycle if (3.25) holds.

From the above analysis, we see that when (3.25) holds, the positive equilibrium E_2 becomes unstable and a limit cycle comes into existence. Such a limit cycle is a result of Hopf bifurcation. Indeed, from the proof of Theorem 3.4.3, we see that E_2 loses its stability and Hopf bifurcation occurs when $\mathrm{tr}(J^*) = J_{11}$ in (3.27) changes sign from negative to positive. Thus, $\mathrm{tr}(J^*) = J_{11} = 0$ gives the condition for Hopf bifurcation. Making use of (3.21), the formula for J_{11} in (3.27) can be simplified to

$$J_{11} = -(a_4 + 2a_5)\bar{v}_2 + a_2 - 2a_5. \tag{3.43}$$

Therefore, sign change of J_{11} from negative to positive is actually equivalent to switch from condition (3.24) to condition (3.25) implying that the limit cycle arises from a Hopf bifurcation.

Next, we deal with the direction of Hopf bifurcation, intending to understand the impact of the fear effect on the Hopf bifurcation and its direction in terms of the fear effect parameter k. We first have the following general theorem on the bifurcation direction.

Theorem 3.4.6 *Let*

$$\begin{aligned}\sigma := &-8\,a_5\,(a_2-2\,a_5)^2\,a_6^2-(a_4+2\,a_5)\,(-a_4+6\,a_4\,a_5-2\,a_5+8\,a_3\,a_5\\&+4\,a_5^2)\,(a_2-2\,a5)\,a_6-a_5\,(a_4+2\,a_5)^2\,(2\,a_3+a_4)\,(a_3+a_4+a_5).\end{aligned}\tag{3.44}$$

Then, the Hopf bifurcation is supercritical if $\sigma<0$ and it is subcritical if $\sigma>0$.

Proof Let $x=u-1, y=v-\overline{v}_2$. Then system (3.18) becomes

$$\begin{aligned}\frac{dx}{dt}&=J_{11}\,x+J_{12}\,y+f_1(x,y),\\\frac{dy}{dt}&=J_{21}\,x+J_{22}\,y+f_2(x,y),\end{aligned}\tag{3.45}$$

where $J_{11}, J_{12}, J_{21}, J_{22}$ are shown in (3.27) and $f_i(x,y)$ for $i=1,2$ represent higher order terms of x, y. We have seen in the above that the Hopf bifurcation occurs when $J_{11}=0$, or equivalently

$$\overline{v}_2=\frac{a_2-2\,a_5}{a_4+2\,a_5}.\tag{3.46}$$

Moreover, by the transformation

$$X=x, Y=J_{11}\,x+J_{12}\,y=J_{12}\,y,$$

system (3.45) is further transformed to

$$\begin{aligned}\frac{dX}{dt}&=Y+f_1\left(X,\frac{Y}{J_{12}}\right),\\\frac{dY}{dt}&=J_{12}\,J_{21}X+J_{12}\,f_2\left(X,\frac{Y}{J_{12}}\right).\end{aligned}\tag{3.47}$$

Let

$$\gamma=-J_{12}\,J_{21}>0, \overline{X}=-X, \overline{Y}=Y/\sqrt{\gamma}.$$

Then system (3.47) becomes

$$\begin{aligned}\frac{d\overline{X}}{dt}&=-\sqrt{\gamma}\,\overline{Y}-f_1\left(-\overline{X},\frac{\sqrt{\gamma}}{J_{12}}\,\overline{Y}\right),\\\frac{d\overline{Y}}{dt}&=\sqrt{\gamma}\,\overline{X}+\frac{J_{12}}{\sqrt{\gamma}}\,f_2\left(-\overline{X},\frac{\sqrt{\gamma}}{J_{12}}\,\overline{Y}\right).\end{aligned}\tag{3.48}$$

Now the Jacobian matrix of (3.48) at $(0,0)$ is of the Jordan Canonical form

$$\begin{bmatrix} 0 & -\sqrt{\gamma} \\ \sqrt{\gamma} & 0 \end{bmatrix}. \tag{3.49}$$

Define F_1 and F_2 by

$$F_1(\overline{X},\overline{Y}) = -f_1\left(-\overline{X}, \frac{\sqrt{\gamma}\,\overline{Y}}{J_{12}}\right), F_2(\overline{X},\overline{Y}) = \frac{J_{12}}{\sqrt{\gamma}}\, f_2\left(-\overline{X}, \frac{\sqrt{\gamma}\,\overline{Y}}{J_{12}}\right).$$

Then the direction of Hopf bifurcation is determined by the sign of the quantity

$$\begin{aligned} \sigma^* := {} & \frac{1}{16}\left(\frac{\partial^3 F_1}{\partial \overline{X}^3} + \frac{\partial^3 F_1}{\partial \overline{X}\partial \overline{Y}^2} + \frac{\partial^3 F_2}{\partial \overline{X}^2 \partial \overline{Y}} + \frac{\partial^3 F_2}{\partial \overline{Y}^3}\right) \\ & + \frac{1}{16\omega}\Big(\frac{\partial^2 F_1}{\partial \overline{X}\partial \overline{Y}}\left(\frac{\partial^2 F_1}{\partial \overline{X}^2} + \frac{\partial^2 F_1}{\partial \overline{Y}^2}\right) - \frac{\partial^2 F_2}{\partial \overline{X}\partial \overline{Y}}\left(\frac{\partial^2 F_2}{\partial \overline{X}^2} + \frac{\partial^2 F_2}{\partial \overline{Y}^2}\right) \\ & - \frac{\partial^2 F_1}{\partial \overline{X}^2}\frac{\partial^2 F_2}{\partial \overline{X}^2} + \frac{\partial^2 F_1}{\partial \overline{Y}^2}\frac{\partial^2 F_2}{\partial \overline{Y}^2}\Big), \end{aligned} \tag{3.50}$$

where $\omega = \sqrt{\gamma} = \sqrt{-J_{12}\,J_{21}}$. Using (3.46) and with the help of Maple software, σ^* is calculated and simplified to the formula given by σ in (3.44). By [33] (Theorem 1 on page 34), Hopf bifurcation is supercritical if $\sigma < 0$ and it is subcritical if $\sigma > 0$.

In order to analyze how the fear affects the direction of Hopf bifurcation, we may choose k as a bifurcation parameter. By (3.19), it is clear that only a_3 and a_6 depend on the parameter k. Letting $h = d/m$, we see that

$$a_3 = a_6 + h. \tag{3.51}$$

By $a_6 = \frac{p}{m}\frac{1}{k}$, we can equivalently take a_6 (instead of k) as the bifurcation parameter in the re-scaled model (3.18). By using (3.51), (3.46) can be simplified to

$$a_6 = \frac{(a_4 + 2\,a_5)(a_4\,a_5 + a_4\,a_1 + a_5\,a_2 + 2\,a_5\,a_1 + 2\,a_5\,h - h\,a_2)}{(a_2 + a_4)(a_2 - 2\,a_5)} =: a_6^* \tag{3.52}$$

an equation with the right hand side independent of k, giving the critical value of a_6 for Hopf bifurcation.

Regarding a_6 as a bifurcation parameter which is chosen at the critical value a_6^*, σ in (3.44) can be expressed, in terms of a_1 as a quadratic function, as

$$\sigma_0 = A_1\,a_1^2 + A_2\,a_1 + A_3, \tag{3.53}$$

the sign of which determines the direction of Hopf bifurcation. In (3.53), we have

$$\begin{aligned} A_1 &= -2\,a_5\,(a_4 + 2\,a_5)^2\,(2\,a_2 - 2\,a_5 + a_4)^2, \\ A_2 &= -(a_4 + 2\,a_5)\,(B_1\,h + B_2), A_3 = D_1\,h^2 + D_2\,h + D_3, \end{aligned} \tag{3.54}$$

where

$$
\begin{aligned}
B_1 &= -4\,a_5\,(-2\,a_5 + a_2)^2\,(2\,a_2 - 2\,a_5 + a_4),\\
B_2 &= (a_2 + a_4)(-2\,a_5\,a_2^2 + 6\,a_4\,a_5\,a_2^2 + 20\,a_2^2\,a_5^2 - a_2^2\,a_4 - 44\,a_5^3\,a_2 + 3\,a_2\,a_5\,a_4^2\\
&\quad + 4\,a_4\,a_2\,a_5 + 8\,a_5^2\,a_2 - 8\,a_4\,a_5^3 - 2\,a_4^2\,a_5^2 - 4\,a_4\,a_5^2 - 8\,a_5^3 + 24\,a_5^4),\\
D_1 &= -2\,a_5\,(-2\,a_5 + a_2)^4,\\
D_2 &= (a_2 - 2\,a_5)^2\,(a_2 + a_4)\,(-a_4\,a_2 + 3\,a_4\,a_2\,a_5 + 10\,a_5^2\,a_2 - 2\,a_5\,a_2\\
&\quad - 2\,a_4\,a_5^2 + 4\,a_5^2 - 12\,a_5^3 + 2\,a_4\,a_5),\\
D_3 &= -a_5\,(a_2 + a_4)^2\,(a_4^2\,a_2^2 + 12\,a_2^2\,a_5^2 - 2\,a_5\,a_2^2 + 7\,a_4\,a_5\,a_2^2 - a_2^2\,a_4 - 12\,a_2\,a_4\,a_5^2\\
&\quad - a_2\,a_5\,a_4^2 - 28\,a_5^3\,a_2 + 8\,a_5^2\,a_2 + 4\,a_4\,a_2\,a_5 - 8\,a_5^3 + 4\,a_4\,a_5^3 - 4\,a_4\,a_5^2 + 16\,a_5^4).
\end{aligned}
\tag{3.55}
$$

From (3.54), it is clear that $A_1 < 0$ because $a_5 > 0$. Let $\Delta = A_2^2 - 4\,A_1\,A_3$. Mathematical analysis show that A_2, A_3 and Δ can be positive or negative under different conditions. Numerical simulations show that all reasonable combinations of A_2, A_3, Δ are possible (see Figures 3.1, 3.2, 3.3).

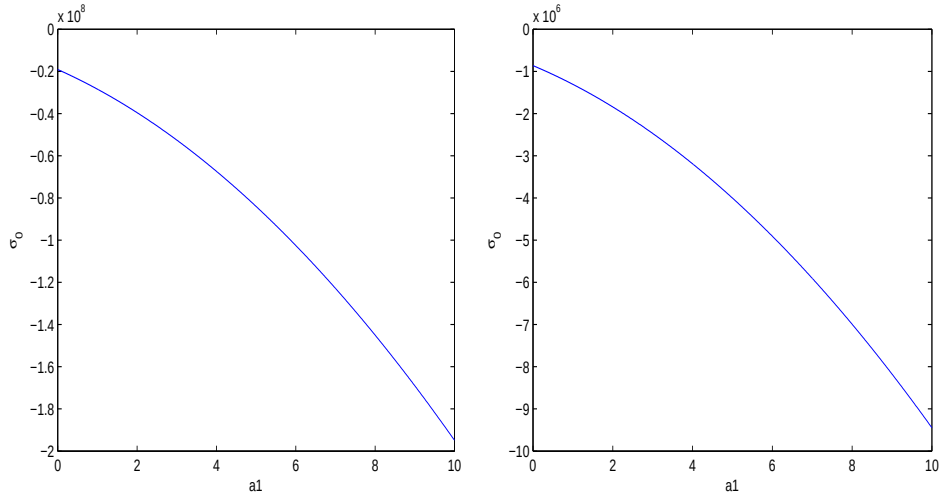

(a) case 1 (b) case 2

Figure 3.1: $A_1 < 0, A_2 < 0, A_3 < 0, \Delta > 0$ and $A_1 < 0, A_2 < 0, A_3 < 0, \Delta < 0$. Parameters are: $a_2 = 9.0639, a_4 = 8.8393, a_5 = 4.4733, h = 0.8866$ and $a_2 = 8.7964, a_4 = 3.82, a_5 = 1.4757, h = 1.3037$ respectively.

Notice that $A_1,\ A_2,\ A_3,\ \Delta$ are all expressions of $a_2,\ a_4,\ a_5,\ h$. Then, by taking different values of a_1, σ_0 can be positive or negative. Let

$$
a_1^+ = \frac{1}{2}\frac{(a_4 + \sqrt{a_4^2 - 4\,a_5\,h})(a_2 + a_4)}{a_5} - h, \tag{3.56}
$$

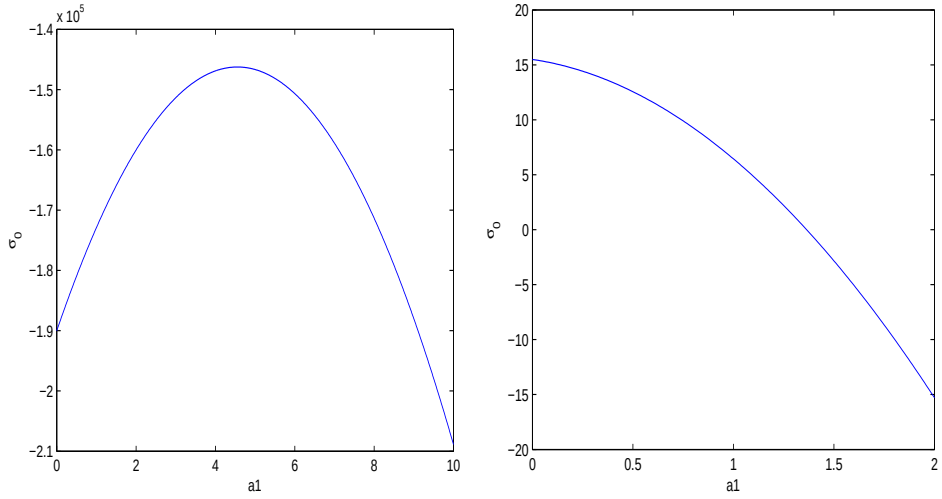

(a) case 3 (b) case 4

Figure 3.2: $A_1 < 0, A_2 > 0, A_3 < 0, \Delta < 0$ and $A_1 < 0, A_2 < 0, A_3 > 0, \Delta > 0$. Parameters are: $a_2 = 3.9703, a_4 = 7.6983, a_5 = 0.0715, h = 35.7226$ and $a_2 = 6.9741, a_4 = 0.1337, a_5 = 0.1194, h = 0.0032$ respectively.

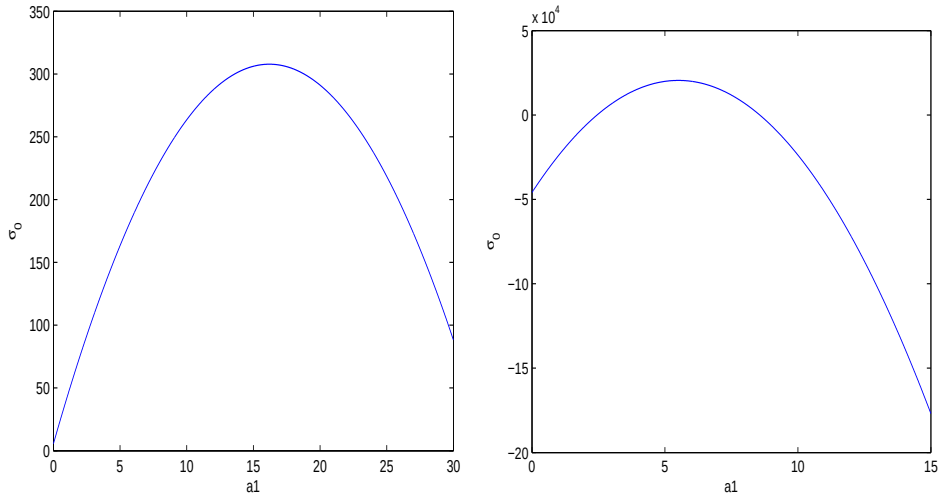

(a) case 5 (b) case 6

Figure 3.3: $A_1 < 0, A_2 > 0, A_3 > 0, \Delta > 0$ and $A_1 < 0, A_2 > 0, A_3 < 0, \Delta > 0$. Parameters are: $a_2 = 8.0115, a_4 = 0.2414, a_5 = 0.0256, h = 0.0131$ and $a_2 = 7.1134, a_4 = 7.3037, a_5 = 0.0436, h = 0.7421$ respectively.

Hopf Direction / Conditions / Cases	A_1	A_2	A_3	Δ	a_1	Hopf Direction
case 1	< 0	< 0	< 0	> 0	a_1^i	Supercritical
case 2	< 0	< 0	< 0	< 0	a_1^i	Supercritical
case 3	< 0	> 0	< 0	< 0	a_1^i	Supercritical
case 4-1	< 0	< 0	> 0	> 0	a_1^+	Supercritical
case 4-2	< 0	< 0	> 0	> 0	a_1^-	Subcritical
case 5-1	< 0	> 0	> 0	> 0	a_1^+	Supercritical
case 5-2	< 0	> 0	> 0	> 0	a_1^-	Subcritical
case 6-1	< 0	> 0	< 0	> 0	$a_1^i, r_2 < a_1^i < r_1$	Subcritical
case 6-2	< 0	> 0	< 0	> 0	$a_1^-, r_2 < a_1^- < r_1 < a_1^+$	Subcritical
case 6-3	< 0	> 0	< 0	> 0	$a_1^i, a_1^- < r_2 < r_1 < a_1^+$	Supercritical
case 6-4	< 0	> 0	< 0	> 0	$a_1^+, r_2 < a_1^- < r_1 < a_1^+$	Supercritical
case 6-5	< 0	> 0	< 0	> 0	$a_1^i, r_1 < a_1^i$	Supercritical

Table 3.1: Direction of Hopf bifurcation by taking a_6 as a bifurcation parameter.
Here $a_1^i, i = +, -$ are defined in (3.56), (3.57) and r_1, r_2 are larger and smaller roots of (3.53) respectively.

and

$$a_1^- = -\frac{1}{2}\frac{(-a_4 + \sqrt{a_4^2 - 4\,a_5\,h})(a_2 + a_4)}{a_5} - h. \tag{3.57}$$

By using a_1^+ and a_1^-, the possibilities of the direction of Hopf bifurcation are summarized in Table 3.1, which shows that the direction of Hopf bifurcation can be supercritical or subcritical depending on different combinations of a_1, a_2, a_4, a_5, h.

3.5 Numerical Simulations

In order to better explore the role that the cost of fear plays in our predator-prey model, we conducted a series of numeric simulations for model (3.12) with parameters in their original scales. In Figure 3.4, the solid curve represents the critical curve which determines the Hopf bifurcation without the fear effect (i.e. $k = 0$) by setting r_0 and q as free parameters. Figure 3.4 shows that the model incorporating the cost of fear requires larger r_0 to admit the existence of Hopf bifurcation, compared to the models without it. From a biological point of view, the cost of fear in prey requires higher compensation for the prey's birth rate to support periodic oscillations in prey and predator populations. As indicated in Figure 3.5(a), the population of the prey and

predator tend toward a globally stable steady state if r_0 and q are located in the region between the dashed curve and the solid curve in Figure 3.4. In this case, no matter how sensitive the prey is to predation risk, periodic oscillations can not occur. Figure 3.5(b) shows that the populations of prey and predator oscillate periodically due to supercritical Hopf bifurcation if the parameters are chosen in the region between the solid line and the dotted line in Figure 3.4. In Figure 3.4, by choosing $q = 0.6$, we can obtain a vertical line which intersects with the solid line and the dotted line when increasing the value of r_0. This indicates that increasing r_0 or equivalently increasing k may lead to change of directions of Hopf bifurcation from forward to backward. Figure 3.6 is a subcritical Hopf bifurcation diagram plotted using Matcont software ([9, 10]). As shown in Figure 3.6, taking k as a bifurcation parameter, there are two branches for the period of oscillation where the lower one corresponds to an unstable limit cycle and the upper one accounts for a stable limit cycle. Biologically, increasing the level of the fear effect in prey may induce a transition from the state where the populations of the prey and predator oscillate periodically to a bi-stability situation. When bi-stability happens, multiple limit cycles occur, as shown in Figure 3.7. In this scenario, the eventual pattern for prey and predators depend on their initial population sizes. Prey and predators tend to a steady state if initial populations are relatively small and stay inside the unstable limit cycle. The populations of prey and predators oscillate periodically if initial populations are relatively large and locate outside the unstable limit cycle. Figure 3.8 shows the relationship between $(k,\ q)$ and $(k,\ r_0)$ along the critical line determining Hopf bifurcation. Figure 3.8(b) indicates that when increasing the value of the prey's birth rate, lower levels of fear are required to obtain Hopf bifurcation no matter how the handling time of food by predators varies. Biologically, this implies that with a higher birth rate, the prey becomes less sensitive in perceiving predation risk.

Similarly, Figure 3.9 again shows that as fear effects become more extreme, it can induce a change in the direction of Hopf bifurcation, from supercritical to subcritical by holding p fixed at some point. The difference between Figure 3.4 and Figure 3.9 lies in that p needs to be large enough to support subcritical bifurcation whereas q has to be in an intermediate interval. Biologically, the attack rate by predators needs to be large enough to instill fear in prey; otherwise, fear will not affect dynamical behaviours of predator-prey systems and bi-stability can not happen. Figure 3.10(a) shows that prey are more willing to show anti-predator behaviours when the attack rate of predators increases and Figure 3.10(b) again confirms that the prey show weaker anti-predator behaviours when the prey's birth rate is greater, regardless of the change in the predators' attack rate.

Another interesting observation is that the natural death rate of predators m needs to be relatively small in order for the model to permit a subcritical Hopf bifurcation, as indicated in Figure 3.11. Biologically, a relatively high density of predators is required to evoke anti-predator

defenses in prey that carry costs large enough to affect prey populations. The cost of fear can not be observed if the population of predators drops too quickly whereby cues signifying predation risk are low, as will be the anti-predator responses of prey.

We also apply different functions in modelling the cost of fear when conducting simulations. Particularly, we test the following two functions

$$f(v) = e^{-k\,v}, \tag{3.58}$$

and

$$f(v) = \frac{1}{1 + k_1\,v + k_2\,v^2}. \tag{3.59}$$

Both functions (3.58) and (3.59) are decreasing functions with respect to v, but with different decreasing rates, compared with (3.11). Our simulation results for Hopf bifurcation and its direction are qualitatively unchanged with either (3.58) or (3.59), which implies that our results are applicable for general monotone decreasing function of v. Moreover, for (3.59), we also obtain a relationship between k_1 and k_2 along the Hopf bifurcation curve as demonstrated in Figure 3.13 indicating that k_2 is indeed linearly decreasing with k_1 on the Hopf bifurcation.

In the context of population control, if all solutions of (3.12) tend to a steady state eventually, then the fear effect will not affect the prey population over the long-term. However, under the same scenario, the predator's eventual population will decrease when k increases (see (3.22)). On the other hand, the populations of the prey and predator may oscillate periodically due to supercritical or subcritical Hopf bifurcation. In this case, Figure 3.14 indicates that the biomass of prey and predators decrease with increasing k along periodic solutions due to supercritical Hopf bifurcation. Biologically, this implies that anti-predator behaviours of prey may impact their long-term overall growth rate, as a cost of fear. Moreover, Figure 3.14 confirms the theoretical arguments that stronger levels of defence result in higher costs, which can decrease the prey's long-term population size. Simulations are also conducted for biomass of prey and predators along periodic solutions with varying k due to subcritical Hopf bifurcation. Results for such a case are consistent with the former one where Hopf bifurcation is supercritical and is thus omitted.

3.6 Conclusions and discussions

In this paper, we have studied a predator-prey model that has incorporated the effect that the fear of predators have on prey with either the linear functional response or the Holling type II functional response. For the case with the linear functional response, mathematical results show that the cost of fear does not change dynamical behaviours of the model and a unique positive equilibrium is globally asymptotically stable when it exists.

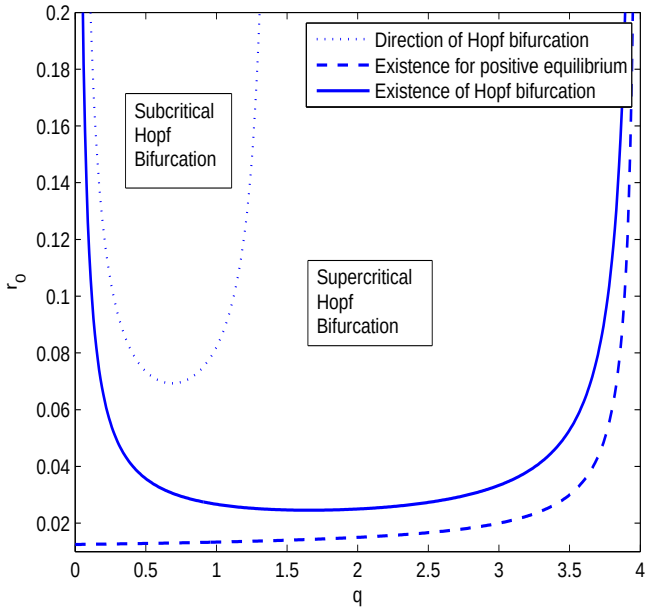

Figure 3.4: Available region of Hopf bifurcation on r_0, q plane. Parameters are: $a = 0.01, p = 0.5, c = 0.4, m = 0.05, d = 0.01$.

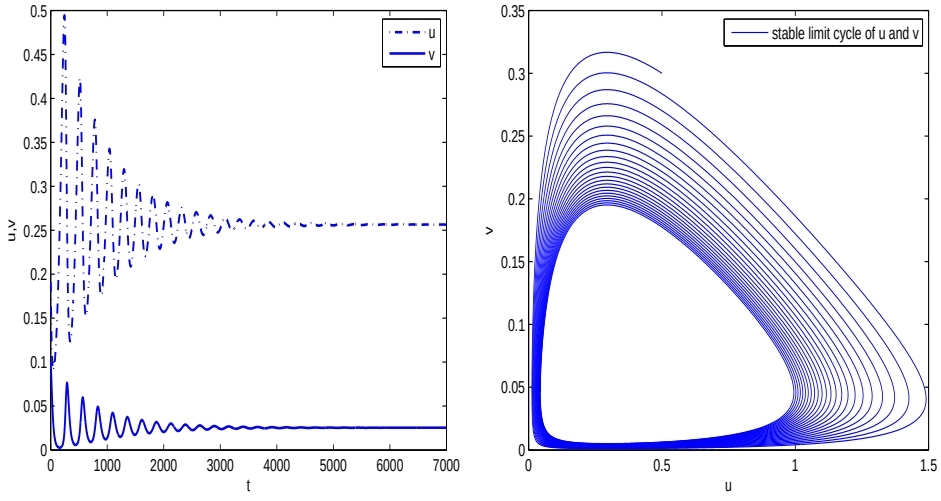

(a) Global stable positive equilibrium (b) Stable limit cycle

Figure 3.5: Different patterns for prey and predators. Parameters for 3.5(a) are: $r_0 = 0.03, k = 0.1, d = 0.01, a = 0.01, p = 0.5, q = 0.1, m = 0.05, c = 0.4$. Parameters for 3.5(b) are: $r_0 = 0.05, k = 10, d = 0.01, a = 0.01, p = 0.5, q = 0.6, m = 0.05, c = 0.4$.

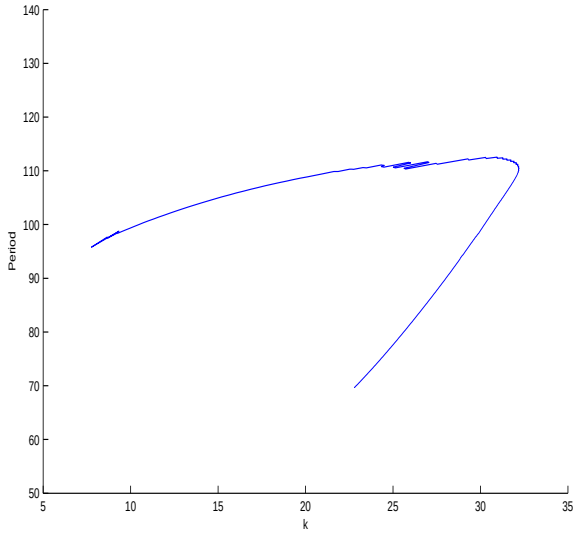

Figure 3.6: Bifurcation diagram for subcritical Hopf bifurcation. Parameters are: $r_0 = 2.671, d = 0.0246, a = 0.0004, p = 0.0673, q = 0.0058, c = 0.0952, m = 0.0505$.

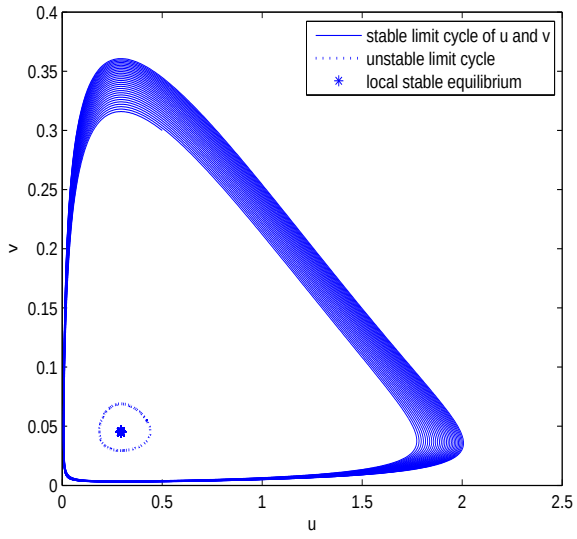

Figure 3.7: Subcritical Hopf bifurcation/Bi-stability. Parameters are: $r_0 = 0.12, k = 60, d = 0.01, a = 0.01, p = 0.5, q = 0.6, m = 0.05, c = 0.4$.

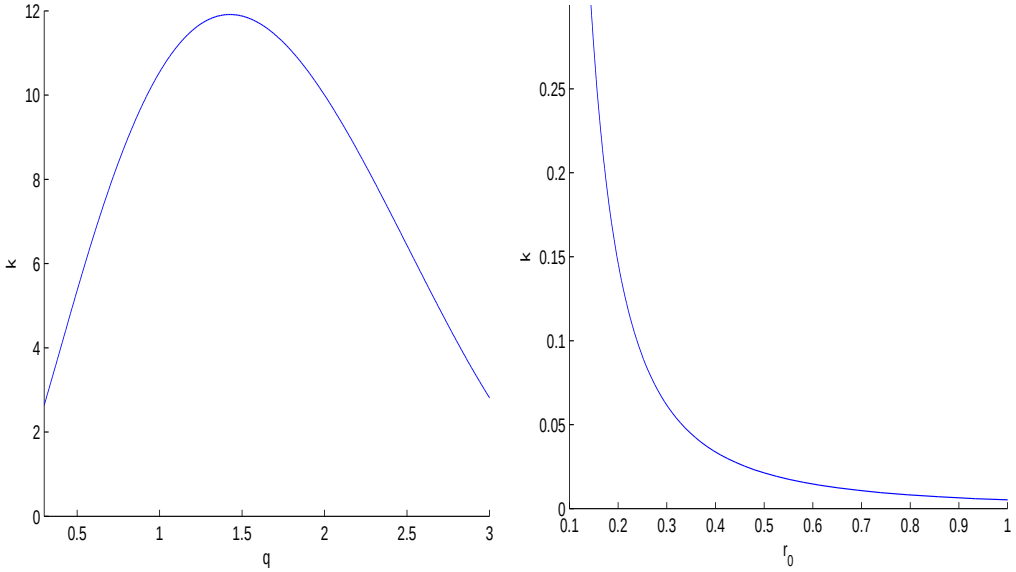

(a) k, q along Hopf bifurcation curve (b) k, r_0 along Hopf bifurcation curve

Figure 3.8: Two dimensional projection of Hopf bifurcation curve when $k \neq 0$ into k, q and k, r_0 respectively.

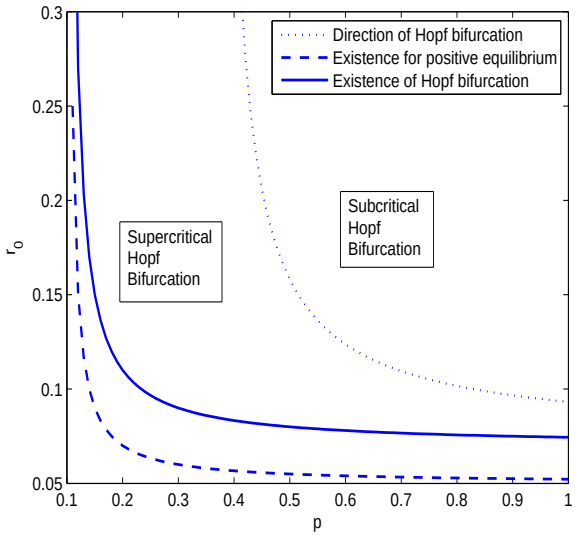

Figure 3.9: Available region of Hopf bifurcation on r_0, p plane. Parameters are: $q = 0.5, c = 0.5, m = 0.1, d = 0.05, a = 0.01$.

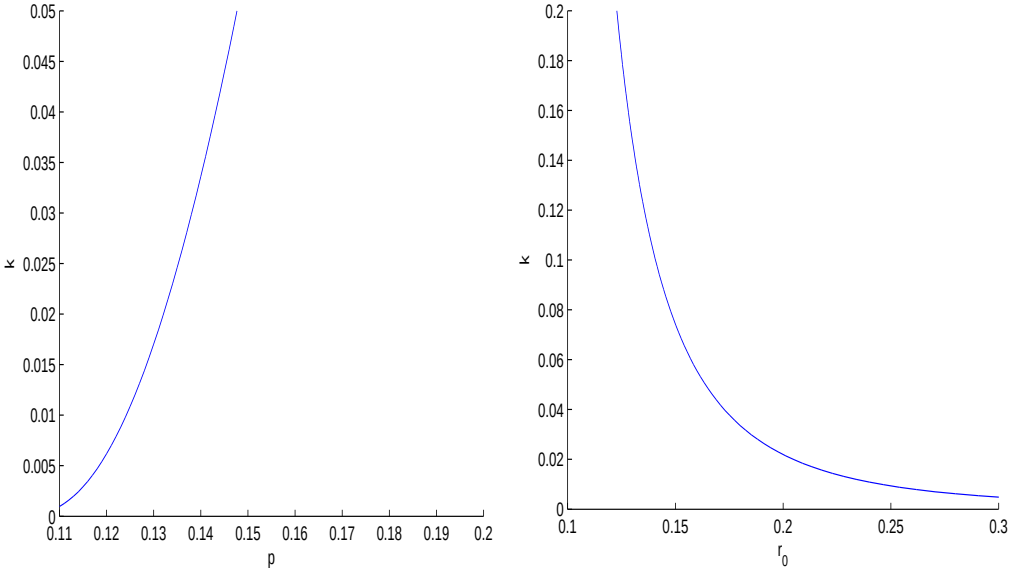

(a) k, p along Hopf bifurcation curve (b) k, r_0 along Hopf bifurcation curve

Figure 3.10: Two dimensional projection of Hopf bifurcation curve when $k \neq 0$ into k, p and k, r_0 respectively.

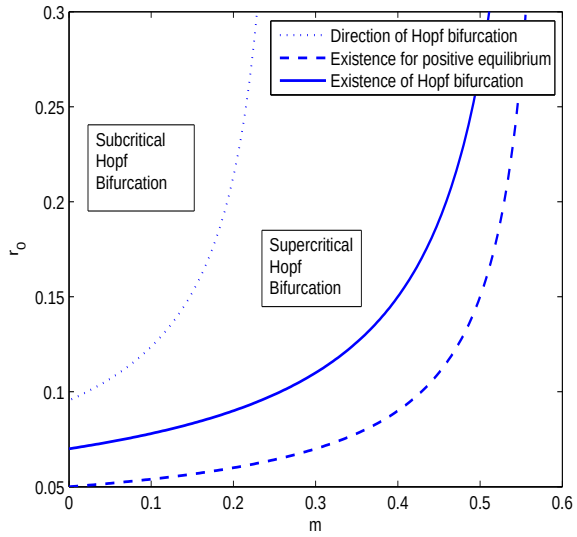

Figure 3.11: Available region of Hopf bifurcation on r_0, m plane. Parameters are: $q = 0.5, p = 0.5, c = 0.6, a = 0.01, d = 0.05$.

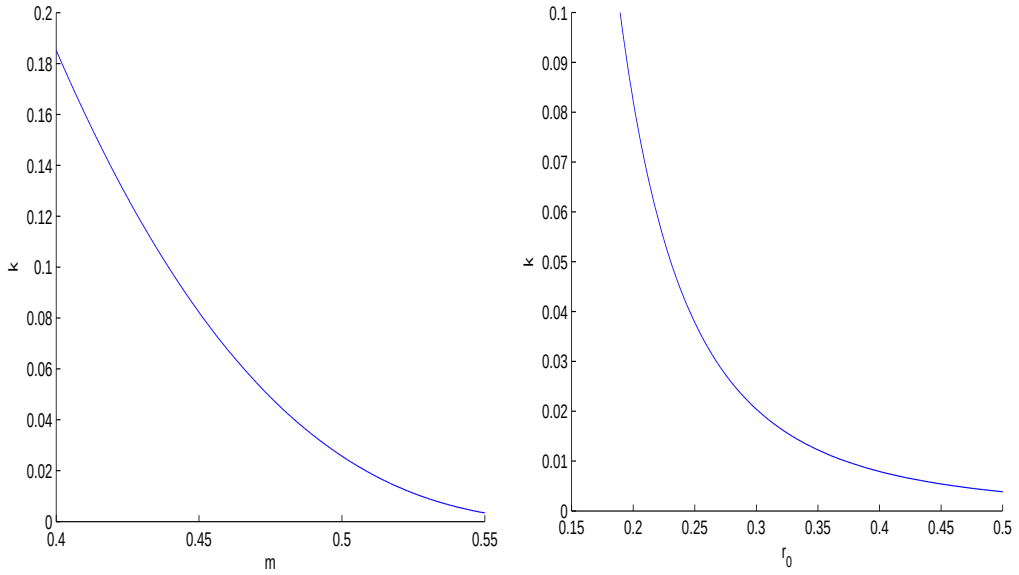

(a) k, m along Hopf bifurcation curve (b) k, r_0 along Hopf bifurcation curve

Figure 3.12: Two dimensional projection of Hopf bifurcation curve when $k \neq 0$.

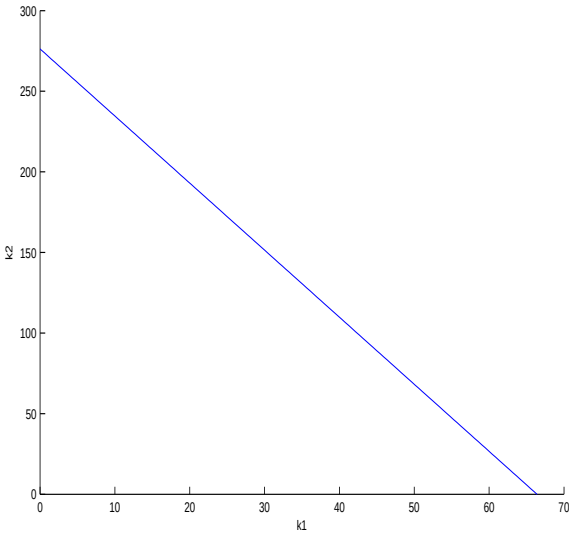

Figure 3.13: Relationship between k_1 and k_2 along the Hopf bifurcation line when taking fear function (3.59).

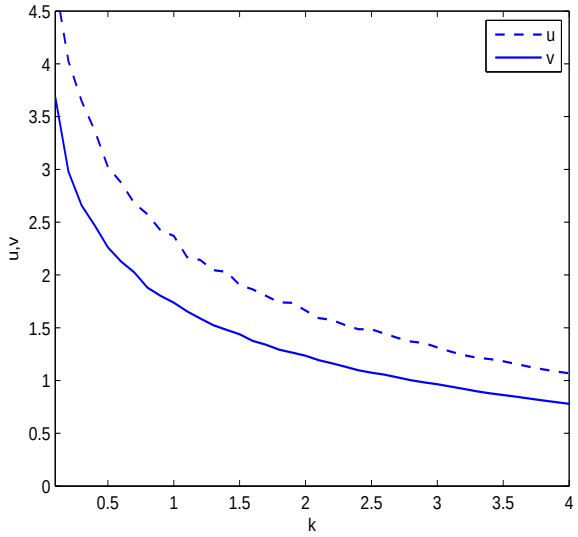

Figure 3.14: The biomass for predators and prey from periodic solutions with varying k due to supercritical Hopf bifurcation. Parameters are: $r_0 = 2, d = 0.2, a = 0.04, p = 0.4, q = 0.2, c = 0.3, m = 0.1$.

However, for the model with the Holling type II functional response, the cost of fear affects predator-prey interactions in several ways. Analytical results show that there exists a globally stable positive equilibrium if the birth rate of prey is not large enough to support fluctuations. In this case, the populations of prey and predators tend to generate positive constants eventually, no matter how sensitive the prey is to potential dangers from predators. When the birth rate of prey is large enough to support oscillations, the positive equilibrium of the predator-prey system is locally asymptotically stable if the fear level is high. In this case, the cost of fear can stabilize the predator-prey system by ruling out periodic solutions. This offers a new mechanism to avoid the "paradox of enrichment " in ecosystems. Periodic solutions can still exist when the fear level is relatively low. Conditions for existence of Hopf bifurcation and conditions determining the direction of Hopf bifurcation are obtained, which indicate that the cost of fear will not only affect the existence of Hopf bifurcation but also change the direction of Hopf bifurcation. Indeed, we have shown that Hopf bifurcation in the model incorporating the cost of fear can be both supercritical and subcritical, which is in contrast to the classic predator-prey models that ignore the predation risk effects where Hopf bifurcation can only be supercritical.

Numerical simulations are conducted to show the potential role that fear effects can play in predator-prey interactions by releasing one or two more parameters free rather than the single k. Under conditions of Hopf bifurcation, increasing fear level may cause a change in the direction of Hopf bifurcation, from supercritical to subcritical, when the birth rate of prey

increases accordingly. Fear generates rich dynamical behaviours including bi-stability, where the solutions tend to a steady state or oscillate periodically depending on the initial population size. Numerical simulations also show that the prey is less sensitive to perceived predation risk when the birth rate of prey is high, regardless of how other parameters change. Moreover, the prey would be more willing to show anti-predator defences when the attack (i.e. predation) rate is high, and would perceive fewer potential dangers as the death rate of predators increases. Simulations with different functions modelling the cost of fear indicate that the results we have obtained in this paper remain valid when other general monotone decreasing functions are adopted.

In our model formulation, we have assumed that the perceived predation risks only reduce the birth rate and survival of offspring, and have ignored the possible impact on the death rate of adult prey. Although Zanette *et al.* ([48]) and Clinchy *et al.* ([4]) argue that fear may increase the adult death rate due to long-term physiological impacts, there is still a lack of direct experimental evidence. For the same reason, we have only considered the case when fear does not affect intra-specific competition in our model, although there is also a theoretical argument in [7] that the fear effect may change the strength of intra-specific competition because of the complexity of food web. Once some experimental evidence becomes available, these should all be incorporated into the model, and such a model would be able shed more light on the prey-predator interactions.

Bibliography

[1] J. R. Beddington. Mutual interference between parasites or predators and its effect on searching efficiency. *The Journal of Animal Ecology*, 44:331–340, 1975.

[2] R. S. Cantrell and C. Cosner. On the dynamics of predator-prey models with the Beddington-DeAngelis functional response. *Journal of Mathematical Analysis and Applications*, 257:206–222, 2001.

[3] C. Castillo-Chavez and H. R. Thieme. Asymptotically autonomous epidemic models. *Mathematical Population Dynamics: Analysis of Heterogeneity*, 1:33–50, 1995.

[4] M. Clinchy, M. J. Sheriff, and L. Y. Zanette. Predator-induced stress and the ecology of fear. *Functional Ecology*, 27:56–65, 2013.

[5] S. Creel and D. Christianson. Relationships between direct predation and risk effects. *Trends in Ecology & Evolution*, 23:194–201, 2008.

[6] S. Creel, D. Christianson, S. Liley, and J. A. Winnie. Predation risk affects reproductive physiology and demography of elk. *Science*, 315:960–960, 2007.

[7] W. Cresswell. Predation in bird populations. *Journal of Ornithology*, 152:251–263, 2011.

[8] D. L. DeAngelis, R. A. Goldstein, and R. V. O'Neill. A model for tropic interaction. *Ecology*, 56:881–892, 1975.

[9] A. Dhooge, W. Govaerts, and Y. A. Kuznetsov. Matcont: a MATLAB package for numerical bifurcation analysis of ODEs. *ACM Transactions on Mathematical Software (TOMS)*, 29:141–164, 2003.

[10] A. Dhooge, W. Govaerts, Y. A. Kuznetsov, H. G. E. Meijer, and B. Sautois. New features of the software Matcont for bifurcation analysis of dynamical systems. *Mathematical and Computer Modelling of Dynamical Systems*, 14:147–175, 2008.

[11] S. Eggers, M. Griesser, and J. Ekman. Predator-induced plasticity in nest visitation rates in the Siberian jay (*perisoreus infaustus)*. *Behavioral Ecology*, 16:309–315, 2005.

[12] S. Eggers, M. Griesser, M. Nystrand, and J. Ekman. Predation risk induces changes in nest-site selection and clutch size in the siberian jay. *Proceedings of the Royal Society of London B: Biological Sciences*, 273:701–706, 2006.

[13] J. J. Fontaine and T. E. Martin. Parent birds assess nest predation risk and adjust their reproductive strategies. *Ecology letters*, 9:428–434, 2006.

[14] H. I. Freedman and G. S. K. Wolkowicz. Predator-prey systems with group defence: The paradox of enrichment revisited. *Bulletin of Mathematical Biology*, 48:493–508, 1986.

[15] C. K. Ghalambor, S. I. Peluc, and T. E. Martin. Plasticity of parental care under the risk of predation: how much should parents reduce care? *Biology Letters*, 9:20130154, 2013.

[16] M. E. Gilpin and M. L. Rosenzweig. Enriched predator-prey systems: theoretical stability. *Science*, 177:902–904, 1972.

[17] C. S. Holling. The functional response of predators to prey density and its role in mimicry and population regulation. *Memoirs of the Entomological Society of Canada*, 97:5–60, 1965.

[18] F. Hua, R. J. Fletcher, K. E. Sieving, and R. M. Dorazio. Too risky to settle: avian community structure changes in response to perceived predation risk on adults and offspring. *Proceedings of the Royal Society of London B: Biological Sciences*, 280:20130762, 2013.

[19] F. Hua, K. E. Sieving, R. J. Fletcher, and C. A. Wright. Increased perception of predation risk to adults and offspring alters avian reproductive strategy and performance. *Behavioral Ecology*, 25:509–519, 2014.

[20] J. Huang, S. Ruan, and J. Song. Bifurcations in a predator-prey system of leslie type with generalized Holling type iii functional response. *Journal of Differential Equations*, 257: 1721–1752, 2014.

[21] T-W Hwang. Global analysis of the predator-prey system with Beddington-DeAngelis functional response. *Journal of Mathematical Analysis and Applications*, 281:395–401, 2003.

[22] T-W Hwang. Uniqueness of limit cycles of the predator-prey system with Beddington-DeAngelis functional response. *Journal of Mathematical Analysis and Applications*, 290: 113–122, 2004.

[23] J. D. Ibáñez-Álamo and M. Soler. Predator-induced female behavior in the absence of male incubation feeding: an experimental study. *Behavioral Ecology and Sociobiology*, 66:1067–1073, 2012.

[24] R. E. Kooij and A. Zegeling. Qualitative properties of two-dimensional predator-prey systems. *Nonlinear Analysis: Theory, Methods & Applications*, 29:693–715, 1997.

[25] Y. Kuang and H. I. Freedman. Uniqueness of limit cycles in Gause-type models of predator-prey systems. *Mathematical Biosciences*, 88:67–84, 1988.

[26] S. L. Lima. Nonlethal effects in the ecology of predator-prey interactions. *Bioscience*, 48: 25–34, 1998.

[27] S. L. Lima. Predators and the breeding bird: behavioral and reproductive flexibility under the risk of predation. *Biological Reviews*, 84:485–513, 2009.

[28] R. M. May. Limit cycles in predator-prey communities. *Science*, 177:900–902, 1972.

[29] C. D. McAllister, R. J. LeBrasseur, T. R. Parsons, and M. L. Rosenzweig. Stability of enriched aquatic ecosystems. *Science*, 175:562–565, 1972.

[30] J. D. Meiss. *Differential dynamical systems*, volume 14. SIAM, 2007.

[31] J. L. Orrock and R. J. Fletcher. An island-wide predator manipulation reveals immediate and long-lasting matching of risk by prey. *Proceedings of the Royal Society of London B: Biological Sciences*, 281:20140391, 2014.

[32] S. D. Peacor, B. L. Peckarsky, G. C. Trussell, and J. R. Vonesh. Costs of predator-induced phenotypic plasticity: a graphical model for predicting the contribution of nonconsumptive and consumptive effects of predators on prey. *Oecologia*, 171:1–10, 2013.

[33] L. Perko. *Differential equations and dynamical systems*, volume 7. Springer Science & Business Media, 2013.

[34] N. Pettorelli, T. Coulson, S. M. Durant, and J-M Gaillard. Predation, individual variability and vertebrate population dynamics. *Oecologia*, 167:305–314, 2011.

[35] E. L. Preisser and D. I. Bolnick. The many faces of fear: comparing the pathways and impacts of nonconsumptive predator effects on prey populations. *PloS One*, 3:e2465, 2008.

[36] J. F. Riebesell. Paradox of enrichment in competitive systems. *Ecology*, 55:183–187, 1974.

[37] M. L. Rosenzweig. Paradox of enrichment: destabilization of exploitation ecosystems in ecological time. *Science*, 171:385–387, 1971.

[38] G. Seo and D. L. DeAngelis. A predator-prey model with a Holling type i functional response including a predator mutual interference. *Journal of Nonlinear Science*, 21: 811–833, 2011.

[39] M. J. Sheriff, C. J. Krebs, and R. Boonstra. The sensitive hare: sublethal effects of predator stress on reproduction in snowshoe hares. *Journal of Animal Ecology*, 78:1249–1258, 2009.

[40] Y. Song and X. Zou. Bifurcation analysis of a diffusive ratio-dependent predator-prey model. *Nonlinear Dynamics*, 78:49–70, 2014.

[41] Y. Song and X. Zou. Spatiotemporal dynamics in a diffusive ratio-dependent predator-prey model near a Hopf-Turing bifurcation point. *Computers & Mathematics with Applications*, 67:1978–1997, 2014.

[42] J. Sugie, R. Kohno, and R. Miyazaki. On a predator-prey system of Holling type. *Proceedings of the American Mathematical Society*, 125:2041–2050, 1997.

[43] T. O. Svennungsen, Ø. H. Holen, and O. Leimar. Inducible defenses: continuous reaction norms or threshold traits? *The American Naturalist*, 178:397–410, 2011.

[44] A. J. Wirsing and W. J. Ripple. A comparison of shark and wolf research reveals similar behavioral responses by prey. *Frontiers in Ecology and the Environment*, 9:335–341, 2011.

[45] G. S. K. Wolkowicz. Bifurcation analysis of a predator-prey system involving group defence. *SIAM Journal on Applied Mathematics*, 48:592–606, 1988.

[46] G. S. K. Wolkowicz, H. Zhu, and S. A. Campbell. Bifurcation analysis of a predator-prey system with nonmonotonic functional response. *SIAM Journal on Applied Mathematics*, 63:636–682, 2003.

[47] D. Xiao and S. Ruan. Global analysis in a predator-prey system with nonmonotonic functional response. *SIAM Journal on Applied Mathematics*, 61:1445–1472, 2001.

[48] L. Y. Zanette, A. F. White, M. C. Allen, and M. Clinchy. Perceived predation risk reduces the number of offspring songbirds produce per year. *Science*, 334:1398–1401, 2011.

Chapter 4

Modelling the fear effect in predator-prey interactions with adaptive avoidance of predators

4.1 Introduction

Studying the mechanism of predator-prey interaction is a central topic in both ecology and evolutionary biology. Direct killing of prey by predators is obviously easy to observe in the field and hence is the focus of mathematical modelling by far. However, it has been argued by theoretical biologists ([6, 14, 15]) that indirect effects caused by anti-predator behaviours of prey may play an even more important role in determining prey demography.

Almost all vertebrates demonstrate plastic behaviours in response to stimuli in the surrounding environment. For prey, the fear of predators drives prey to avoid direct predation, which may increase short-term survival probability of prey but may cause a long-term loss in the prey population as a consequence ([8]). Such indirect effects exist commonly in species with different life stages in their life span, for example, birds. Breeding birds may fly away from nests and leave juvenile birds unprotected and less looked after when adults perceive predation risk ([8]). Even temporary absence of adult birds may lower survival probability of juveniles because juveniles may experience less suitable living conditions and face higher risk of predation. In such a scenario, the overall fitness of the bird species may decrease because fear may lead to a reduction of reproduction success although temporary survival probability may increase.

Some recent field experiments supported the aforementioned theoretical arguments about the significant effect that such anti-predator behaviours may have. For example, Zanette *et al.* ([27]) conducted a field experiment on song sparrows during a whole breeding season by using

electrical fence to eliminate direct predation of both juvenile and adult song sparrows. No direct killing can happen in the experiment, however, broadcast of vocal cues of known predators in the field was employed to mimic predation risk. Two groups of female song sparrows were tested, among which one group was exposed to predator sounds while the other group was not. The authors ([27]) found that the group of song sparrows exposed to predator vocal cues produced 40% less offspring than the other group because fewer eggs were laid, fewer eggs were successfully hatched, and fewer nestlings survived eventually. Behavioural changes of adult song sparrows when predation risk existed were also observed and documented in [27], including less time of adult song sparrows on brood and less feeding to nestlings during breeding period, and these were all believed to be responsible for the total cost of 40% reduction in offspring population. Some correlative experiments on other birds or other vertebrate species also reported that even though there was no direct killing between predators and prey, the presence of predators did cause a large reduction of prey population due to anti-predator behaviours of prey ([7, 18, 25]).

Based on the experiment in Zanette *et al.* [27], Wang *et al.* ([23]) studied a predator-prey model with the cost of fear incorporated. The authors found that strong anti-predator behaviours or equivalently the large cost of fear may exclude the existence of periodic solutions and thus eliminate the phenomenon 'paradox of enrichment'. In addition, under relatively low cost of fear, periodic solutions still exist arising from either supercritical or subcritical Hopf bifurcation ([23]). Wang's study ignored age-structure of prey, while Zanette's experiment distinguished the life stages of song sparrows with regards to their behaviours. In addition, the cost of anti-predator defense of adult prey does not only exist in the birth rate of juvenile prey but also been observed in the survival rates including both natural death rate and predation rate of juveniles. All this evidence demands the incorporation of age structures into a mathematical model. In fact, the anti-predator behaviour of adult prey can be viewed as a plastic trait or strategy which is adaptive to the environment ([20, 26]). Under selection, adult prey tend to choose a defense level that would increase their survival probability and reduce the reproduction loss but maximize the individual fitness ([1]). There have been a few mathematical models that describe such adaptive behaviours of prey. Křivan ([12]) studied the trade-off between foraging and predation based on classic Lotka-Volterra model where either prey or predator or both were adaptive to maximize their individual fitness. Peacor *et al.* ([17]) employed a graphical model to study the strength of anti-predator behaviours and conditions when the indirect effects dominate predator-prey interactions by regarding the defense level of prey as an adaptive trait. Takeuchi *et al.* ([21]) studied the conflict between investing time on taking care of juveniles and searching for resources of adult prey in the absence of direct predation, where they assumed that adults adapt their parental care time through learning.

Motivated by the above existing works and the experimental evidence of [27] for song sparrows, and as an extension of [23], in this paper, we formulate, in Section 2, a predator-prey model with age structure and allowing adaptive avoidance of predators. The model divides the prey population into a juvenile stage and an adult stage, and is naturally represented by a system of delay differential equations (DDEs) with the delay accounting for the maturation time. Adult prey in the model are assumed to adapt defense level in terms of the total growth rate of both juveniles and adults. In Section 3, we address the well-posedness of the model with properly posed initial conditions. In Section 4, we analyze the dynamics of the model with either a constant defense level or an adaptive defense level respectively, with focus on a simplified version of the model. The reason is that for the full model in the general form, analysis becomes more difficult, as such, we mainly present some numerical simulation results and discuss some biological implications, with focus on the impact of some key model parameters. We conclude the paper by Section 5 in which we briefly summarize this work and in the mean time, discuss some possible future topics related to this paper.

4.2 Model formulation

Based on the experiment in [27], there exists different stages of song sparrows, in which song sparrows behave very differently. This naturally suggests use of age structured model for study of population dynamics of birds. For simplicity, we only consider two stages —a juvenile stage and an adult stage, and follow the standard and frequently used approach (see references [2, 4, 5, 10, 16, 22]) to incorporate the two stages of prey into the model. Apparently there is a maturation delay between juvenile prey and adult prey, which is denoted as τ in our model. Noting that Zanette *et al.* reported in [27] that juvenile song sparrows can't live independently and must live under the protection of adult song sparrows to survive, we assume that juvenile birds do not show anti-predator behaviours. In other words, only adult prey perceive predation risk and are able to avoid potential attacking by flying away from nests. Such an anti-predator defense of adult prey positively impacts the individual survival but in the mean time, results in a cost as well ([6]). This is because anti-predator behaviours of adult prey increase the possibility for them to escape from direct killing by predator but more frequent and defensive flying of adults will consume extra energy and time, which are essential for reproduction. Moreover, too frequent flying of parent birds will leave the juveniles less looked after and less protected, leading to a higher risk of predation. In addition, as documented in [27], adult song sparrows feed less to juveniles if they are scared, and this leads to a higher death rate of juvenile song sparrows even in the absence of direct killing.

Taking into consideration the aforementioned facts/observations due to fear effect of adult

prey, we can formulate a mathematical model as below. Let $\alpha \in [0, 1]$ denote the level of anti-predator defense of adult prey, with larger value of α accounting for stronger anti-predation defense and smaller value corresponding to weaker response. Denote the populations of juvenile prey and adult prey by x_1 and x_2 respectively, and the population of predator by y. Adopting the simple mass action predation mechanism and incorporating the effect of the anti-predation response represented by α, the dynamics of x_1 and x_2 can be described by the following differential equations:

$$\begin{cases} \dfrac{dx_1}{dt} = b(\alpha, x_2)\, x_2 - (d_0 + d_1\,\alpha)\, x_1 - (s_0 + s_1\,\alpha)\, x_1\, y \\ \qquad\quad - b(\alpha, x_2(t-\tau))\, x_2(t-\tau) e^{-(d_0 + s_0\, y + (d_1 + s_1\, y)\,\alpha)\,\tau}, \\ \dfrac{dx_2}{dt} = b(\alpha, x_2(t-\tau))\, x_2(t-\tau) e^{-(d_0 + s_0\, y + (d_1 + s_1\, y)\,\alpha)\,\tau} \\ \qquad\quad - d_2\, x_2 - s(\alpha)\, x_2\, y. \end{cases} \tag{4.1}$$

Here, d_0 is the natural death rate of juveniles, s_0 is the death rate of juveniles due to direct predation, d_1 and s_1 are death rates of juveniles induced by the cost of anti-predator behaviours of adult prey, d_2 is the natural death rate of adult prey. Here in this work, to avoid making things too complicated, we assume that the predator population y is a constant. This corresponds to a scenario that the predator is a generalist which lives on many other species of prey, and this also reflects the environment of the field experiment by Zanette *et. al.* ([27]) in which the presence of predators is represented by the strength of vocal cues which can be controlled as a constant level.

In model (4.1), $b(\alpha, x_2)$ is the birth rate function and $s(\alpha)$ is the predation rate function for adult prey. Both of them depend on the anti-predation behaviours of adult prey and should be decreasing in α, followed by the aforementioned discussions on the fear effect. Typically $b(\alpha, x_2)$ is also decreasing in x_2. To be specific, we choose the following form for $b(\alpha, x_2)$:

$$b(\alpha, x_2) = \begin{cases} (b_0 - b_1\,\alpha)^{\theta_1} e^{(-a\, x_2)}, \quad \text{if } \ 0 \le \alpha < \dfrac{b_0}{b_1}, \\ 0, \quad \text{if } \ \dfrac{b_0}{b_1} \le \alpha \le 1, \end{cases} \tag{4.2}$$

where $0 < b_0 < b_1$ and $\theta_1 \ge 1$. This assumes a threshold b_0/b_1 below which, the birth function is of the Ricker type with the maximal birth rate adjusted by $\alpha \in [0, b_0/b_1)$, and above which (extremely fearful case) there is no birth at all. For $s(\alpha)$, for convenience we also choose the following similar form:

$$s(\alpha) = \begin{cases} (s_2 - s_3\,\alpha)^{\theta_2}, \quad \text{if } \ 0 \le \alpha < \dfrac{s_2}{s_3}, \\ 0, \quad \text{if } \ \dfrac{s_2}{s_3} \le \alpha \le 1, \end{cases} \tag{4.3}$$

where $0 < s_2 < s_3$ and $\theta_2 \geq 1$. Again a threshold s_2/s_3 is assumed above which, the adults can fully escape from predation. We point out that depending on the particular species of predator and prey, the two threshold values b_0/b_1 and s_2/s_3 may vary. For convenience of subsequent discussions, we assume, in the rest of the paper, that $s_2/s_3 < b_0/b_1$, accounting for a situation of relatively mild predation.

Because adult prey can perceive predation risk to some extent and *adapt* their behaviours to the change of the surrounding environment ([8]), we may consider the anti-predator defense level of the adult prey (i.e., α) to be adaptive. According to [20], it is reasonable to regard α as a trait, which should evolve toward maximizing the fitness of the prey species ([1]). For a prey with stage structure, following the idea in [21], we consider the scenario that adult prey act adaptively so that the *instant total growth rate of the total species* will be benefitted. With this consideration and following [21], we adopt the following quantity for the fitness of prey with respect to anti-predator defense level α

$$\begin{aligned}\Phi &= \frac{dx_1}{dt} + \frac{dx_2}{dt} \\ &= b(\alpha, x_2)\, x_2 - (d_0 + d_1\,\alpha)\, x_1 - (s_0 + s_1\,\alpha)\, y\, x_1 - d_2\, x_2 - s(\alpha)\, x_2\, y. \end{aligned} \tag{4.4}$$

Then, according to [21], the evolution of α is governed by

$$\begin{aligned}\frac{d\alpha}{dt} &= \gamma(\alpha)\,\frac{\partial \Phi}{\partial \alpha} \\ &= \gamma(\alpha)\left(\frac{\partial b(\alpha, x_2)}{\partial \alpha} x_2 - d_1\, x_1 - s_1\, y\, x_1 - \frac{ds(\alpha)}{d\alpha} x_2\, y\right), \end{aligned} \tag{4.5}$$

where $\gamma(\alpha) = k\,\alpha\,(1-\alpha)$ ensures that the defense level α remains between 0 and 1, provided that $\alpha(0) \in [0, 1]$. Summarizing, as far as the adaptive anti-predator response is concerned, we will consider the following stage structured predator-prey model with adaptive avoidance of predation and fear effect:

$$\begin{cases} \dfrac{dx_1}{dt} = b(\alpha, x_2)\, x_2 - (d_0 + d_1\,\alpha)\, x_1 - (s_0 + s_1\,\alpha)\, x_1\, y \\ - b(\alpha(t-\tau), x_2(t-\tau))\, x_2(t-\tau) \exp\left(-\displaystyle\int_{t-\tau}^{t} (d_0 + s_0\, y + (d_1 + s_1\, y)\,\alpha(s))ds\right), \\ \dfrac{dx_2}{dt} = b(\alpha(t-\tau), x_2(t-\tau))\, x_2(t-\tau) \exp\left(-\displaystyle\int_{t-\tau}^{t} (d_0 + s_0\, y + (d_1 + s_1\, y)\,\alpha(s))ds\right) \\ - d_2\, x_2 - s(\alpha)\, x_2\, y, \\ \dfrac{d\alpha}{dt} = k\,\alpha\,(1-\alpha)\left(\dfrac{\partial b(\alpha, x_2)}{\partial \alpha}\, x_2 - d_1\, x_1 - s_1\, y\, x_1 - \dfrac{ds(\alpha)}{d\alpha}\, x_2\, y\right). \end{cases} \tag{4.6}$$

4.3 Well-posedness of the model

The model (4.6) should be associated with non-negative initial values:

$$x_2(\theta) \geq 0, \quad \alpha(\theta) \in [0,1] \quad \text{with} \quad x_2(0) > 0. \tag{4.7}$$

As for the variable x_1, there is also a compatibility issue. To see this, we can integrate the equation for x_1 in (4.6) to obtain

$$x_1(t) = \int_{t-\tau}^{t} b(\alpha(\eta), x_2(\eta))\, x_2(\eta) \exp\left(-\int_{\eta}^{t} (d_0 + s_0\, y + d_1\, \alpha(u) + s_1\, y\, \alpha(u))\, du\right) d\eta. \tag{4.8}$$

At $t = 0$, the above equation gives a constraint on the initial values:

$$x_1(0) = \int_{-\tau}^{0} b(\alpha(\eta), x_2(\eta))\, x_2(\eta) \exp\left(-\int_{\eta}^{0} (d_0 + s_0\, y + d_1\, \alpha(u) + s_1\, y\, \alpha(u))\, du\right) d\eta. \tag{4.9}$$

This condition is also biologically reasonable because it simply says that the total juvenile population at $t = 0$ is a result of the newborns during the interval $[-\tau, 0]$ mediated by the death during this period ([13]).

The existence and uniqueness of solutions of (4.6) can be easily established by the standard method of steps. Now when the initial values are non-negative and the compatibility condition (4.9) holds, we can confirm the well-posedness in the sense stated in the following lemma.

Lemma 4.3.1 *Let $x_2(\theta), \alpha(\theta) \geq 0$ on $-\tau \leq \theta < 0$ and $x_2(0) > 0, b_0/b_1 > \alpha(0) > 0$, and assume that $x_1(0)$ satisfies* (4.9)*. Then the solution of* (4.6) *stays positive and is ultimately bounded.*

Proof Let

$$h(t) = \frac{\partial \Phi}{\partial \alpha}(t) = \frac{\partial b(\alpha(t), x_2(t))}{\partial \alpha}\, x_2(t) - d_1\, x_1(t) - s_1\, y\, x_1(t) - \frac{ds(\alpha(t))}{d\alpha(t)}\, y\, x_2(t). \tag{4.10}$$

Then, $\alpha(t)$ can be expressed as

$$\alpha(t) = \frac{\alpha(0)\, \exp\left(\int_0^t k\, h(\eta) d\eta\right)}{1 - \alpha(0) + \alpha(0) \exp\left(\int_0^t k\, h(\eta) d\eta\right)}. \tag{4.11}$$

Thus, it is clear that $\alpha(t) = 0$ for all $t \geq 0$ if $\alpha(0) = 0$, $\alpha(t) = 1$ for all $t \geq 0$ if $\alpha(0) = 1$, and $0 < \alpha(t) < 1$ for $t \geq 0$ if $0 < \alpha(0) < 1$.

Since we assume $x_2(\theta), \alpha(\theta) \geq 0$ on $-\tau \leq \theta < 0$, from equation of x_2 in (4.6), we obtain

$$\frac{dx_2(t)}{dt} \geq -d_2\, x_2 - s(\alpha)\, x_2\, y \geq -(d_2 + s_2^2\, y)\, x_2, \quad t \in [0, \tau]. \tag{4.12}$$

By a comparison argument and from (4.12), we obtain

$$x_2(t) \geq x_2(0)e^{-(d_2+s_2^2 y)t}, \quad t \in [0, \tau] \tag{4.13}$$

which shows that $x_2(t) > 0$ if $x_2(0) > 0$ for $t \in [0, \tau]$. Repeating the argument, we obtain the positivity in $[\tau, 2\tau]$, $[2\tau, 3\tau]$, $\cdots$, and hence for all $t \geq 0$ indeed. The positivity of $x_1(t)$ is just a consequence of combining (4.8) and the positivity of $x_2(t)$ and $\alpha(t)$.

Next, we show boundedness of solutions of (4.6). In the above, we have shown that $\alpha(t)$ is bounded between 0 and 1. Thus it only remains to show the boundedness of x_1 and x_2. From (4.6), we have

$$\begin{aligned} \frac{dx_1}{dt} &\leq b(\alpha, x_2)\, x_2 - (d_0 + d_1\, \alpha)\, x_1 - (s_0 + s_1\, \alpha)\, x_1\, y \\ &\leq b_0^{\theta_1}\, e^{-a\, x_2}\, x_2 - (d_0 + s_0\, y)\, x_1 \\ &\leq \frac{b_0^{\theta_1}}{e\, a} - (d_0 + s_0\, y)\, x_1. \end{aligned} \tag{4.14}$$

Therefore, we obtain

$$\limsup_{t\to\infty}(x_1(t)) \leq \frac{b_0^{\theta_1}}{e\, a\, (d_0 + s_0\, y)}.$$

Furthermore, adding the first two equations of (4.6) gives

$$\begin{aligned} \frac{d(x_1 + x_2)}{dt} &\leq b(\alpha, x_2)\, x_2 - d_0\, x_1 - d_2\, x_2 \\ &\leq b(\alpha, x_2)\, x_2 - \gamma(x_1 + x_2) \\ &\leq \frac{b_0^{\theta_1}}{e\, a} - \gamma(x_1 + x_2), \end{aligned} \tag{4.15}$$

where $\gamma = \min\{d_0, d_2\}$. Thus

$$\limsup_{t\to\infty}(x_1(t) + x_2(t)) \leq \frac{b_0^{\theta_1}}{e\, a\, \gamma}. \tag{4.16}$$

By (4.16) and the positivity of x_1 and x_2, we conclude that x_1 and x_2 are ultimately bounded, completing the proof of the lemma.

4.4 Long term dynamics of the model

In this section, we investigate the dynamics of the model. We start by looking at two special cases first, in subsections 4.4.1 and 4.4.2 respectively, before considering the full model in subsection 4.4.3.

4.4.1 Model with constant defense level

Before we consider the adaptive defense described by (4.6), it would be helpful and useful to look at the case when the defense level α is a constant. In this case, the equation of x_2 is decoupled from x_1, and the dynamics of system (4.1) is completely determined by

$$\frac{dx_2}{dt} = b(\alpha, x_2(t-\tau))\, x_2(t-\tau) e^{-(d_0 + s_0\, y + (d_1 + s_1\, y)\, \alpha)\, \tau} - d_2\, x_2 - s(\alpha)\, x_2\, y, \tag{4.17}$$

where $b(\alpha, x_2)$, $s(\alpha)$ are defined in (4.2) and (4.3) respectively. In order to simplify analysis, let $p = d_0 + s_0\, y$, $q = d_1 + s_1\, y$, $\delta_0(\alpha) = p + q\, \alpha$, and $\delta(\alpha) = d_2 + s(\alpha)\, y$.

When the defense level is too strong in the sense that $\alpha \in [b_0/b_1, 1]$, by (4.2), $b(\alpha, x_2) = 0$, meaning the species is fully devoted to defend predation so that there is no birth at all. Then (4.17) becomes

$$\frac{dx_2}{dt} = -d_2\, x_2 - s(\alpha)\, x_2\, y, \tag{4.18}$$

implying that $x_2(t)$ dies out exponentially. Accordingly, by the first equation in (4.6), $x_1(t)$ also approaches zero.

Next, consider the case of mild defence, that is, $\alpha \in [0, b_b/b_1)$. Then, plugging in the birth function given in (4.2) into (4.17) leads to

$$\frac{dx_2}{dt} = (b_0 - b_1\alpha)^{\theta_1} e^{-\delta_0(\alpha)\tau} e^{-a x_2(t-\tau)} x_2(t-\tau) - \delta(\alpha) x_2. \tag{4.19}$$

This is in the form of the well-known Nicholson blowflies equation which has been extensively studied in the literature, see, e.g., [4, 9, 11, 19, 24] and the references therein. In terms of the so called basic reproduction number

$$\mathcal{R}_0 = \frac{(b_0 - b_1\alpha)^{\theta_1}\, e^{-\delta_0(\alpha)\tau}}{\delta(\alpha)}, \tag{4.20}$$

the main results about (4.19) related to the topics of this paper are summarized below:

(C1) If $\mathcal{R}_0 \le 1$, then the trivial equilibrium $x_2 = 0$ is globally asymptotically stable.

(C2) If $\mathcal{R}_0 > 1$, then the trivial equilibrium becomes unstable and there exists a unique positive equilibrium given by $x_2^+ = \frac{1}{a} \ln \mathcal{R}_0$. In this case, for any fixed $\tau > 0$,

(C2-i) either x_2^+ is asymptotically stable;

(C2-ii) or x_2^+ is unstable but there is an asymptotically stable periodic solution $x_{2p}(t)$ that is a sustained oscillation about x_2^+.

Since in both (C2-i) and (C2-ii), $x_2^+ = \frac{1}{a}\ln\mathcal{R}_0$ represents the average persistence level of the population, it is interesting and significant to explore at what value of $\alpha \in [0, b_0/b_1)$, $\mathcal{R}_0 = \mathcal{R}_0(\alpha)$ will be maximized. Note that $s(\alpha) = 0$ for $\alpha \in [s_2/s_3, 1]$, and hence $\mathcal{R}_0(\alpha)$ is deceasing in $[s_2/s_3, 1]$. Thus, $\mathcal{R}_0$ should be maximized in the interval $[0, s_2/s_3]$. The following theorem gives an answer to the problem when $\theta_1 = 1 = \theta_2$.

Theorem 4.4.1 *Let $\theta_1 = 1 = \theta_2$. Then, $\mathcal{R}_0$ is maximized at $\alpha = 0$ if*

$$\exp\left(\frac{q\,\tau\,s_2}{s_3}\right) > \frac{(d_2 + s_2\,y)\,(b_0\,s_3 - b_1\,s_2)}{b_0\,d_2\,s_3}, \tag{4.21}$$

and it is maximized at $\alpha = s_2/s_3$ if (4.21) *is reversed.*

Proof For $0 \le \alpha \le s_2/s_3$, we have

$$\frac{d\mathcal{R}_0}{d\alpha} = \frac{-e^{-p\tau}e^{-q\tau\alpha}}{(d_2 + ys_2 - ys_3\alpha)^2}\left[a_1\,\alpha^2 + a_2\,\alpha + a_3\right] \tag{4.22}$$

where

$$\begin{aligned} &a_1 = q\,\tau\,b_1\,y\,s_3,\; a_2 = -q\,\tau\,(b_1\,d_2 + b_1\,y\,s_2 + s_3\,y\,b_0)\,,\\ &a_3 = q\,\tau\,b_0\,(d_2 + s_2\,y) + b_1\,d_2 - y\,(b_0\,s_3 - b_1\,s_2)\,. \end{aligned} \tag{4.23}$$

Let

$$\Delta = a_2^2 - 4\,a_1\,a_3 = q\,\tau\,(s_3\,y\,b_0 - b_1\,d_2 - b_1\,y\,s_2)\,(q\,\tau\,b_0\,y\,s_3 + 4\,b_1\,s_3\,y - q\,\tau\,b_1\,y\,s_2 - q\,\tau\,b_1\,d_2)\,. \tag{4.24}$$

If $a_3 > 0$ and $\Delta < 0$, (4.22) has not real root and $\mathcal{R}_0$ is maximized either at $\alpha = 0$ or $\alpha = s_2/s_3$. If $a_3 > 0$ and $\Delta > 0$, then (4.22) has two distinct positive roots

$$\bar{\alpha}_1 = \frac{-a_2 - \sqrt{\Delta}}{2\,a_1},\; \bar{\alpha}_2 = \frac{-a_2 + \sqrt{\Delta}}{2\,a_1},$$

where $\bar{\alpha}_2 > s_2/s_3$ and hence should be excluded. Direct calculations show that $\alpha = \bar{\alpha}_1$ is the local minimum point of R_0, and hence $\mathcal{R}_0$ is maximized either at $\alpha = 0$ or $\alpha = s_2/s_3$. If $a_3 < 0$, then (4.22) has a single positive root $\bar{\alpha}_2$ which is in $[s_2/s_3, 1]$. Summarizing, in the interval $0 \le \alpha \le s_2/s_3$, $\mathcal{R}_0$ can only be maximized either at $\alpha = 0$ or at $\alpha = s_2/s_3$. Evaluating of $\mathcal{R}_0(0)$ and $\mathcal{R}_0(s_2/s_3)$ leads to the conclusion of the theorem, and the proof is completed.

For other values of θ_1 and θ_2, one may also do similar things but it typically becomes more difficult for analytic results. However, one can always explore numerically to gain useful information on this topic. For example, for $\theta_1 = \theta_2 = 2$ and with parameters given, numerical results show that an optimal defense level α may exist in the interval $0 < \alpha < s_2/s_3$, as demonstrated in Figure 4.1.

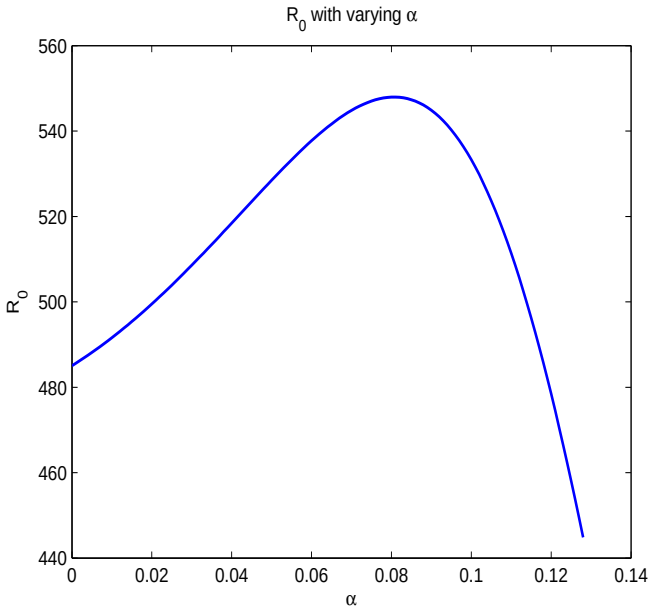

Figure 4.1: If $\theta_1 = \theta_2 = 2$, optimal defense level α exists in interval $[0, s_2/s_3]$. Other parameters are $b_0 = 9.4609$, $b_1 = 13.2741$, $p = 0.0856$, $q = 3.0554$, $d_2 = 0.0467$, $s_2 = 0.2009$, $s_3 = 1.5685$, $y = 2.6194$, $\tau = 2.2335$.

4.4.2 Model with adaptive defense level—a special case: $d_1 = 0, \quad s_1 = 0$

In this subsection, we first consider a special case where the anti-predation response of adult prey has no impact on the death and predation of juveniles. This is reflected by assuming $d_1 = 0,\ s_1 = 0$ in (4.6), leading to the following simplified version of the model:

$$\begin{aligned}
\frac{dx_1}{dt} &= b(\alpha,\ x_2)\, x_2 - (s_0\, y + d_0)\, x_1 - b(\alpha(t-\tau), x_2(t-\tau))\, x_2(t-\tau) e^{-(d_0 + s_0\, y)\tau}, \\
\frac{dx_2}{dt} &= b(\alpha(t-\tau), x_2(t-\tau))\, x_2(t-\tau) e^{-(d_0 + s_0\, y)\,\tau} - d_2\, x_2 - s(\alpha)\, x_2\, y, \\
\frac{d\alpha}{dt} &= k\,\alpha\,(1-\alpha)\left(\frac{\partial b(\alpha, x_2)}{\partial \alpha}\, x_2 - \frac{ds(\alpha)}{d\alpha}\, x_2\, y\right),
\end{aligned} \tag{4.25}$$

where $b(\alpha, x_2)$ and $s(\alpha)$ are the same functions defined in (4.2) and (4.3) respectively. To be more concrete, we will choose $\theta_1 = \theta_2 = 2$ in this subsection.

Notice that the equations for $x_2'(t)$ and $\alpha'(t)$ in (4.25) are decoupled from the equation for $x_1'(t)$. Therefore, we only need, in the rest of this subsection, to study subsystem

$$\begin{aligned}
\frac{dx_2}{dt} &= b(\alpha(t-\tau), x_2(t-\tau))\, x_2(t-\tau) e^{-p\,\tau} - d_2\, x_2 - s(\alpha)\, x_2\, y, \\
\frac{d\alpha}{dt} &= k\,\alpha\,(1-\alpha)\left(\frac{\partial b(\alpha, x_2)}{\partial \alpha}\, x_2 - \frac{ds(\alpha)}{d\alpha}\, x_2\, y\right),
\end{aligned} \tag{4.26}$$

where $p = d_0 + s_0\, y$.

4.4.2.1 Equilibria of system (4.26)

For (4.26), the basic reproduction number reduces to

$$\mathcal{R}_0(\alpha) = \frac{(b_0 - b_1\alpha)^2\, e^{-p\,\tau}}{d_2 + (s_2 - s_3\alpha)^2\, y}. \tag{4.27}$$

Let $\mathcal{R}_0^0 = \mathcal{R}_0(0)$. There are two extinction equilibrium: $E_{b0} = (0,\, 0)$ and $E_{b1} = (0,\, 1)$. Straightforward and simple stability analysis shows that E_{b1} is always stable, and E_{b0} is stable if $\mathcal{R}_0^0 < 1$ and is unstable if $\mathcal{R}_0^0 > 1$.

A semi-trivial equilibrium $E_s = (\bar{x}_{20}, 0)$ exists if $\mathcal{R}_0^0 > 1$ where

$$\bar{x}_{20} = \frac{1}{a}\,\ln \mathcal{R}_0^0.$$

Properties of (4.2) and (4.3) give

$$\begin{aligned} \frac{d\alpha}{dt} &= k\,\alpha\,(1-\alpha)\left[-2\,b_1\,(b_0 - b_1\,\alpha)\,e^{-a\,x_2}\,x_2\right] \\ &< 0, \qquad \text{if} \quad \frac{s_2}{s_3} \le \alpha < \frac{b_0}{b_1}. \end{aligned} \tag{4.28}$$

Similarly, we obtain

$$\frac{dx_2}{dt} = -d_2\,x_2, \qquad \text{if} \quad \frac{b_0}{b_1} \le \alpha \le 1. \tag{4.29}$$

By (4.28) and (4.29), it is clear that positive equilibrium can exist only if $0 \le \alpha < s_2/s_3$.

Setting the right hand side of the second equation in (4.26) to zero and solving for α in terms of $\psi = e^{-ax_2}$, we see that a positive equilibrium $E(\bar{x}_2,\, \bar{\alpha})$ must satisfy

$$\bar{x}_2 = -\frac{1}{a}\,\ln(\psi), \qquad \bar{\alpha} = \frac{b_0\,b_1\,\psi - s_2\,s_3\,y}{b_1^2\,\psi - s_3^2\,y} =: H(\psi) \tag{4.30}$$

where, by plugging the formula for $\bar{\alpha}$ in (4.30) into the right hand side of the first equation in (4.26), ψ is determined by

$$F(\psi) := \rho_1\,\psi^2 + \rho_2\,\psi + \rho_3 = 0. \tag{4.31}$$

Here in (4.31) we have

$$\begin{aligned} \rho_1 &= -b_1^2\left(b_1^2\,d_2 + y\,(b_1\,s_2 - b_0\,s_3)^2\right), \\ \rho_2 &= y\,s_3^2\left(e^{-p\,\tau}\,y\,(b_0\,s_3 - b_1\,s_2)^2 + 2\,b_1^2\,d_2\right), \quad \rho_3 = -d_2\,y^2\,s_3^4. \end{aligned} \tag{4.32}$$

Noting that with the assumption of $s_2/s_3 < b_0/b_1$, $H(\psi)$ is decreasing in $\psi \in (0, 1)$ with $H(0) = s_2/s_s$, which automatically ensures that $\bar{\alpha} < s_2/s_3$. Now the other requirement of $\bar{\alpha} > 0$ leads to another constraint for ψ : $\psi < s_2 s_3 y/b_0 b_1$, which is obtained by solving $H(\psi) = 0$ for ψ. Thus, we need to look for real roots of (4.31) in the interval $(0, \psi_0)$ where

$$\psi_0 = \min\left\{\frac{s_2\,s_3\,y}{b_0\,b_1},\, 1\right\}. \tag{4.33}$$

Let

$$\Delta = \rho_2^2 - 4\,\rho_1\,\rho_3. \tag{4.34}$$

From (4.32), it is obvious that $\rho_1 < 0$, $\rho_2 > 0$, $\rho_3 < 0$, thus $F(0) = \rho_3 < 0$ and $F'(0) = \rho_2 > 0$. Therefore, (4.31) has no positive root if $\Delta < 0$, and (4.31) has two distinct positive roots if $\Delta > 0$. For the latter case, denote the two positive roots of (4.31) by ψ_1, ψ_2 respectively and assume $\psi_1 < \psi_2$ without loss of generality. Thus, system (4.26) admits a unique positive equilibrium ψ_1 if $\Delta > 0$, $F(\psi_0) > 0$ and it has two distinct equilibria if $\Delta > 0$, $\psi_2 < \psi_0$. Note that the condition $\Delta > 0$ is equivalent to

$$e^{p\,\tau} < \frac{b_1\,d_2 + \sqrt{(b_1\,d_2)^2 + d_2\,y\,(b_0\,s_3 - b_1\,s_2)^2}}{2\,b_1\,d_2}. \tag{4.35}$$

Summarizing the above analysis and expressing in terms of the model parameters, we obtain the following two theorems about the existence of positive equilibrium/equilibria.

Theorem 4.4.2 *Assume that* (4.35) *holds. Then, a unique positive equilibrium* $E_{p1} = (\bar{x}_{21},\, \bar{\alpha}_1)$ *of* (4.26) *exists if*

$$\begin{cases} y \geq \dfrac{b_0\,b_1}{s_2\,s_3} \qquad (\textit{corresponding to} \quad \psi_0 = 1), \\ \left(d_2\,s_3^4\,y^2 + b_1^2\left((b_1\,s_2 - b_0\,s_3)^2 - 2\,d_2\,s_3^2\right)\,y + d_2\,b_1^4\right)e^{p\,\tau} < y^2\,s_3^2\,(b_0\,s_3 - b_1\,s_2)^2 \;\; (\,F(\psi_0) > 0\,); \end{cases} \tag{4.36}$$

or

$$\begin{cases} y < \dfrac{b_0\,b_1}{s_2\,s_3} \qquad \left(\textit{corresponding to} \;\; \psi_0 = \dfrac{s_2 s_3 y}{b_0 b_1}\right), \\ e^{p\,\tau} < \dfrac{s_2\,s_3\,b_0\,y}{b_1\left(d_2 + y\,s_2^2\right)} \quad (\,F(\psi_0) > 0\,) \end{cases} \tag{4.37}$$

where

$$\bar{x}_{21} = \frac{-1}{a}\,\ln\left(\frac{-\rho_2 + \sqrt{\Delta}}{2\,\rho_1}\right), \;\; \bar{\alpha}_1 = \frac{b_0\,b_1\left(\left(-\rho_2 + \sqrt{\Delta}\right)/(2\,\rho_1)\right) - s_2\,s_3\,y}{b_1^2\left(\left(-\rho_2 + \sqrt{\Delta}\right)/(2\,\rho_1)\right) - s_3^2\,y}. \tag{4.38}$$

In Theorem 4.4.2, Δ, ρ_1, ρ_2 are defined in (4.34) and (4.32) respectively.

Theorem 4.4.3 *Assume that* (4.35) *holds. Then, two distinct positive equilibria* $E_{p1} = (\bar{x}_{21},\, \bar{\alpha}_1)$, $E_{p2} = (\bar{x}_{22},\, \bar{\alpha}_2)$ *of* (4.26) *exist if*

$$\begin{cases} y \geq \dfrac{b_0\,b_1}{s_2\,s_3} \qquad (\textit{corresponding to} \quad \psi_0 = 1), \\ y^2\,s_3^2\,(b_0\,s_3 - b_1\,s_2)^2 < \left(d_2\,s_3^4\,y^2 + b_1^2\left((b_1\,s_2 - b_0\,s_3)^2 - 2\,d_2\,s_3^2\right)\,y + d_2\,b_1^4\right)e^{p\,\tau} \;\; (\,F(\psi_0) < 0\,), \\ y^2\,s_3^2\,(b_0\,s_3 - b_1\,s_2)^2 < 2\,b_1^2\left(d_2\,(b_1^2 - y\,s_3^2) + y\,(b_0\,s_3 - b_1\,s_2)^2\right)\,e^{p\,\tau} \;\; (\,\psi_2 < \psi_0\,); \end{cases} \tag{4.39}$$

or

$$\begin{cases} y < \dfrac{b_0\, b_1}{s_2\, s_3} \qquad \left(\textit{corresponding to } \ \psi_0 = \dfrac{s_2 s_3 y}{b_0 b_1}\right), \\ s_2\, s_3\, b_0\, y < b_1\,(d_2 + y\, s_2^2) e^{p\,\tau} \ \ (\,F(\psi_0) < 0\,), \\ b_0\, s_3\, y\,(b_0\, s_3 - b_1\, s_2) < 2\, b_1\ (s_2\, y\,(b_0\, s_3 - b_1\, s_2) - b_1\, d_2)\ e^{p\,\tau} \ \ (\,\psi_2 < \psi_0\,), \end{cases} \tag{4.40}$$

where $\bar{x}_{21}$, $\bar{\alpha}_1$ *are the same as* (4.38)*, and*

$$\bar{x}_{22} = \frac{-1}{a}\ \ln\left(\frac{-\rho_2 - \sqrt{\Delta}}{2\,\rho_1}\right), \quad \bar{\alpha}_2 = \frac{b_0\, b_1\ \left(\left(-\rho_2 - \sqrt{\Delta}\right)/(2\,\rho_1)\right) - s_2\, s_3\, y}{b_1^2\ \left(\left(-\rho_2 - \sqrt{\Delta}\right)/(2\,\rho_1)\right) - s_3^2\, y}. \tag{4.41}$$

4.4.2.2 Dynamics of system (4.26)

We begin with analyzing local stability of the semi-trivial equilibrium E_s. The linearization of (4.26) at E_s is

$$\begin{aligned} \frac{dx_2}{dt} &= f_{11}\, x_2 + f_{12}\, \alpha + f_{13}\, x_2(t-\tau) + f_{14}\, \alpha(t-\tau), \\ \frac{d\alpha}{dt} &= f_{22}\, \alpha, \end{aligned} \tag{4.42}$$

where

$$\begin{aligned} f_{11} &= -d_2 - s_2^2\, y, \\ f_{12} &= 2\, s_2\, s_3\, \bar{x}_{20}\, y, \\ f_{13} &= \left(d_2 + s_2^2\, y\right)(1 - a\bar{x}_{20})\,, \\ f_{14} &= -2\, b_1\, \bar{x}_{20}\, \left(\frac{d_2 + s_2^2\, y}{b_0}\right), \\ f_{22} &= k\, \bar{x}_{20}\, \left(-2\, b_0\, b_1\, e^{-a\,\bar{x}_{20}} + 2\, s_2\, s_3\, y\right). \end{aligned} \tag{4.43}$$

Plugging $(x_2,\, \alpha) = e^{(\lambda\, t)}(v_1,\, v_2)$ into (4.42), we obtain the characteristic equation at E_s

$$G(\lambda,\, \tau) := \left[\lambda - \left(f_{11} + f_{13}\, e^{-\lambda\,\tau}\right)\right](\lambda - f_{22}) = 0. \tag{4.44}$$

When $\tau = 0$, the characteristic equation (4.44) reduces to

$$G(\lambda) = \left[\lambda + (d_2 + s_2^2 y)\ln \mathcal{R}_0^0\right] \cdot \left[\lambda + 2k\bar{x}_{20}\left(\frac{b_0 b_1}{\mathcal{R}_0^0} - s_2 s_3 y\right)\right] \tag{4.45}$$

where $\bar{x}_{20} = \frac{1}{a}\ln\left(b_0^2/(d_2 + s_2^2\, y)\right) = \frac{1}{a}\ln R_0^0$. By (4.45), we obtain the local stability of E_s when $\tau = 0$, which is shown in the following theorem.

Theorem 4.4.4 *Consider the case of* $\tau = 0$ *and* $b_0 b_1 > s_2 s_3 y$*. Assume* $\mathcal{R}_0^0 > 1$ *so that the semi-trivial equilibrium* $E_s = (\bar{x}_{20},\, 0)$ *exists. Then,* E_s *is locally asymptotically stable if*

$$\mathcal{R}_0^0 = \frac{b_0^2}{d_2 + s_2^2 y} < \frac{b_0 b_1}{s_2 s_3 y} \quad \left(\Longleftrightarrow \frac{b_0}{b_1} - \frac{s_2}{s_3} < \frac{d_2}{s_2 s_3 y}\right), \tag{4.46}$$

and it is unstable if (4.46) *is reversed.*

Next we analyze how the delay τ affects the stability of E_s. To this end, we assume that E_s is locally stable when $\tau = 0$ (i.e. (4.46) holds). Now we consider the case where $\tau > 0$. Note that $\mathcal{R}_0^0$ depends on τ, being decreasing in τ.

Theorem 4.4.5 *Let $b_0 b_1 > s_2 s_3 y$ and assume that $\mathcal{R}_0^0 > 1$ so that E_s exists. Then E_s is locally asymptotically stable if*

$$\mathcal{R}_0^0 < \frac{b_0\, b_1}{s_2\, s_3\, y} \quad \textit{and} \quad \mathcal{R}_0^0 \le e^2. \tag{4.47}$$

Proof The characteristic equation (4.44) has one real eigenvalue

$$\lambda = f_{22} = -2\, k\, \bar{x}_{20} \left(\frac{b_0\, b_1}{\mathcal{R}_0^0} - s_2\, s_3\, y \right)$$

which is negative if and only if

$$\mathcal{R}_0^0 < \frac{b_0\, b_1}{s_2\, s_3\, y}. \tag{4.48}$$

All other eigenvalues of (4.44) are determined by

$$D(\lambda, \tau) := P(\lambda, \tau) + Q(\lambda, \tau)\, e^{-\lambda \tau} = 0, \tag{4.49}$$

where

$$\begin{aligned} P(\lambda, \tau) &= \lambda - f_{11} = \lambda + (d_2 + s_2^2\, y), \\ Q(\lambda, \tau) &= -f_{13} = -\left(d_2 + s_2^2\, y\right)(1 - a\, \bar{x}_{20}). \end{aligned} \tag{4.50}$$

Because $D(0, \tau) = \left(d_2 + s_2^2\, y\right) a \bar{x}_{20} > 0$, $\lambda = 0$ is not a characteristic root of (4.49) for any $\tau > 0$. Therefore, stability of E_s can change only through the occurrence of pure imaginary roots of (4.49). Assume $\lambda = i\, \omega$ with $\omega > 0$. Because $|P(i\, \omega, \tau)| = |-Q(i\, \omega, \tau)\, \exp(-i\, \omega\, \tau)| = |Q(i\, \omega, \tau)|$ (by (4.49)), $\omega > 0$ must satisfy

$$\begin{aligned} 0 = F(\omega, \tau) &= |P(i\, \omega, \tau)|^2 - |Q(i\, \omega, \tau)|^2 \\ &= \omega^2 + (d_2 + s_2^2\, y)^2 - (d_2 + s_2^2\, y)^2\, (1 - a\, \bar{x}_{20})^2 \\ &= \omega^2 + (d_2 + s_2^2\, y)^2 \left[1 - (1 - a \bar{x}_{20})^2 \right]. \end{aligned} \tag{4.51}$$

Obviously, (4.51) has no positive solution if $a \bar{x}_{20} \le 2$, implying that there is no pure imaginary root for (4.49). Simple calculation shows that

$$a\, \bar{x}_{20} \le 2 \Longleftrightarrow \mathcal{R}_0^0 \le e^2. \tag{4.52}$$

Indeed, if (4.52) holds, then (4.49) also has no root with *positive real part*. To see this, we assume $\lambda = r + i\, \omega$ is a root of (4.49) with $r > 0$ and $\omega > 0$. By substituting $\lambda = r + i\, \omega$ into (4.49), we obtain

$$r + \left(d_2 + s_2^2\, y\right) + i\, \omega = \left(d_2 + s_2^2\, y\right)(1 - a\, \bar{x}_{20}) e^{-r\, \tau} e^{-i\, \omega\, \tau},$$

which gives

$$|r + \left(d_2 + s_2^2\, y\right) + i\,\omega| = |\left(d_2 + s_2^2\, y\right)(1 - a\,\bar{x}_{20})e^{-r\,\tau}e^{-i\,\omega\,\tau}|. \tag{4.53}$$

Because $r > 0$ by assumption, (4.53) implies

$$\begin{aligned} &\left(d_2 + s_2^2\, y\right)^2 < \left(r + d_2 + s_2^2\, y\right)^2 < \left(r + d_2 + s_2^2\, y\right)^2 + \omega^2 \\ &= \left(d_2 + s_2^2\, y\right)^2 \,(1 - a\,\bar{x}_{20})^2\, e^{-2\,r\,\tau} < \left(d_2 + s_2^2\, y\right)^2 \,(1 - a\,\bar{x}_{20})^2, \end{aligned} \tag{4.54}$$

implying that $2 < a\,\bar{x}_{20}$ which contradicts to (4.52). Therefore, every eigenvalue $\lambda = r + i\,\omega$ of (4.49) must have $r < 0$ if (4.52) holds. As a consequence, local stability of E_s remains valid for $\tau > 0$ if (4.48) and (4.52) hold.

Noting that $\mathcal{R}_0^0$ is decreasing in τ, we immediately have the following corollary.

Corollary 4.4.6 *Assume that*

$$\frac{b_0^2}{d_2 + s_2^2 y} < \min\left\{\frac{b_0 b_1}{s_2 s_3 y},\, e^2\right\}.$$

Then E_s is asymptotically stable as long as it exists (i.e., provided that $\mathcal{R}_0^0 > 1$.)

From the proof of Theorem 4.4.5, we can see that violation of condition (4.48) leads to the sign change of a real eigenvalue from negative to positive, and loss of stability of E_s results in the occurrence of a positive equilibrium (see the condition (4.37) in Theorem 4.4.2), which will be discussed later. The violation of the other condition (4.52), on the other hand, makes it possible for a pair of complex eigenvalues to cross the imaginary axis from the left half plane to the right in the complex plane, and this is expected to cause Hopf bifurcation. We explore a bit more along this line below. The focus is on the impact of the delay $\tau > 0$, and accordingly, we assume that (4.46) holds so that E_s is asymptotically stable when $\tau = 0$, and we follow the framework of [3] to proceed.

Assume the opposite of (4.52), that is

$$a\,\bar{x}_{20} > 2 \quad (\text{equivalently } \mathcal{R}_0^0 > e^2). \tag{4.55}$$

Under (4.55), equation (4.51) admits a unique positive root given by

$$\omega(\tau) = \left(d_2 + s_2^2\, y\right)\sqrt{(1 - a\,\bar{x}_{20})^2 - 1}. \tag{4.56}$$

Following [3], let I denote the interval in which $\omega(\tau)$ in (4.56) is defined. Solving (4.55) for τ then gives

$$I = \left[0, \frac{1}{p}\ln\frac{b_0^2}{(d_2 + s_2^2 y)e^2}\right).$$

Let $\theta(\tau): I \to \mathbb{R}_+$ be the solution of

$$\sin\theta(\tau) = -\frac{\omega(\tau)}{(d_2 + s_2^2\, y)(1 - a\,\bar{x}_{20})}, \quad \cos\theta(\tau) = \frac{1}{1 - a\,\bar{x}_{20}}. \tag{4.57}$$

Then, by [3], stability switch of E_s may occur when τ is a zero of

$$S_n(\tau) := \tau - \frac{\theta(\tau) + n\,2\,\pi}{\omega(\tau)}, \quad \tau \in I, \quad n \in \mathbb{N}. \tag{4.58}$$

To finally confirm the stability switch, we need to verify the transversality condition at zeros of $S_n(\tau)$, $\tau \in I$. To this end, we use the implicit differentiation in (4.49) to obtain

$$\frac{d\lambda}{d\tau} = \frac{(f_{13}^{'} - f_{13}\,\lambda)\, e^{-\lambda\,\tau}}{1 + f_{13}\,\tau\, e^{-\lambda\,\tau}}, \tag{4.59}$$

where f_{13} is shown in (4.43). We point out that it is more convenient to consider

$$\left(\frac{d\lambda}{d\tau}\right)^{-1} = \frac{e^{\lambda\,\tau} + f_{13}\,\tau}{f_{13}^{'} - f_{13}\lambda} = \frac{f_{13}/(\lambda - f_{11}) + f_{13}\tau}{f_{13}^{'} - f_{13}\lambda}. \tag{4.60}$$

At a zero τ^* of $S_n(\tau)$, we have $\lambda(\tau^*) = iw(\tau^*)$. This observation together with (4.49) and (4.51) help us to simplify (4.60) to

$$\begin{aligned}\left(\frac{d\lambda}{d\tau}\right)^{-1}\Big|_{\lambda = i\,\omega(\tau_i)} &= \frac{-f_{11} + f_{13}^2\,\tau - \omega\, i}{\omega\,\omega' - f_{13}^2\,\omega\, i} \\ &= \frac{1}{\omega^2\,\omega'^2 + f_{13}^4\,\omega^2}\left(\left(-f_{11} + f_{13}^2\,\tau\right)\omega\,\omega' + \omega^2\, f_{13}^2 + \left(f_{13}^2\,\omega - \omega^2\,\omega'\right) i\right).\end{aligned} \tag{4.61}$$

By (4.61), we obtain

$$\left.\frac{d\,\mathrm{Re}(\lambda)}{d\tau}\right|_{\lambda = i\,\omega(\tau_i)} = \frac{\left(-f_{11} + f_{13}^2\,\tau\right)\omega\,\omega' + \omega^2\, f_{13}^2}{\omega^2\,\omega'^2 + f_{13}^4\,\omega^2}. \tag{4.62}$$

The formula in (4.62) can be used to determine the transversality for Hopf bifurcation. Unfortunately, we cannot confirm the sign of this formula for general model parameters. However, once the values of parameters are given, it is straightforward and easy to numerically calculate the zeros of $S_n(\tau)$ and evaluate (4.62) at these zeros, and thereby, determine whether Hopf bifurcation will occur. For examples, for parameters chosen in Figure 4.2, by numerically solving $S_n(\tau) = 0$, we find that there are two zeros for $S_0(\tau)$, which are $\tau_1 = 0.5$ and $\tau_2 = 4.782$, as shown in Figure 4.2, but none for $S_n(\tau)$, $n = 1, \cdots$. Moreover, numerical evaluations of (4.62) at τ_1 and τ_2 indicate that $d\,\mathrm{Re}(\lambda)/d\tau > 0$ at τ_1 and $d\,\mathrm{Re}(\lambda)/d\tau < 0$ at τ_2. This implies that the model (4.26) undergoes Hopf bifurcation at these two critical values: when τ increases to pass τ_1, E_s loses its stability leading to sustained oscillation of the population; while when τ

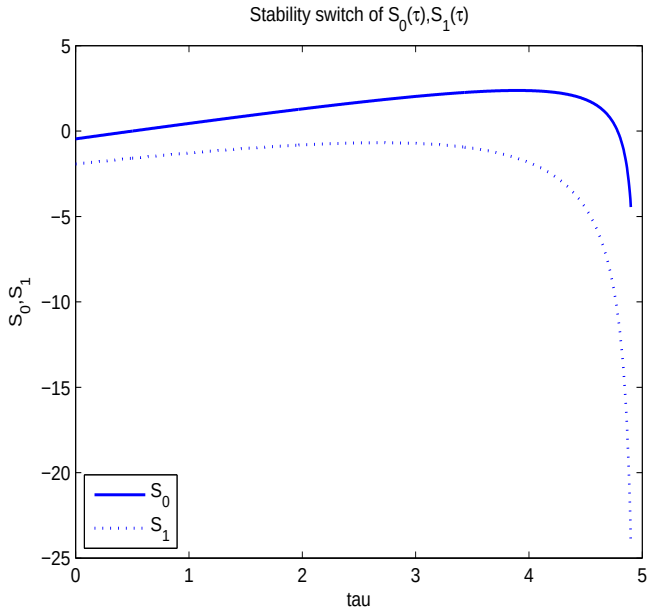

Figure 4.2: Stability switch of E_s. Parameters are: $b_0 = 8.1311$, $b_1 = 9.1252$, $a = 0.9858$, $p = 0.3290$, $s_2 = 1.3924$, $s_3 = 2.4989$, $y = 0.5376$, $d_2 = 0.7139$, $k = 1$.

further increases to pass τ_2, the periodic solutions disappear and E_s regains its stability. These are confirmed by numerical simulations of the model (4.26), as shown in Figure 4.3.

The above analyses have shown that the semi-trivial equilibrium E_s may lose its stability to a stable periodic solution with an intermediate value of τ and regain its stability when τ is large, through Hopf bifurcation. In addition to this, as we mentioned before, E_s may also lose its stability to a positive equilibrium through equilibrium bifurcation, reflected by a real eigenvalue crossing the pure imaginary axis from the left to the right in the complex plane. Such a positive equilibrium is interesting since it represents a persistent anti-predator defense. Thus, the stability/instability of such a positive equilibrium is of great importance.

Note that Theorem 4.4.2 and 4.4.3 have confirmed that one positive equilibrium or two positive equilibria may exist under different conditions. However, if $\tau = 0$, E_{p2} in Theorem 4.4.3 can not exist because the conditions for its existence are contradictory in this case. Hence, we first consider the case where a unique positive equilibrium E_{p1} exists (i.e. where conditions in Theorem 4.4.2 hold) when $\tau \geq 0$ and then proceed to the case where Theorem 4.4.3 holds by restricting $\tau > 0$. The procedure is exactly the same as the one for the stability/instability of E_s above, mainly using the framework in [3], as such, we will try to be brief below, omitting many details.

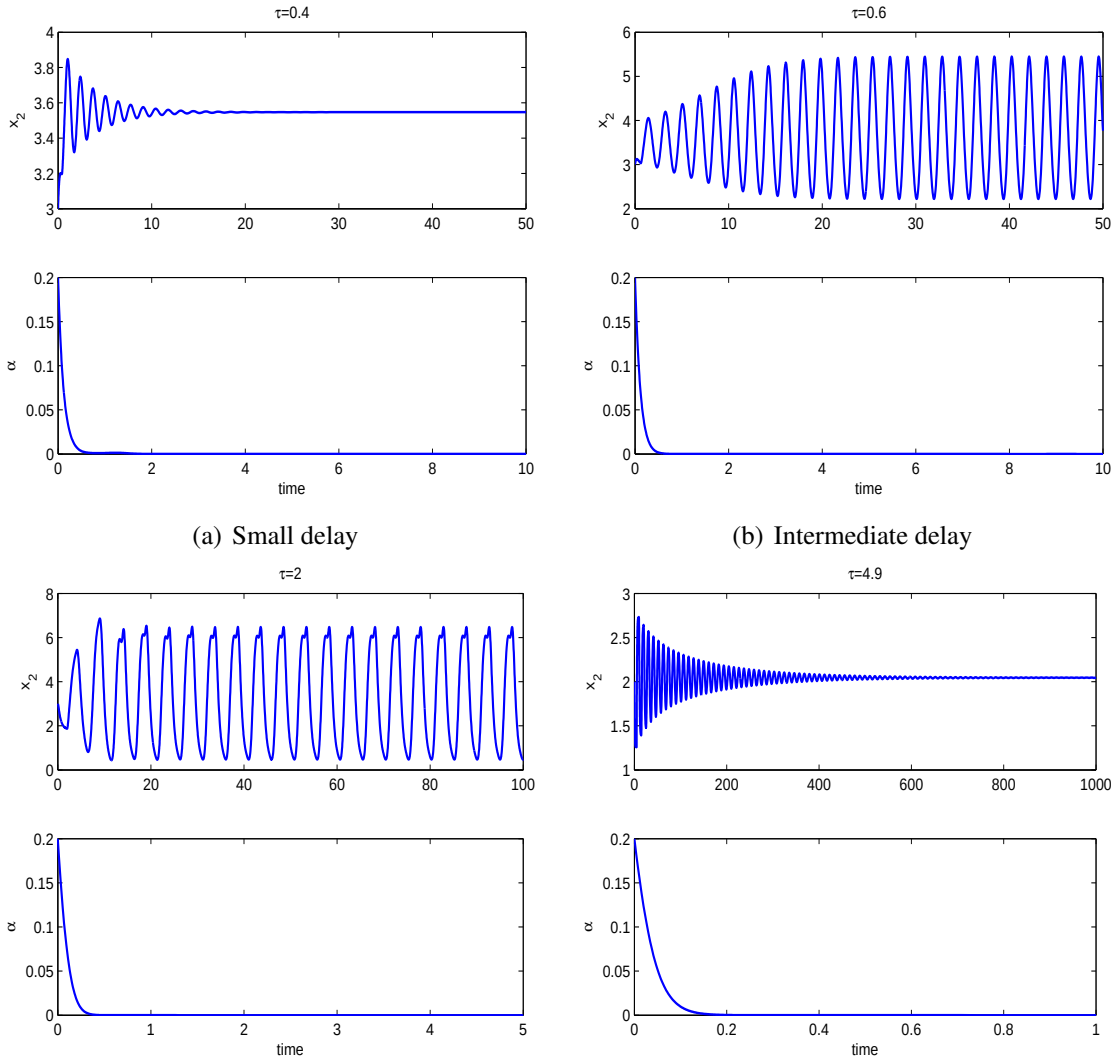

(a) Small delay

(b) Intermediate delay

(c) Intermediate delay

(d) Large delay

Figure 4.3: Stability switch of E_s with varying τ. Parameters are: $b_0 = 8.1311$, $b_1 = 9.1252$, $a = 0.9858$, $p = 0.3290$, $s_2 = 1.3924$, $s_3 = 2.4989$, $y = 0.5376$, $d_2 = 0.7139$, $k = 1$.

By linearizing (4.26) at E_{p1}, we obtain characteristic equation at E_{p1}:

$$G(\lambda,\,\tau) := \lambda^2 - (g_{11}+g_{22})\,\lambda + (g_{11}\,g_{22} - g_{21}\,g_{12}) + (-g_{13}\,\lambda + g_{13}\,g_{22} - g_{21}\,g_{14})\,e^{-\lambda\,\tau} = 0, \quad (4.63)$$

where

$$\begin{aligned}
g_{11} &= -d_2 - (s_2 - s_3\,\bar{\alpha}_1)^2\,y,\\
g_{12} &= 2\,s_3\,(s_2 - s_3\,\bar{\alpha}_1)\bar{x}_{21}\,y,\\
g_{13} &= (b_0 - b_1\,\bar{\alpha}_1)^2\,e^{-a\,\bar{x}_{21}}\,e^{-p\,\tau}(1 - a\,\bar{x}_{21}),\\
g_{14} &= -2\,(b_0 - b_1\,\bar{\alpha}_1)\,e^{-a\,\bar{x}_{21}}\,\bar{x}_{21}\,e^{-p\,\tau}\,b_1,\\
g_{21} &= 2\,k\,\bar{\alpha}_1(1-\bar{\alpha}_1)\,a\,s_3\,(s_2 - s_3\,\bar{\alpha}_1)\,y\,\bar{x}_{21},\\
g_{22} &= 2\,k\,\bar{x}_{21}\,\bar{\alpha}_1\,(1-\bar{\alpha}_1)\,\left(b_1^2\,e^{-a\,\bar{x}_{21}}\,\bar{x}_{21} - s_3^2\,y\right).
\end{aligned} \quad (4.64)$$

When $\tau = 0$, (4.63) reduces to a simplified equation

$$\begin{aligned}
&G(\lambda,0) = 0 \Longleftrightarrow \left[\lambda\,y\,(b_0\,s_3 - b_1\,s_2)^2 - \left(y\,(b_0\,s_3 - b_1\,s_2)^2 + b_1^2\,d_2\right)\,d_2\,\ln(\psi)\right]\\
&\left[\lambda\,\left(y\,(b_0\,s_3 - b_1\,s_2)^2 + b_1^2\,d_2\right)\,a + 2\,k\,[(s_2 - s_3)\,(b_0\,s_3 - b_1\,s_2)\,y - b_1\,d_2]\right.\\
&\left.[(b_0\,s_3 - b_1\,s_2)\,s_2\,y - b_1\,d_2]\,\ln(\psi)\right] = 0.
\end{aligned} \quad (4.65)$$

In fact, when $\tau = 0$, the existence condition of E_{p1}, which is $\psi < \psi_0$ as discussed in the above section, can be simplified to

$$\begin{cases}
\dfrac{d_2\,s_3^2\,y}{y\,(b_0\,s_3 - b_1\,s_2)^2 + b_1^2\,d_2} < 1 \quad \Longleftrightarrow \psi < 1,\\
\mathcal{R}_0^0 = \dfrac{b_0^2}{d_2 + s_2^2 y} > \dfrac{b_0 b_1}{s_2 s_3 y} \quad \Longleftrightarrow \psi < \dfrac{s_2\,s_3\,y}{b_0\,b_1}.
\end{cases} \quad (4.66)$$

When (4.66) holds, it is clear that (4.65) gives negative real eigenvalues, which leads to the following theorem.

Theorem 4.4.7 *If $\tau = 0$, a unique positive equilibrium $E_{p1} = (\bar{x}_{21}, \bar{\alpha}_1)$ is always locally stable when it exists.*

Again, we hope to see whether delay τ would induce stability switch of E_{p1}. Assuming (4.66) holds, we seek pure imaginary root $i\,\omega$ of (4.63) to find possible stability switch of E_{p1} when $\tau > 0$. Similar to the proof of Theorem 4.4.5, we substitute $i\,\omega$ with $\omega > 0$ into (4.63) and obtain

$$\begin{aligned}
F(\omega,\,\tau) &= \omega^4 - \omega^2\,\left(g_{13}^2 + 2\,(g_{11}\,g_{22} - g_{21}\,g_{12}) - (g_{11}+g_{22})^2\right)\\
&+ \left((g_{11}\,g_{22} - g_{21}\,g_{12})^2 - (g_{13}\,g_{22} - g_{21}\,g_{14})^2\right) = 0,
\end{aligned} \quad (4.67)$$

where g_{11}, g_{12}, g_{13}, g_{14}, g_{21}, g_{22} are shown in (4.64). Let

$$\Delta = \left[g_{13}^2 + 2\,(g_{11}\,g_{22} - g_{21}\,g_{12}) - (g_{11}+g_{22})^2\right]^2 - 4\,\left[(g_{11}\,g_{22} - g_{21}\,g_{12})^2 - (g_{13}\,g_{22} - g_{21}\,g_{14})^2\right]. \quad (4.68)$$

By (4.68), we know that (4.67) admits two positive equilibria ω_1^2, ω_2^2 with $\omega_1^2(\tau) < \omega_2^2(\tau)$ if $\Delta > 0$, where

$$\begin{aligned}\omega_1^2(\tau) &= \frac{1}{2}\left[\left(g_{13}^2 + 2\,(g_{11}\,g_{22} - g_{21}\,g_{12}) - (g_{11}+g_{22})^2\right) - \sqrt{\Delta}\right],\\ \omega_2^2(\tau) &= \frac{1}{2}\left[\left(g_{13}^2 + 2\,(g_{11}\,g_{22} - g_{21}\,g_{12}) - (g_{11}+g_{22})^2\right) + \sqrt{\Delta}\right].\end{aligned} \tag{4.69}$$

We first consider possible stability switch of E_{p1} where only ω_2^2 exists. Similar to (4.57) and (4.58), define $\theta(\tau) \in [0,\, 2\,\pi)$ such that

$$\begin{aligned}\sin(\theta(\tau)) &= \frac{\left((g_{11}\,g_{22} - g_{21}\,g_{12}) - \omega_2^2\right)\,\omega_2\,g_{13} - \omega_2\,(g_{11}+g_{22})\,(g_{13}\,g_{22} - g_{21}\,g_{14})}{\omega_2^2\,g_{13}^2 + (g_{13}\,g_{22} - g_{21}\,g_{14})^2},\\ \cos(\theta(\tau)) &= -\frac{\left((g_{11}\,g_{22} - g_{21}\,g_{12}) - \omega_2^2\right)\,(g_{13}\,g_{22} - g_{21}\,g_{14}) + \omega_2^2\,(g_{11}+g_{22})\,g_{13}}{\omega_2^2\,g_{13}^2 + (g_{13}\,g_{22} - g_{21}\,g_{14})^2}.\end{aligned} \tag{4.70}$$

Then stability switch of E_{p1} occurs when τ passes zeros of

$$S_n^0(\tau) := \tau - \frac{\theta(\tau) + n\,2\,\pi}{\omega_2(\tau)},\quad n \in \mathbb{N}, \tag{4.71}$$

where θ is obtained by solving (4.70). Based on [3] and again employing numerical tools, zeros of (4.71) can be obtained. For example, for the set of parameter values in Figure 4.4, by numerically solving $S_0^0(\tau) = 0$, we obtain two zeros $\tau_1 = 0.123$ and $\tau_2 = 0.154$, as shown in Figure 4.4. Because E_{p1} is locally stable when $\tau = 0$, E_{p1} switches from stable to unstable when τ increase to pass $\tau_1 = 0.123$. Again, numerical simulation of the model, as shown in Figure 4.5, confirms that when maturation delay τ is relatively small, the local stability of E_{p1} will not change. However, if τ is larger ($\tau > \tau_1$), delay will destroy the stability of E_{p1} causing periodic oscillations for *both* x_2 and α (in contrast to the situation when E_s loses stability due to Hopf bifurcation in which only $x_2(t)$ oscillates), as demonstrated in Figures 4.5(b) and 4.5(c). When τ further increases to pass the second critical value τ_2 shown in Figure 4.4, E_{p1} regains its stability and both $(x_2(t), \alpha(t))$ tends to the equilibrium E_{p1} again, as indicated in Figure 4.5(d). Here in (4.71), only $S_0^0(\tau) = 0$ has real roots. Hence there are no other critical values of τ other than τ_1 and τ_2 that could induce stability switch of E_{p1}. We point out that parameters chosen in Figure 4.4 only admits positive $\omega_2^2(\tau)$ but $\omega_1^2(\tau)$ is negative, and hence, only allows a unique positive equilibrium of (4.67). Although we cannot prove analytically, our extensive numerical simulations show that $\omega_1^2(\tau)$ is always negative.

As for the case when there are two positive equilibria E_{p1} and E_{p2} under the conditions in Theorem 4.4.3, by numerical simulations, we find that under such conditions, E_{p2} is always unstable. In this case, going through the same procedure of constructing $S_n^0(\tau)$ and numerically solving $S_n^0(\tau) = 0$ reveals that the delay induced instability of E_{p1} is different from the previous

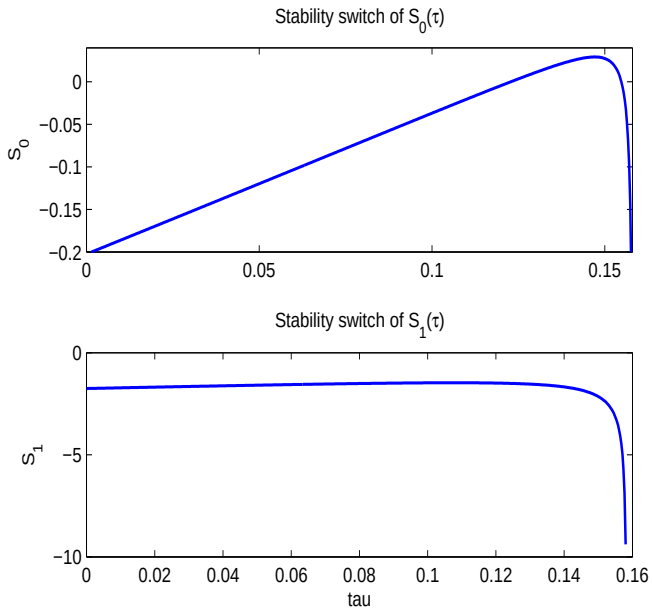

Figure 4.4: Stability switch of E_{p1} where only E_{p1} exists as a positive equilibrium. Parameters are: $b_0 = 3.07552$, $b_1 = 4.33876$, $a = 0.38976$, $p = 0.750396$, $s_2 = 0.562070$, $s_3 = 1.21206$, $y = 4.89360$, $d_2 = 0.552225$, $k = 31.0047$.

case where E_{p2} doesn't exist. As shown in Figure 4.6, $S_n^0(\tau)$ has only a unique positive root, which is different from Figure 4.4 where two distinct positive roots of $S_n^0(\tau)$ exist. Accordingly, E_{p1} will remain asymptotically stable when $\tau > 0$ and is small, and will lose its stability to a periodic solution when τ increases to pass the unique critical value $\tau_c > 0$ through Hopf bifurcation; however, E_{p1} cannot regain its stability through Hopf bifurcation. These numerical observations are illustrated in Figure 4.7, where the parameters gives a unique $\tau_c \approx 2$ from $S_0^0(\tau) = 0$.

4.4.3 Full model

In this section, we consider the original 3-d model (4.6). Since the full model involves three equations with delays and is much more complicated, we will mainly explore it numerically. Before that and in order to simplify the notations, let $p = d_0 + s_0\, y, q = d_1 + s_1\, y$. Similar to the analysis of the reduced 2-d model (4.26), and still making use of $\mathcal{R}_0(\alpha)$ defined in (4.27), we may determine the existence of a semi-trivial equilibrium of (4.6), as stated in the following lemma.

Lemma 4.4.8 *A semi-trivial equilibrium* $E_{s0} = (\bar{x}_{10}, \bar{x}_{20}, 0)$ *exists if*

$$\mathcal{R}_0 > 1, \quad \tau > 0, \tag{4.72}$$

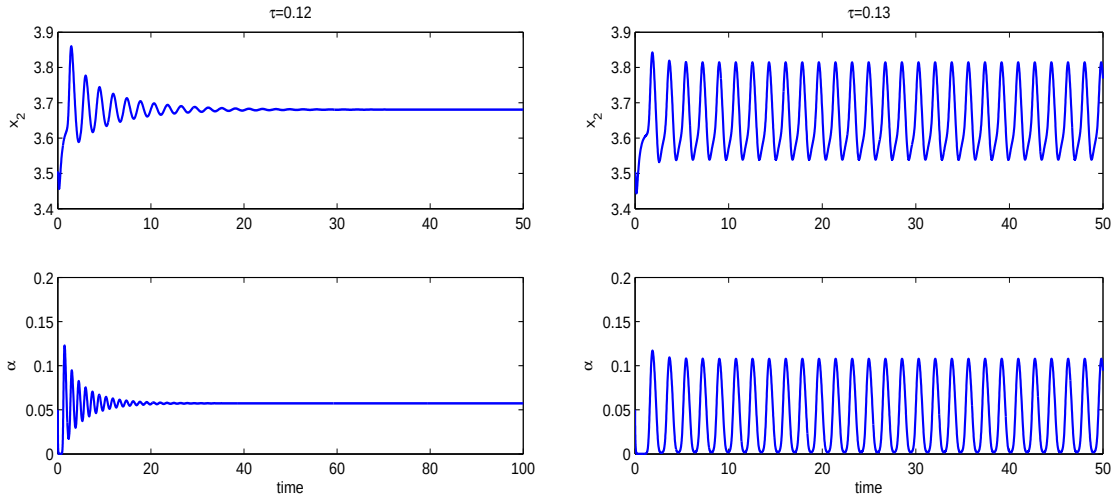

(a) Small delay (b) Intermediate delay

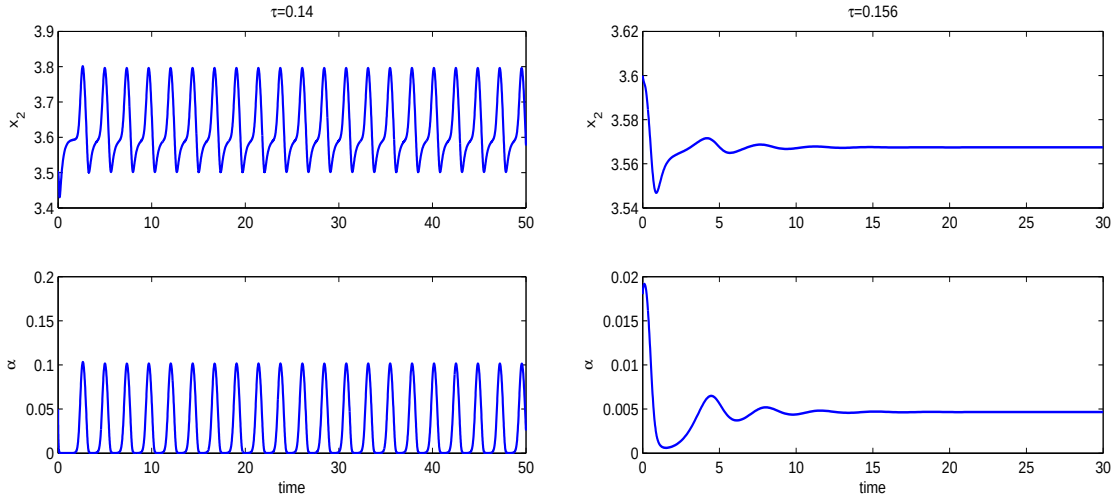

(c) Intermediate delay (d) Large delay

Figure 4.5: Stability switch of E_{p1} with varying τ. Parameters are: $b_0 = 3.07552$, $b_1 = 4.33876$, $a = 0.38976$, $p = 0.750396$, $s_2 = 0.562070$, $s_3 = 1.21206$, $y = 4.89360$, $d_2 = 0.552225$, $k = 31.0047$.

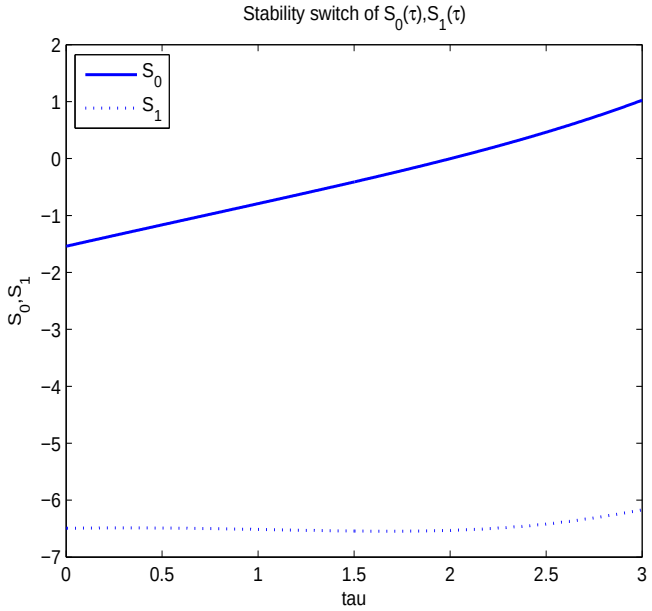

Figure 4.6: Stability switch of E_{p1} where both E_{p1} and E_{p2} may exist. Parameters are: $b_0 = 4.6332$, $b_1 = 5.4762$, $a = 0.1694$, $p = 0.3781$, $d_2 = 0.5693$, $s_2 = 0.5797$, $s_3 = 3.7623$, $y = 4.7052$, $k = 0.7519$.

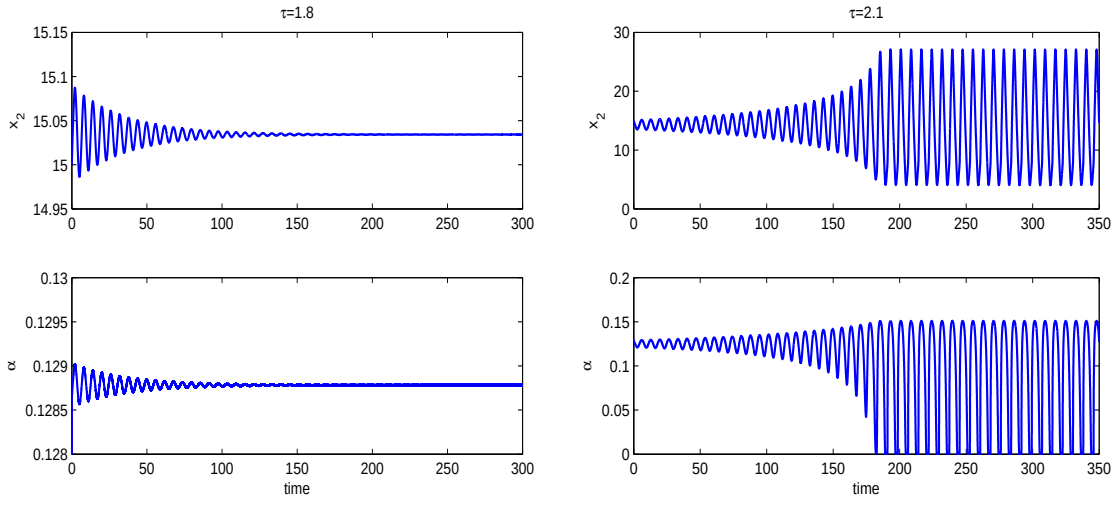

(a) Small delay (b) Large delay

Figure 4.7: Stability switch of E_{p1} with varying τ. Parameters are: $b_0 = 4.6332$, $b_1 = 5.4762$, $a = 0.1694$, $p = 0.3781$, $d_2 = 0.5693$, $s_2 = 0.5797$, $s_3 = 3.7623$, $y = 4.7052$, $k = 0.7519$.

where

$$\begin{aligned} \bar{x}_{10} &= \frac{(d_2 + s_2^2\, y)\,(e^{p\,\tau} - 1)}{a\, p} \ln \mathcal{R}_0, \\ \bar{x}_{20} &= \frac{1}{a} \ln \mathcal{R}_0. \end{aligned} \tag{4.73}$$

Theorem 4.4.9 *Assume that* $\mathcal{R}_0 > 1$, $\tau > 0$ *so that the semi-trivial equilibrium* $E_{s0} = (\bar{x}_{10}, \bar{x}_{20}, 0)$ *exists. Then it is locally asymptotically stable if*

$$\mathcal{R}_0 < \frac{b_0\ (2\, b_1\, p + q\, b_0)}{2\, s_2\, s_3\, y\, p + q\, d_2 + q\, y\, s_2^2} \ \ \textit{and} \ \ \mathcal{R}_0 \le e^2. \tag{4.74}$$

Proof The characteristic equation of system (4.6) at E_{s0} is

$$\begin{aligned} &G(\lambda, \tau) := (\lambda + p)\left[\lambda + k\left(2\, b_0\, b_1\, e^{-a\,\bar{x}_{20}} \bar{x}_{20} + q\, \bar{x}_{10} - 2\, s_2\, s_3\, \bar{x}_{20}\, y\right)\right] \\ &\left[\lambda + d_2 + y\, s_2^2 + e^{-a\,\bar{x}_{20}}\, e^{-p\,\tau}\, b_0^2 (a\, \bar{x}_{20} - 1)\, e^{-\lambda\,\tau}\right], \end{aligned} \tag{4.75}$$

where $\bar{x}_{10}, \bar{x}_{20}$ are shown in (4.73). Equation (4.75) has two real eigenvalues

$$\lambda_1 = -p < 0, \quad \lambda_2 = -k\left(2\, b_0\, b_1\, e^{-a\,\bar{x}_{20}} \bar{x}_{20} + q\, \bar{x}_{10} - 2\, s_2\, s_3\, y\, \bar{x}_{20}\right). \tag{4.76}$$

From (4.76), one can easily verify that

$$\lambda_2 < 0 \quad \text{if} \quad \mathcal{R}_0 < \frac{b_0\ (2\, b_1\, p + q\, b_0)}{2\, s_2\, s_3\, y\, p + q\, d_2 + q\, y\, s_2^2}. \tag{4.77}$$

All other eigenvalues of (4.75) are determined by the same equation as (4.49). The remaining part of the proof is the same as the proof in Theorem 4.4.5 and is thus omitted.

Next, we numerically explore the model dynamics, hoping to gain some information and insights about the roles that anti-predator defense of adult prey play in predator-prey interactions.

We start by considering the impact of the parameter k which represents the sensitivity of adaptive anti-predator response. Figure 4.8(a) illustrates that, for relatively small k, the populations of both juvenile and adult prey, as well as the adaptive defense level of adult prey all converge to positive constants. However, for relatively large k, we have observed periodic oscillations of the solutions of the model, as is shown in Figure 4.8(b). This indicates that, in addition to the maturation delay τ, this parameter of sensitivity may also destabilize an otherwise stable positive equilibrium, leading to the occurrence of periodic solutions.

Note that the parameter b_1 in the function $b(\alpha, x_2)$ describes how fast $b(\alpha, x_2)$ decreases with respect to the increase of α, and hence, accounts for the cost of the anti-predation response in the reproduction. The simulation results show that this parameter can also destabilize an otherwise stable positive equilibrium, as demonstrated in Figure 4.9. Similar destabilizing

effect by another parameter d_1, the cost of the fear in the death rate of the juveniles due to less sufficient care from the parental prey, has also been observed, see Figure 4.10.

Our model assumes a simplest scenario for the predator population: constant predator population y (see the justification for this in the introduction). We now investigate the impact of this parameter. Interestingly, we have found that within certain range of other parameters, increasing y can stabilize an otherwise unstable positive equilibrium, see the simulation results in Figure 4.11.

It is also interesting to examine the impact of key parameters on the components of a positive equilibrium. Figure 4.12 describes the dependence of E_{p1} on predator population y: Figure 4.12(a) indicates that the population of both juveniles and adult prey decreases with increasing population of predators, and Figure 4.12(b) shows that anti-predator defense level of adult prey increases with larger predator population–this is biologically reasonable (not surprising) because adult prey are easier to perceive predation risk with higher density of predators and demonstrate stronger anti-predator behaviours. Figure 4.13 shows the dependence of E_{p1} on the cost of fear b_1 in the reproduction while fixing other parameters. Figure 4.13(a) demonstrates that adult prey population decreases with increasing cost of fear. Figure 4.13(b) indicates that adult prey show weaker anti-predator behaviours if the cost of such behaviours becomes too larger. Notice that from Figure 4.13(a), the population of juvenile increases slowly with large b_1. This is because adult prey devote more energy in juvenile's reproduction and protection of juveniles with larger cost of anti-predator defense. As a consequence, the population of juvenile prey increases slightly.

We also compare the effects that the adaptive defense level of adult prey α has on adult prey population with the case where α is a constant, i.e. the case when there is no adaptation for the strategy α. As shown in Figure 4.14, the steady state population of adult prey $\bar{x}_{21}$ in E_{p1} is always larger than the steady state population of adult prey x_2^+ in (4.17) when $0 \leq \alpha \leq s_2/s_3$. Figure 4.14 indicates that adaptive defense of adults will have more benefit for prey in terms of its long term population.

4.5 Conclusion and discussion

Motivated by a recent experimental field study on the fear effect of prey, we proposed a mathematical model to examine the impact of the fear effect on the population dynamics of prey. The model is in the form of a system of delay differential equations. The novelty lies in the incorporation of *cost of the anti-predation response* of the prey both in the offspring reproduction (produce less) and the death of juveniles (high death rate due to less sufficient care from the parent prey), as well as the *adaptive* defense level. We have theoretically analyzed the

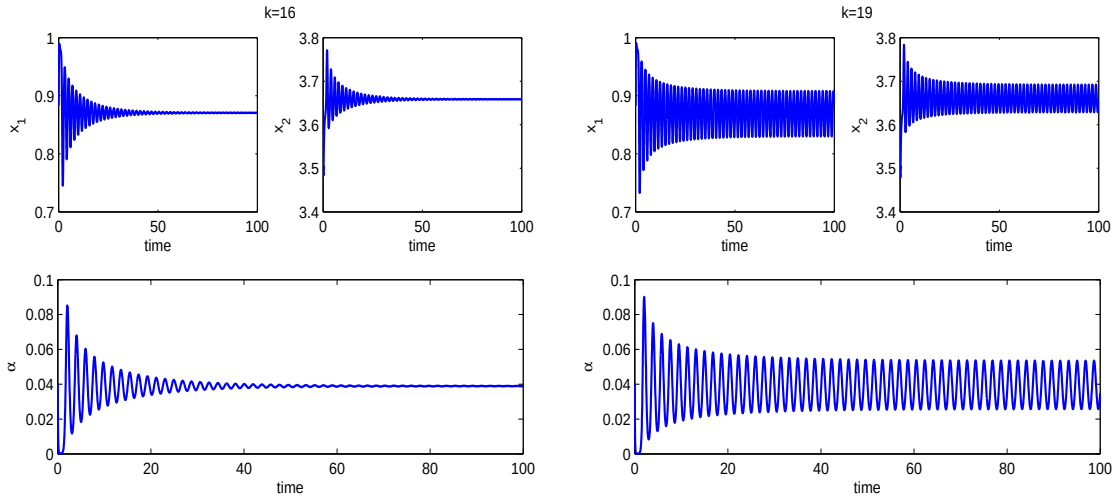

(a) Small k (b) Large k

Figure 4.8: Steady state or oscillation of system (4.6) with varying k. Parameters are: $b_0 = 3.07552$, $b_1 = 4.33876$, $a = 0.38976$, $p = 0.750396$, $q = 0.2$, $s_2 = 0.562070$, $s_3 = 1.21206$, $y = 4.89360$, $\tau = 0.12276$, $d_2 = 0.552225$, $k = 16$ or $k = 19$.

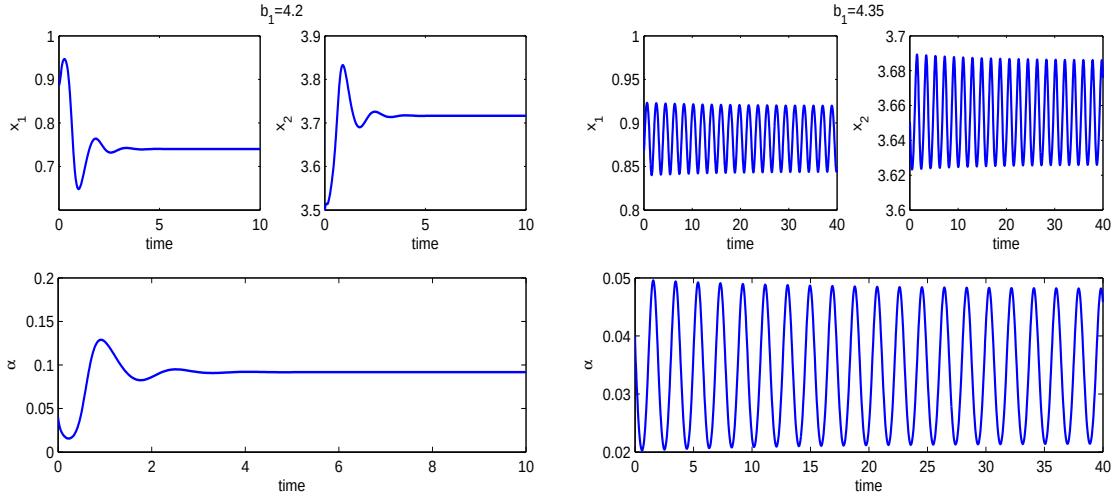

(a) Small b_1 (b) Large b_1

Figure 4.9: Steady state or oscillation of system (4.6) with varying b_1. Parameters are: $b_0 = 3.07552$, $a = 0.38976$, $p = 0.750396$, $q = 0.2$, $s_2 = 0.562070$, $s_3 = 1.21206$, $y = 4.89360$, $\tau = 0.12276$, $d_2 = 0.552225$, $k = 18.31767$, $b_1 = 4.2$ or 4.35.

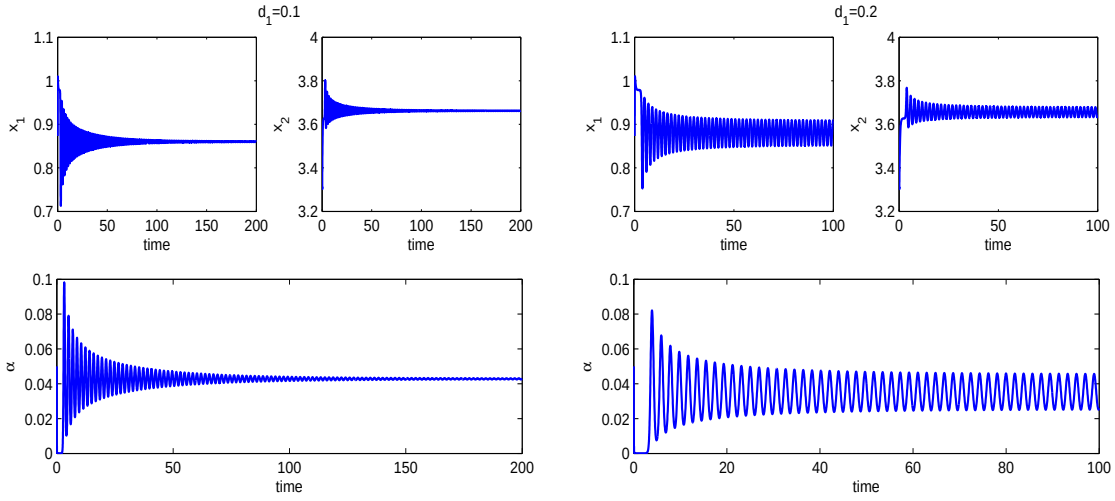

(a) Small d_1 (b) Large d_1

Figure 4.10: Steady state or oscillation of system (4.6) with varying d_1. Parameters are: $b_0 = 3.07552$, $b_1 = 4.33876$, $a = 0.38976$, $p = 0.750396$, $s_2 = 0.562070$, $s_3 = 1.21206$, $\tau = 0.12276$, $d_2 = 0.552225$, $k = 18.31767$, $y = 4.8936$, $s_1 = 0.01$, $d_1 = 0.1$ or 0.2.

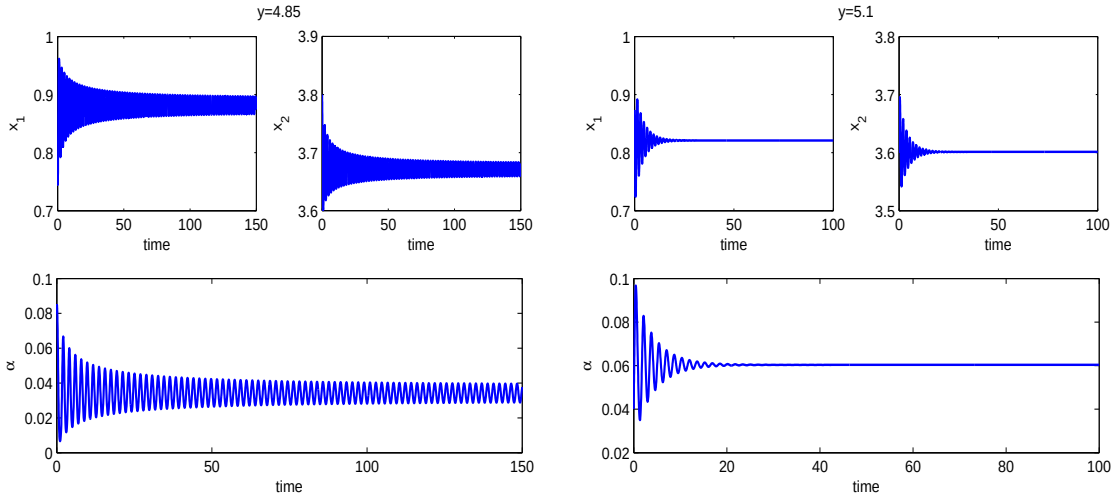

(a) Small y (b) Large y

Figure 4.11: Steady state or oscillation of system (4.6) with varying y. Parameters are: $b_0 = 3.07552$, $b_1 = 4.33876$, $a = 0.38976$, $p = 0.750396$, $q = 0.2$, $s_2 = 0.562070$, $s_3 = 1.21206$, $\tau = 0.12276$, $d_2 = 0.552225$, $k = 18.31767$, $y = 4.85$ or 5.1.

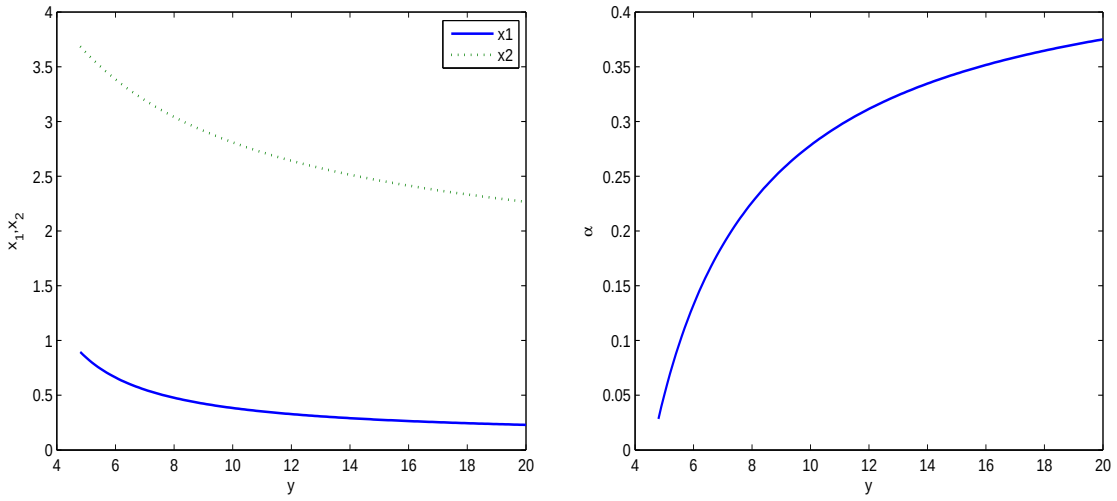

(a) Impact of y on $\bar{x}_1, \bar{x}_2$ (b) Impact of y on α

Figure 4.12: Impact of y on the positive equilibrium $E_{p1}(\bar{x}_1, \bar{x}_2, \bar{\alpha})$. Parameters are: $b_0 = 3.07552$, $b_1 = 4.33876$, $a = 0.38976$, $p = 0.750396$, $q = 0.2$, $s_2 = 0.562070$, $s_3 = 1.21206$, $\tau = 0.12276$, $d_2 = 0.552225$.

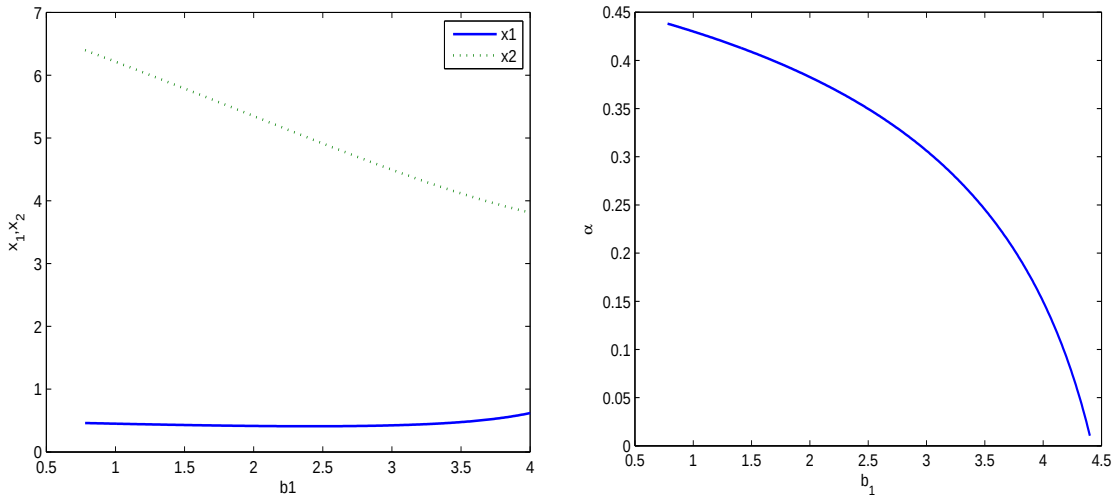

(a) Impact of b_1 on $\bar{x}_1, \bar{x}_2$ (b) Impact of b_1 on α

Figure 4.13: Impact of b_1 on the positive equilibrium $E_{p1}(\bar{x}_1, \bar{x}_2, \bar{\alpha})$. Parameters are: $b_0 = 3.07552$, $a = 0.38976$, $p = 0.750396$, $q = 0.2$, $s_2 = 0.562070$, $s_3 = 1.21206$, $\tau = 0.12276$, $d_2 = 0.552225$, $y = 4.8936$.

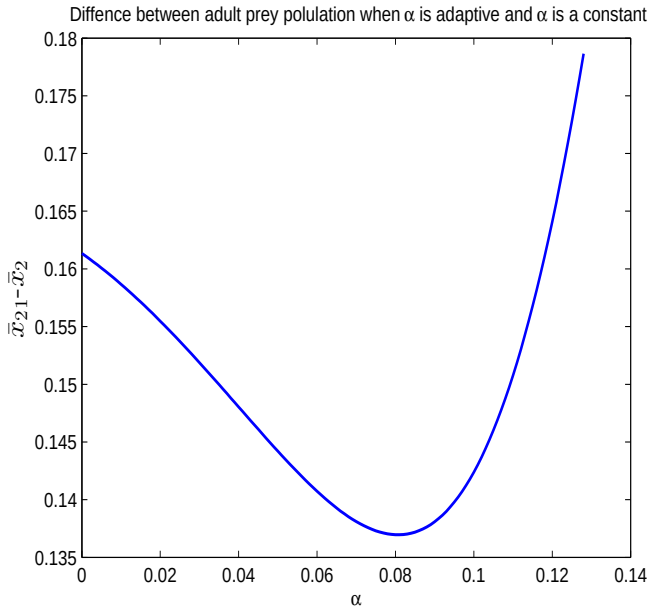

Figure 4.14: Difference between $\bar{x}_{21}$ in $E_{p1}(\bar{x}_{21}, \bar{\alpha}_1)$ and x_2^+ in (4.17). Parameters are: $b_0 = 9.4609$, $b_1 = 13.2741$, $p = 0.0856$, $q = 3.0554$, $d_2 = 0.0467$, $s_2 = 0.2009$, $s_3 = 1.5685$, $y = 2.6194$, $\tau = 2.2335\, a = 5$.

model dynamics for two simpler cases, and numerically explored the full model in the general case with focus on the impact that some key model parameters has on the long term behaviours of solutions of the model.

Results show that, in addition to the maturation delay which has been found to destroy the stability of an equilibrium and cause periodic oscillations in many delay differential equation models, some other essential parameters can also affect the stability of an equilibrium, as illustrated in Section 4. While more rigorous and thorough analysis is still needed to obtain more qualitative and quantitative results about the full 3-d model, the numerical results based on the framework of the model have already provided some important information on the role that an anti-predator response may play in determining the long term population dynamics. For example, in the case of a constant defense level, there may exist an optimal anti-predator defense level, and in the adaptive defense level case, within the certain ranges of parameters, periodic defense levels may be a choice. Most importantly, these results, together with those recent field experimental results offered strong evidences of the significance of the fear effect in predator-prey interactions. All these seem to suggest the incorporation of the fear effect in existing predator-prey models, and consideration of such a new mechanism may lead to interesting and significant findings. For example, our recent work [23] on a simpler model with the fear effect offered an alternative way to eliminate the so-called 'paradox of enrichment'.

In the model, the predator population is assumed to remain as a constant. Although there are numerous situations that fit in such a scenario, as we explained in the introduction, a case where the predator population is not an constant may intrigue further extensions. However, the corresponding model with non-constant predator population is obviously very challenging and difficult to analyze. Furthermore, as far as the predator-prey interaction is concerned, spatial effect is an important factor due to foraging behaviors of both prey and predators. This suggests models with spatial dispersal, in addition to the spatial implicitly predation, anti-predator defense of prey, and the corresponding cost on prey population. All the aforementioned possible extensions are interesting, biologically important but yet mathematically challenging, and we have to leave them for future research projects.

Bibliography

[1] P. A. Abrams. The evolution of predator-prey interactions: theory and evidence. *Annual Review of Ecology and Systematics*, 31:79–105, 2000.

[2] S. M. Baer, B. W. Kooi, Y. A. Kuznetsov, and H. R. Thieme. Multicodimensional bifurcation analysis of a basic two stage population model. *SIAM Journal on Applied Mathematics*, 66:1339–1365, 2006.

[3] E. Beretta and Y. Kuang. Geometric stability switch criteria in delay differential systems with delay dependent parameters. *SIAM Journal on Mathematical Analysis*, 33:1144–1165, 2002.

[4] K. Cooke, P. Van den Driessche, and X. Zou. Interaction of maturation delay and nonlinear birth in population and epidemic models. *Journal of Mathematical Biology*, 39:332–352, 1999.

[5] K. L. Cooke, R. H. Elderkin, and W. Huang. Predator-prey interactions with delays due to juvenile maturation. *SIAM Journal on Applied Mathematics*, 66:1050–1079, 2006.

[6] S. Creel and D. Christianson. Relationships between direct predation and risk effects. *Trends in Ecology & Evolution*, 23:194–201, 2008.

[7] S. Creel, D. Christianson, S. Liley, and J. A. Winnie. Predation risk affects reproductive physiology and demography of elk. *Science*, 315:960–960, 2007.

[8] W. Cresswell. Predation in bird populations. *Journal of Ornithology*, 152:251–263, 2011.

[9] T. Faria. Asymptotic stability for delayed logistic type equations. *Mathematical and Computer Modelling*, 43:433–445, 2006.

[10] S. A. Gourley and Y. Kuang. A stage structured predator-prey model and its dependence on maturation delay and death rate. *Journal of Mathematical Biology*, 49:188–200, 2004.

[11] I. Győri and S. I. Trofimchuk. On the existence of rapidly oscillatory solutions in the Nicholson blowflies equation. *Nonlinear Analysis: Theory, Methods & Applications*, 48: 1033–1042, 2002.

[12] V. Křivan. The Lotka-Volterra predator-prey model with foraging-predation risk trade-offs. *The American Naturalist*, 170:771–782, 2007.

[13] Y. Kuang and J. W-H So. Analysis of a delayed two-stage population model with space-limited recruitment. *SIAM Journal on Applied Mathematics*, 55:1675–1696, 1995.

[14] S. L. Lima. Nonlethal effects in the ecology of predator-prey interactions. *Bioscience*, 48: 25–34, 1998.

[15] S. L. Lima. Predators and the breeding bird: behavioral and reproductive flexibility under the risk of predation. *Biological Reviews*, 84:485–513, 2009.

[16] S. Liu and E. Beretta. A stage-structured predator-prey model of Beddington-DeAngelis type. *SIAM Journal on Applied Mathematics*, 66:1101–1129, 2006.

[17] S. D. Peacor, B. L. Peckarsky, G. C. Trussell, and J. R. Vonesh. Costs of predator-induced phenotypic plasticity: a graphical model for predicting the contribution of nonconsumptive and consumptive effects of predators on prey. *Oecologia*, 171:1–10, 2013.

[18] M. J. Sheriff, C. J. Krebs, and R. Boonstra. The sensitive hare: sublethal effects of predator stress on reproduction in snowshoe hares. *Journal of Animal Ecology*, 78:1249–1258, 2009.

[19] H. Shu, L. Wang, and J. Wu. Global dynamics of Nicholsons blowflies equation revisited: Onset and termination of nonlinear oscillations. *Journal of Differential Equations*, 255: 2565–2586, 2013.

[20] T. O. Svennungsen, Ø. H. Holen, and O. Leimar. Inducible defenses: continuous reaction norms or threshold traits? *The American Naturalist*, 178:397–410, 2011.

[21] Y. Takeuchi, W. Wang, S. Nakaoka, and S. Iwami. Dynamical adaptation of parental care. *Bulletin of Mathematical Biology*, 71:931–951, 2009.

[22] W. Wang, S. Nakaoka, and Y. Takeuchi. Invest conflicts of adult predators. *Journal of Theoretical Biology*, 253:12–23, 2008.

[23] X. Wang, L. Y. Zanette, and X. Zou. Modelling the fear effect in predatorprey interactions. *Journal of Mathematical Biology*, 2016. doi: 10.1007/s00285-016-0989-1.

[24] J. Wei and M. Li. Hopf bifurcation analysis in a delayed Nicholson blowflies equation. *Nonlinear Analysis: Theory, Methods & Applications*, 60:1351–1367, 2005.

[25] A. J. Wirsing and W. J. Ripple. A comparison of shark and wolf research reveals similar behavioral responses by prey. *Frontiers in Ecology and the Environment*, 9:335–341, 2011.

[26] M. Yamamichi, T. Yoshida, and A. Sasaki. Comparing the effects of rapid evolution and phenotypic plasticity on predator-prey dynamics. *The American Naturalist*, 178:287–304, 2011.

[27] L. Y. Zanette, A. F. White, M. C. Allen, and M. Clinchy. Perceived predation risk reduces the number of offspring songbirds produce per year. *Science*, 334:1398–1401, 2011.

Chapter 5

Pattern formation of a predator-prey model with the cost of anti-predator behaviors

5.1 Introduction

In ecological systems, spatially heterogeneous distributions of many species have been observed, for example, patchiness of plankton in aquatic systems ([27]). Although such heterogeneity of species may be attributed to unevenly distributed landscapes, it may also occur in a closely homogeneous environment ([17, 27]). One interesting question is that what are the mechanisms behind the spatial heterogeneity of a species in homogeneous environment? Generally, movement or dispersal of a species and its interactions with other species may lead to pattern formation, and predator-prey type is such an interaction.

Pattern formation of predator-prey systems has been studied extensively (see [3, 20, 24, 26] for example). In general, if both prey and predators move randomly in habitats, prey-dependent only functional responses, including the Holling type I, II, III functional responses, can't generate spatially heterogeneous distributions. In such systems, the density-dependent death rate of predators or the Allee effect in prey's growth plays a critical role in determining spatial patterns ([19, 20]). On the other hand, competition between predators alone may allow pattern formation in predator-prey systems, which includes ratio-dependent functional response, the Beddington-DeAngelis functional response, and their generalizations ([3, 24, 26]).

In addition to pure random movement of prey and predators, directed movement of predators has attracted much attention in recent years and has inspired numerous researches about the so called prey-taxis problems (see [1, 8, 16, 28, 29, 32] for example). A common feature of

the models in the aforementioned papers lies in that the movement of predators is affected by the density gradient of prey, in addition to random movement. In analogy to the well-known chemotaxis, predators are attracted by prey-taxis and tend to move to habitats with higher prey density. Such biased movement allows predators to forage prey more effectively. In [1, 28], the global existence of weak solution and classical solution were proved respectively. As an extension of [1, 28], the authors in [32] proved the global existence of classical solution with more general local reaction terms and established the uniform persistence of the solutions as well. In [16], pattern formation was studied under various functional responses between prey and predators. The authors concluded that pattern formation may occur if the prey-taxis was small and certain functional responses or growth functions were chosen ([16]).

Besides the fact that predators forage prey, prey may avoid predators actively as well. Almost all species perceive predation risk to some extent and avoid predation by showing various anti-predator behaviors ([9, 10]). More importantly, such anti-predator behaviors carry a cost on the reproduction success of prey ([33]). Zanette *et al.* [33] experimentally verified that anti-predator behaviors alone caused a 40% reduction in the reproduction rate of song-sparrows when all direct predations were eliminated (see [30] for a thorough discussion about the cost of fear). Recent work of Ryan and Cantrell [23] modelled avoidance behaviors of prey in an intraguild predation community with heterogeneous distribution of resources. Biktashev *et al.* [8] also considered avoided prey but in a homogeneous environment and identified several patterns numerically. However, the cost of anti-predator behaviors of prey is ignored in the models of Ryan and Cantrell and Biktashev *et al.* [8, 23].

In this paper, we extend the model based on Wang *et al.* by explicitly incorporating spatial effects, where spatial structures are ignored in [30]. We study how the anti-predator behaviors and the corresponding cost would affect the spatial distribution of prey and predators. In Section 2, the model formulation including the so-called predator-taxis is proposed. In Section 3, the global existence of classical solution is established. In Section 4, pattern formation is analyzed both theoretically and numerically for different functional responses. We end the paper in Section 5 by giving conclusions and discussions.

5.2 Model Formulation

Let $u(x,t)$ and $v(x,t)$ represent the densities of prey and predators at position x and time t respectively. As discussed in the introduction, we assume that predators move randomly to forage prey but prey can perceive predation risk and act accordingly to avoid predators actively ([9, 10]). As a consequence, the dispersal of prey is a directed movement towards lower density of predators in addition to random movement. Ideally, the avoidance behavior of prey leads to a

repulsion of prey to lower gradient of predator density. Therefore, the flux of prey is

$$J_u = -d_u \nabla u - \gamma(u, v)\, u \nabla v,$$

and the flux of predators is

$$J_v = -d_v \nabla v,$$

where $\gamma(u, v) \geq 0$ represents the repulsion effect of the predator-taxis. Hence, a general reaction-diffusion-advection model with avoidance behaviors of prey is

$$\begin{aligned} u_t &= \nabla \cdot (d_u \nabla u + \gamma(u, v)\, u \nabla v) + f(u, v), \\ v_t &= d_v \Delta v + g(u, v), \end{aligned} \tag{5.1}$$

where $f(u, v)$ and $g(u, v)$ represent local interactions of predators and prey, d_u, d_v are random diffusion rates of prey and predators respectively, $\gamma(u, v)$ is the sensitivity of prey to predation risk (i.e. predator-taxis). Here, we assume that

$$\gamma(u, v) = \beta(u)\, \alpha(v). \tag{5.2}$$

Taking into account the volume filling effect ([12, 13, 22]) for $\gamma(u, v)$, we adopt $\alpha(v) = \alpha$ as a constant and

$$\beta(u) = \begin{cases} 1 - \dfrac{u}{M}, & \text{if } \ 0 \leq u \leq M, \\ 0, & \text{if } \ M < u, \end{cases} \tag{5.3}$$

where M measures the maximum number of prey that a unit volume can accommodate. If the number of prey goes beyond the volume M, prey can no longer squeeze into nearby space and therefore the tendency of directed movement goes to 0. For local reaction terms, we consider

$$\begin{aligned} f(u, v) &= f_0(k_0\, \alpha, v)\, r_0\, u - d\, u - a\, u^2 - u\, p(u, v)\, v, \\ g(u, v) &= v\, (-m(v) + c\, u\, p(u, v)), \end{aligned} \tag{5.4}$$

where

$$f_0(k_0\, \alpha, v) = \frac{1}{1 + k_0\, \alpha\, v} \tag{5.5}$$

satisfies the same hypotheses as $f(k, v)$ in [30] with k_0 as a nonnegative constant. In fact, this function models the cost of anti-predator responses in the reproduction rate of prey. The successful reproduction rate of prey decreases if the defense level or equivalently predator-taxis sensitivity α increases. Similarly, higher predator density also decreases the local reproduction rate of prey because it would be easier for the prey to perceive predation risk and adopt corresponding avoidance behaviors in the presence of more predators. Here k_0 is a constant which reflects the magnitude that anti-predators behaviors exert on the local reproduction of

prey. In (5.4), d is the natural death rate of prey, a represents the death due to intra-species competition, $p(u, v)$ denotes the functional response between predators and prey, and $m(v)$ is the death rate of predators. We consider either density-independent death rate or density-dependent death rate of predators, i.e.

$$m(v) = m_1 \quad \text{or} \quad m(v) = m_1 + m_2\, v. \tag{5.6}$$

As indicated in [19, 20], the density dependence of predator mortality plays a critical role in pattern formation under certain situations.

We assume that individuals live in an isolated bounded domain $\Omega \in R^n$ with homogeneous environment and $\partial\Omega$ is smooth. Hence, no-flux boundary condition is imposed

$$\begin{aligned} J_u \cdot n &= d_u \frac{\partial u}{\partial \mu} + \gamma(u, v)\, u\, \frac{\partial v}{\partial \mu} = 0, \\ J_v \cdot n &= d_v \frac{\partial v}{\partial \mu} = 0, \end{aligned} \tag{5.7}$$

where μ is the unit outward normal vector at $\partial\Omega$. In fact, no-flux boundary condition (5.7) is equivalent to Neumann boundary condition

$$\frac{\partial u}{\partial \mu} = 0, \frac{\partial v}{\partial \mu} = 0, \quad \forall x \in \partial\Omega. \tag{5.8}$$

Therefore, by (5.1), (5.2), (5.4) and (5.8), we obtain a spatial model with the avoidance behaviors of prey and the cost of anti-predator behaviors, given by the following system

$$\begin{aligned} &\frac{\partial u}{\partial t} = d_u\, \Delta u + \alpha \nabla \cdot (\beta(u)\, u \nabla v) + \frac{r_0\, u}{1 + k_0\, \alpha\, v} - d\, u - a\, u^2 - u\, p(u, v)\, v, \\ &\frac{\partial v}{\partial t} = d_v\, \Delta v + v\, (-m(v) + c\, u\, p(u, v)), \\ &\frac{\partial u}{\partial \mu} = 0, \frac{\partial v}{\partial \mu} = 0, \quad \forall x \in \partial\Omega, \\ &u(x, 0) = u_0(x) \geq 0, v(x, 0) = v_0(x) \geq 0, \end{aligned} \tag{5.9}$$

where $u_0(x), v_0(x)$ are continuous functions.

5.3 Global existence of classical solution

First, we establish the global existence of classical solutions of (5.9). It is clear that the carrying capacity of prey in (5.9) is $K = (r_0 - d)/a$. By [22], we assume that

$$M > \frac{r_0 - d}{a}, \tag{5.10}$$

which is reasonable because K measures the maximum capacity of the environment but M merely represents the maximum number that one unit volume can be filled by prey. Notice that $\beta(u)$ is not differentiable at $u = M$. In order to obtain classical solutions, similar to [31], we make a smooth extension of $\beta(u)$ by

$$\bar{\beta}(u) = \begin{cases} > 1, & u < 0, \\ \beta(u), & 0 \le u \le M, \\ < 0, & M < u. \end{cases} \tag{5.11}$$

By proving the global existence of classical solutions of system

$$\begin{aligned} &\frac{\partial u}{\partial t} = d_u \Delta u + \alpha \nabla \cdot (\bar{\beta}(u)\, u \nabla v) + \frac{r_0\, u}{1 + k_0\, \alpha\, v} - d\, u - a\, u^2 - u\, p(u, v)\, v, \\ &\frac{\partial v}{\partial t} = d_v \Delta v + v\,(-m(v) + c\, u\, p(u, v)), \\ &\frac{\partial u}{\partial \mu} = 0, \frac{\partial v}{\partial \mu} = 0, \quad \forall x \in \partial\Omega, \\ &u(x, 0) = u_0(x) \ge 0, v(x, 0) = v_0(x) \ge 0, \end{aligned} \tag{5.12}$$

we obtain the global existence of classical solutions of (5.9) because $\beta(u) = \bar{\beta}(u)$ if $0 \le u \le M$ and we will show that $u \in [0, M]$ later. Let $\rho \in (n, +\infty)$, then $W^{1,\rho}\left(\bar{\Omega}, R^2\right)$ is continuously embedded in $C\left(\Omega, R^2\right)$. We consider solutions of (5.12) in

$$X := \left\{ \omega \in W^{1,\rho}\left(\Omega, R^2\right) | \, \frac{\partial \omega}{\partial \mu} = 0 \ \text{ on } \ \partial\Omega \right\}.$$

Then we have the following lemma.

Lemma 5.3.1 *The following statements hold:*

(i) System (5.12) *has a unique solution* $(u(x,t), v(x,t)) \in X$ *defined on* $\Omega \times (0, T)$ *satisfying* $(u, v) \in C((0, T), X) \cap C^{2,1}\left((0, T) \times \bar{\Omega}, R^2\right)$, *where* T *depends on initial data* $(u_0, v_0) \in X$.

(ii) Define $X_1 = \{(u, v) \in R^2 | \, 0 \le u \le M, \ v \ge 0\}$ *at* $G \subset R^2$ *such that* $X_1 \subset G$. *If for every* $G \subset R^2$ *containing* X_1, (u, v) *is bounded away from the boundary of* G *in* $L^\infty(\Omega)$ *norm for* $t \in (0, T)$, *then* $T = \infty$, *meaning that the solution* (u, v) *exists globally.*

Proof Let $\omega = (u, v)^{\mathsf{T}}$. Then system (5.12) can be written as

$$\begin{cases} \omega_t = \nabla \cdot (a(\omega) \nabla \omega) + \mathcal{F}(\omega) \quad \text{in } \ \Omega \times (0, +\infty), \\ \mathcal{B}\omega = 0 \quad \text{on } \ \partial\Omega \times (0, +\infty), \\ \omega(\cdot, 0) = (u_0, v_0)^{\mathsf{T}} \quad \text{in } \ \Omega, \end{cases} \tag{5.13}$$

where

$$a(\omega) = \begin{pmatrix} d_u & \alpha\bar{\beta}(u)\,u \\ 0 & d_v \end{pmatrix}, \tag{5.14}$$

and

$$\begin{aligned} \mathcal{F}(\omega) &= \left(\frac{r_0\,u}{1+k_0\,\alpha\,v} - d\,u - a\,u^2 - u\,p(u,v)\,v, \quad v\,(-m(v) + c\,u\,p(u,v))\right)^{\mathsf{T}}, \\ \mathcal{B}\omega &= \frac{\partial\omega}{\partial n}. \end{aligned} \tag{5.15}$$

Because eigenvalues of $a(\omega)$ are all positive, then (5.13) is normally elliptic ([5, 6]). Hence local existence in (i) follows from Theorem 7.3 in [5]. Because (5.13) is an upper-triangular system, global existence of solution in (ii) follows from Theorem 5.2 in [4].

From (ii) of Lemma 5.3.1, to prove the global existence of solutions, it remains to show that (u, v) are bounded away from the boundary of G in L^∞ norm.

Theorem 5.3.2 *Assume that* $0 \le u_0 \le M$, *then the solution* (u, v) *satisfies* $u(x,t) \ge 0,\ v(x,t) \ge 0$, *and it exists globally in time.*

Proof Define the operator

$$\mathcal{L}u = u_t - d_u\,\Delta u - \alpha\nabla(\bar{\beta}(u)\,u\nabla v) - \frac{r_0\,u}{1+k_0\,\alpha\,v} + d\,u + a\,u^2 + p(u,v)\,u\,v. \tag{5.16}$$

Because $0 \le u_0$, $u = 0$ is a lower solution of the equation. Plug in $u = M$ into (5.16) to obtain

$$\begin{aligned} \mathcal{L}M &= -\frac{r_0\,M}{1+k_0\,\alpha\,v} + d\,M + a\,M^2 + p(M,v)\,M\,v \\ &= M\left(d + a\,M + p(M,v)\,v - \frac{r_0}{1+k_0\,\alpha\,v}\right). \end{aligned} \tag{5.17}$$

If $v \ge 0$, then we obtain

$$\mathcal{L}M \ge M\,(d + a\,M - r_0)\,. \tag{5.18}$$

Because of the restriction (5.10), choosing sufficiently large M gives

$$\mathcal{L}M \ge 0. \tag{5.19}$$

In addition, we have

$$\frac{\partial M}{\partial\mu} = 0, \qquad M \ge u_0. \tag{5.20}$$

By (5.19) and (5.20), we know that $u = M$ is an upper solution of the u equation. Therefore, by comparison principle of parabolic equations ([25]), we have

$$0 \le u \le M. \tag{5.21}$$

Now we prove the L^∞ norm of v is bounded. Here we show only the proof for the case of $m(v) = m_1$ because the proof of the case where $m(v) = m_1 + m_2\, v$ is similar and is thus omitted. Choose $v(0) = v_0 \geq 0$. Then it is obvious that $v = 0$ is a lower solution of the v equation, which gives $v \geq 0$. It remains to show that $\|v\|_{L^\infty(\Omega)}$ is bounded. Integrating the first equation of (5.12), we obtain

$$\begin{aligned}\int_\Omega u_t\, dx &= \int_\Omega \nabla\cdot\Big(d_u\,\nabla u + \alpha\,\bar\beta(u)\,u\,\nabla v\Big)\,dx + \int_\Omega\left(\frac{r_0\,u}{1+k_0\,\alpha\,v} - d\,u - a\,u^2 - p(u,v)\,u\,v\right)dx\\ &= \int_{\partial\Omega}\Big(d_u\,\nabla u + \alpha\,\bar\beta(u)\,u\,\nabla v\Big)\cdot n\,dS + \int_\Omega\left(\frac{r_0\,u}{1+k_0\,\alpha\,v} - d\,u - a\,u^2 - p(u,v)\,u\,v\right)dx\\ &= \int_\Omega\left(\frac{r_0\,u}{1+k_0\,\alpha\,v} - d\,u - a\,u^2 - p(u,v)\,u\,v\right)dx.\end{aligned} \tag{5.22}$$

Similarly, integrating the second equation of (5.12) gives

$$\int_\Omega v_t\,dx = \int_\Omega v\,(-m_1 + c\,p(u,v)\,u)\,dx. \tag{5.23}$$

Multiplying (5.22) by c and adding the resulting equation to (5.23) gives

$$\begin{aligned}\frac{d}{dt}\int_\Omega (c\,u+v)\,dx &= \int_\Omega\left(\frac{r_0\,c\,u}{1+k_0\,\alpha\,v} - c\,d\,u - c\,a\,u^2 - m_1\,v\right)dx\\ &= c\int_\Omega\left(\frac{r_0}{1+k_0\,\alpha\,v} + m_1 - d - a\,u\right)u\,dx - m_1\int_\Omega (c\,u+v)\,dx\\ &\leq c\int_\Omega (r_0+m_1)\;u\,dx - m_1\int_\Omega (c\,u+v)\;dx\\ &\leq c\,|\Omega|(r_0+m_1)\,M - m_1\int_\Omega (c\,u+v)\;dx.\end{aligned} \tag{5.24}$$

By (5.24), we obtain

$$\frac{d}{dt}\|c\,u+v\|_{L^1} \leq c\,|\Omega|(r_0+m_1)\,M - m_1\,\|c\,u+v\|_{L^1} \tag{5.25}$$

From (5.25), we obtain that

$$\limsup_{t\to\infty}\|c\,u+v\|_{L^1} \leq \frac{c\,|\Omega|(r_0+m_1)\,M}{m_1},$$

which shows that $\|c\,u+v\|_{L^1}$ is bounded. From (5.12), the growth of v is dependent only on u, (i.e. predators are specialist predators), which falls into "food pyramid" condition in [2]. Hence by Theorem 3.1. in [2], the boundedness of $\|v\|_{L^1}$ implies that of $\|v\|_{L^\infty}$ and this completes the proof.

5.4 Pattern Formation

Now we analyze the pattern formation of (5.9) with general reaction terms defined in (5.4). Assume that (u_s, v_s) is a spatially homogeneous steady state of (5.9). Let

$$u(x,t) = u_s + \epsilon\,\tilde{u}(x,t), \quad v(x,t) = v_s + \epsilon\,\tilde{v}(x,t), \tag{5.26}$$

where $\epsilon \ll 1$. By substituting (5.26) into (5.9) with general reaction terms, equating first-order terms with respect to ϵ and neglecting higher-order terms, we obtain the linearized system at (u_s, v_s) :

$$\begin{aligned} \frac{\partial u}{\partial t} &= d_u\,\Delta u + \alpha\,\beta(u_s)\,u_s\,\Delta v + f_u(u_s, v_s)\,u + f_v(u_s, v_s)\,v, \\ \frac{\partial v}{\partial t} &= d_v\,\Delta v + g_u(u_s, v_s)\,u + g_v(u_s, v_s)\,v, \end{aligned} \tag{5.27}$$

where $u(x,t), v(x,t)$ are still used instead of $\tilde{u}(x,t), \tilde{v}(x,t)$ for notational convenience. The linearized system (5.27) can be written as the matrix form:

$$\frac{\partial \omega}{\partial t} = D\,\Delta\omega + A\,\omega, \tag{5.28}$$

where

$$\omega = \begin{pmatrix} u \\ v \end{pmatrix}, \quad D = \begin{pmatrix} d_u & \alpha\,\beta(u_s)\,u_s \\ 0 & d_v \end{pmatrix}, \quad A = \begin{pmatrix} f_u & f_v \\ g_u & g_v \end{pmatrix}.$$

By (5.28), the characteristic polynomial of the linearized system at (u_s, v_s) is

$$|\lambda\,\mathrm{I} + k^2\,D - A| = 0, \tag{5.29}$$

where $k \geq 0$ is the wave number ([21]). Expanding the left side of (5.29), we obtain that

$$\lambda^2 + a\left(k^2\right)\,\lambda + b\left(k^2\right) = 0, \tag{5.30}$$

where

$$\begin{aligned} a\left(k^2\right) &= (d_u + d_v)\,k^2 - (f_u + g_v)\,, \\ b\left(k^2\right) &= d_u\,d_v\,k^4 + (g_u\,\alpha\,\beta(u_s)\,u_s - f_u\,d_v - g_v\,d_u)\,k^2 + f_u\,g_v - f_v\,g_u. \end{aligned} \tag{5.31}$$

Here in (5.30), $\lambda = \lambda\,(k)$ are eigenvalues which determine the stability of the steady state (u_s, v_s). For $k = 0$, the two roots of (5.30) satisfy

$$\lambda_1^0 + \lambda_2^0 = f_u + g_v, \quad \lambda_1^0\,\lambda_2^0 = f_u\,g_v - f_v\,g_u. \tag{5.32}$$

Assume that

$$f_u + g_v < 0,\ f_u\,g_v - f_v\,g_u > 0, \tag{5.33}$$

meaning that the steady state (u_s, v_s) is linearly stable when there is no spatial effect. Now for $k > 0$, the two roots of (5.30) satisfy

$$\begin{cases} \lambda_1^k + \lambda_2^k = (f_u + g_v) - (d_u + d_v)\ k^2, \\ \lambda_1^k\, \lambda_2^k = d_u\, d_v\, k^4 + (g_u\, \alpha\, \beta(u_s)\, u_s - f_u\, d_v - g_v\, d_u)\, k^2 + f_u\, g_v - f_v\, g_u. \end{cases} \tag{5.34}$$

Because of $d_u > 0, d_v > 0$ and assumption (5.33), we obtain that $\lambda_1^k + \lambda_2^k < 0$ for all $k = 1, 2 \cdots$ from (5.34). Therefore, if $\lambda_1^k\, \lambda_2^k > 0$ for all $k > 0$, then (u_s, v_s) remains stable. If $\lambda_1^k\, \lambda_2^k < 0$ for some $k > 0$, then (u_s, v_s) becomes unstable, and such diffusion driven instability is often referred to as the Turing instability, which will lead to occurrence of spatially heterogeneous steady state, implying formation of spatial patterns. Summarizing the above analysis, we have the following Theorem.

Theorem 5.4.1 *Assume* (5.33) *holds, spatial homogeneous steady state* (u_s, v_s) *of* (5.9) *may lose stability only if*

$$g_u\, \alpha\, \beta(u_s)\, u_s - f_u\, d_v - g_v\, d_u < 0, \tag{5.35}$$

$$(g_u\, \alpha\, \beta(u_s)\, u_s - f_u\, d_v - g_v\, d_u)^2 - 4\, d_u\, d_v\ (f_u\, g_v - f_v\, g_u) > 0 \tag{5.36}$$

hold.

Remark 5.4.2 *Under the assumption* (5.33)*,* $f_u\, g_v - f_v\, g_u > 0$*, and hence, by Theorem 5.4.1, pattern formation of* (5.9) *can not occur if*

$$g_u\, \alpha\, \beta(u_s)\, u_s > f_u\, d_v + g_v\, d_u. \tag{5.37}$$

5.4.1 Linear functional response

Following above general analysis of pattern formation of spatial homogeneous equilibrium, we now proceed to further detailed analysis when a particular functional response is chosen. First, we analyze possible pattern formation of (5.9) with the linear functional response, where $p(u, v) = p$ in (5.9). Either for the density-independent death rate or for the density-dependent death rate of predators in (5.6), system (5.9) admits several spatial homogeneous steady states. For (5.9), in addition to a trivial equilibrium $E_0(0, 0)$, a semi-trivial equilibrium $E_1((r_0 - d)/a, 0)$ exists if $r_0 > d$ is satisfied. There exists a unique positive equilibrium $E(\bar{u}, \bar{v})$ for either predator death function in (5.6) if

$$r_0 > d + \frac{a\, m_1}{c\, p} \tag{5.38}$$

holds. However, formulas for $E(\bar{u}, \bar{v})$ are different for each function, where

$$\begin{cases} \bar{u} = \dfrac{m_1}{c\,p},\ \bar{v} = \dfrac{\left(\alpha\,c\,d\,k_0\,p + a\,\alpha\,k_0\,m_1 + c\,p^2\right) - \sqrt{\Delta_1}}{-2\,k_0\,\alpha\,p^2\,c}, \\ \Delta_1 = 4\,\alpha\,c\,k_0\,p^2\,(-c\,d\,p + c\,p\,r_0 - a\,m_1) + (-\alpha\,c\,d\,k_0\,p - a\,\alpha\,k_0\,m_1 - c\,p^2)^2 \end{cases} \tag{5.39}$$

if $m(v) = m_1$ while

$$\begin{cases} \bar{v} = \dfrac{\left(c\,p^2 + a\,m_2 + k_0\,\alpha\,(d\,c\,p + a\,m_1)\right) - \sqrt{\Delta_2}}{-2\,k_0\,\alpha\,(c\,p^2 + a\,m_2)},\ \bar{u} = \dfrac{m_1 + m_2\,\bar{v}}{c\,p}, \\ \Delta_2 = 4\,k_0\,\alpha\,(c\,p^2 + a\,m_2)\,(-c\,d\,p + c\,p\,r_0 - a\,m_1) + (-\alpha\,c\,d\,k_0\,p - a\,\alpha\,k_0\,m_1 - c\,p^2 - a\,m_2)^2 \end{cases} \tag{5.40}$$

if $m(v) = m_1 + m_2\,v$. Direct calculations show that pattern formation can not occur around any constant steady state if the functional response is linear, which leads to the following proposition.

Proposition 5.4.3 *Either for $m(v) = m_1$ or for $m(v) = m_1 + m_2\,v$, pattern formation can not occur around any of the constant steady states E_0, E_1, and $E(\bar{u}, \bar{v})$.*

Proof Because the proofs for all steady states are similar, we show only the proof of non-existence of pattern formation around $E(\bar{u}, \bar{v})$ when $m(v) = m_1$ here. Calculations give

$$f_u = -a\,\bar{u} < 0,\ f_v = \bar{u}\left(-\frac{r_0\,k_0\,\alpha}{(1 + k_0\,\alpha\,\bar{v})^2} - p\right) < 0,\ g_u = c\,p\,\bar{v},\ g_v = 0. \tag{5.41}$$

This immediately verifies (5.33), implying that $E(\bar{u},\ \bar{v})$ is locally stable if it exists when there is no spatial effect. Further substitution of (5.41) also shows that (5.37) holds, and then there is no pattern formation around $E(\bar{u}, \bar{v})$, by Remark 5.4.2.

In fact, under additional conditions, we can prove that the unique positive equilibrium $E(\bar{u}, \bar{v})$ is globally stable if $m(v) = m_1 + m_2\,v$.

Theorem 5.4.4 *Under existence condition* (5.38) *for $E(\bar{u}, \bar{v})$, with density-dependent death rate $m(v) = m_1 + m_2\,v$ for the predator, $E(\bar{u}, \bar{v})$ is globally asymptotically stable if*

$$\begin{cases} c\,p\,M > m_1,\ 4\,d_u\,d_v\,\bar{v} > c\,\alpha^2\,\bar{u}\,v^{*2}, \\ \min\left\{a, \dfrac{m_2}{c}\right\} > \dfrac{r_0\,k_0\,\alpha}{2\,(1 + k_0\,\alpha\,\bar{v})} \end{cases} \tag{5.42}$$

hold, where $v^* = (c\,p\,M - m_1)/m_2$ and $\bar{u}, \bar{v}$ are given in (5.40).

Proof As indicated in the proof of Lemma 5.3.1, the L^∞ norm of $v(x, t)$ is bounded for either $m(v) = m_1$ or $m(v) = m_1 + m_2\,v$. In fact, if the death rate of predators is the density-dependent one, then a constant upper solution for the v equation exists. Define

$$\mathcal{F}\,v = v_t - d_v\,\Delta v - v\,(-m_1 - m_2\,v + c\,p\,u)\,. \tag{5.43}$$

Then by substituting $v = v^*$ into (5.43), we obtain

$$\mathcal{F} v^* = -v^* \ (-m_1 - m_2 \, v^* + c \, p \, u) \geq 0 \tag{5.44}$$

because $0 \leq u \leq M$. By the parabolic comparison principle ([25]), we obtain that $v = v^*$ is an upper solution of $v(x,t)$ if $v_0(x,t) \leq v^*$. Therefore, $X := \{(u,v) \in R^2 | 0 \leq u \leq M, \ 0 \leq v \leq v^*\}$ is positive invariant for (5.9). Choose a Lyapunov functional as

$$V(u,v) = \int_\Omega \left(\int_{\bar{u}}^{u} \frac{u - \bar{u}}{u} du + \frac{1}{c} \int_{\bar{v}}^{v} \frac{v - \bar{v}}{v} dv \right) dx. \tag{5.45}$$

If (u,v) is the solution to system (5.9), then we obtain

$$\begin{aligned} \frac{dV(u,v)}{dt} &= \int_\Omega \left(\frac{u - \bar{u}}{u} u_t + \frac{1}{c} \frac{v - \bar{v}}{v} v_t \right) dx \\ &= \int_\Omega \frac{u - \bar{u}}{u} \left(d_u \, \Delta u + \alpha \nabla \cdot (\beta(u) \, u \nabla v) + \frac{r_0 \, u}{1 + k_0 \, \alpha \, v} - d \, u - a \, u^2 - p \, u \, v \right) dx \\ &+ \frac{1}{c} \int_\Omega \frac{v - \bar{v}}{v} \left(d_v \, \Delta_v + v(-m_1 - m_2 \, v + c \, p \, u) \right) dx. \end{aligned} \tag{5.46}$$

Rearranging (5.46) by separating the reaction and dispersal terms gives

$$\frac{dV(u,v)}{dt} = V_1(u,v) + V_2(u,v), \tag{5.47}$$

where

$$\begin{aligned} V_1(u,v) &= \int_\Omega \frac{u - \bar{u}}{u} [d_u \, \Delta u + \alpha \nabla \cdot (\beta(u) \, u \nabla v)] + \frac{v - \bar{v}}{c \, v} d_v \, \Delta v \, dx, \\ V_2(u,v) &= \int_\Omega (u - \bar{u}) \left(\frac{r_0}{1 + k_0 \, \alpha \, v} - d - a \, u - p \, v \right) + \frac{v - \bar{v}}{c} (-m_1 - m_2 \, v + c \, p \, u) \, dx. \end{aligned} \tag{5.48}$$

By using Neumann boundary condition (5.8) and divergence theorem, we obtain that

$$\begin{aligned} V_1(u,v) &= -d_u \int_\Omega \nabla \left(\frac{u - \bar{u}}{u} \right) \cdot \nabla u \, dx - \frac{d_v}{c} \int_\Omega \nabla v \cdot \ \nabla \left(\frac{v - \bar{v}}{v} \right) dx \\ &- \alpha \int_\Omega \beta(u) \, u \, \nabla v \ \cdot \nabla \left(\frac{u - \bar{u}}{u} \right) dx \\ &\leq -d_u \, \bar{u} \int_\Omega \frac{|\nabla u|^2}{u^2} \, dx - \frac{d_v \, \bar{v}}{c} \int_\Omega \frac{|\nabla v|^2}{v^2} \, dx + \alpha \, \bar{u} \int_\Omega \frac{\beta(u)}{u} |\nabla u| \, |\nabla v| \, dx \\ &= - \int_\Omega X^\mathsf{T} A \, X \end{aligned} \tag{5.49}$$

where

$$X = \begin{pmatrix} |\nabla u| \\ |\nabla v| \end{pmatrix}, \quad A = \begin{pmatrix} \dfrac{d_u \, \bar{u}}{u^2} & -\dfrac{\alpha \, \bar{u} \, \beta(u)}{2 \, u} \\ -\dfrac{\alpha \, \bar{u} \, \beta(u)}{2 \, u} & \dfrac{d_v \, \bar{v}}{c \, v^2} \end{pmatrix}.$$

It is clear that $V_1(u,v) < 0$ if A is a positive definite matrix, which is equivalent to show that the trace and determinant of A are positive. The trace of A, which is $\operatorname{tr} A = (d_u\,\bar{u})/(u^2) + (d_v\,\bar{v})/(2\,v^2)$ is clearly positive. The determinant of A is

$$\det A = \frac{d_u\,d_v\,\bar{u}\,\bar{v}}{c\,u^2\,v^2} - \frac{\alpha^2\,\bar{u}^2\,\beta^2(u)}{4\,u^2}. \tag{5.50}$$

From (5.50), we obtain that $\det A > 0$ is equivalent to

$$4\,d_u\,d_v\,\bar{v} > c\,\alpha^2\,\bar{u}\,v^2\,\beta^2(u). \tag{5.51}$$

Because $0 \le u \le M, 0 \le v \le v^*$, a sufficient condition for (5.51) to hold is

$$f_1 := 4\,d_u\,d_v\,\bar{v} > c\,\alpha^2\,\bar{u}\,{v^*}^2. \tag{5.52}$$

Therefore, we obtain that

$$V_1(u,v) = -\int_\Omega X^{\mathsf{T}}\,A\,X \le 0 \tag{5.53}$$

if (5.52) is satisfied.

Now we estimate $V_2(u,v)$ as

$$\begin{aligned}
V_2(u,v) &= \int_\Omega (u-\bar{u})\left(\frac{r_0}{1+k_0\,\alpha\,v} - a\,u - p\,v - \left(\frac{r_0}{1+k_0\,\alpha\,\bar{v}} - a\,\bar{u} - p\,\bar{v}\right)\right) \\
&\quad + \frac{v-\bar{v}}{c}\,(m_2\,\bar{v} - c\,p\,\bar{u} - m_2\,v + c\,p\,u)\;dx \\
&= -a\int_\Omega (u-\bar{u})^2\,dx - \frac{m_2}{c}\int_\Omega (v-\bar{v})^2\,dx - \int_\Omega \frac{r_0\,k_0\,\alpha}{1+k_0\,\alpha\,\bar{v}}\,\frac{(u-\bar{u})(v-\bar{v})}{1+k_0\,\alpha\,v}\,dx \\
&\le -a\int_\Omega (u-\bar{u})^2\,dx - \frac{m_2}{c}\int_\Omega (v-\bar{v})^2\,dx + \int_\Omega \frac{r_0\,k_0\,\alpha}{1+k_0\,\alpha\,\bar{v}}\,\frac{1}{1+k_0\,\alpha\,v}\,|(u-\bar{u})||(v-\bar{v})|\,dx \\
&\le -a\int_\Omega (u-\bar{u})^2\,dx - \frac{m_2}{c}\int_\Omega (v-\bar{v})^2\,dx + \frac{r_0\,k_0\,\alpha}{2\,(1+k_0\,\alpha\,\bar{v})}\int_\Omega \left((u-\bar{u})^2 + (v-\bar{v})^2\right)dx \\
&= -\left(a - \frac{r_0\,k_0\,\alpha}{2\,(1+k_0\,\alpha\,\bar{v})}\right)\int_\Omega (u-\bar{u})^2\,dx - \left(\frac{m_2}{c} - \frac{r_0\,k_0\,\alpha}{2\,(1+k_0\,\alpha\,\bar{v})}\right)\int_\Omega (v-\bar{v})^2\,dx \\
&\le 0
\end{aligned} \tag{5.54}$$

if

$$f_2 := \min\left\{a, \frac{m_2}{c}\right\} > \frac{r_0\,k_0\,\alpha}{2\,(1+k_0\,\alpha\,\bar{v})} \tag{5.55}$$

holds. From (5.54), under (5.55), the only possibility such that $\dot{V}(u,v) = 0$ is $(u,v) = (\bar{u},\bar{v})$. Hence, by the LaSalle invariance principle ([18]), we obtain the global stability of $E(\bar{u},\bar{v})$ if (5.42) holds.

By checking conditions in (5.42), we can not obtain an explicit formula for the predator-taxis sensitivity α due to the complex expressions of α in $E(\bar{u}, \bar{v})$. Hence, we employ numerical simulations to explore the role that α plays in global stability of $E(\bar{u}, \bar{v})$ by testing the parameter dependence of α in (5.52) and (5.55). As shown in Figure 5.1, we see that $E(\bar{u}, \bar{v})$ is globally asymptotically stable if α is small. Similarly, by examining the impact of k_0 on the global stability of $E(\bar{u}, \bar{v})$, we observe that $E(\bar{u}, \bar{v})$ is globally asymptotically stable if k_0 is small, as indicated in Figure 5.2. In biological interpretation, Figures 5.1 and 5.2 show that prey and predators will tend to a steady state if prey are less sensitive to perceive predation risk or the cost of anti-predator defense on the local reproduction rate of prey is small, regardless of spatial effect, provided that the linear functional response is adopted.

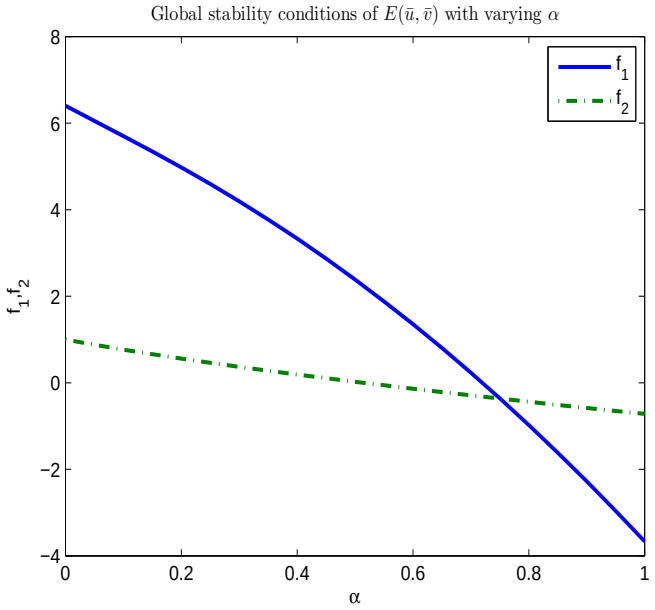

Figure 5.1: Conditions of global stability of $E(\bar{u}, \bar{v})$ when α varies with $m(v) = m_1 + m_2\, v$ and $p(u, v) = p$. Parameters are: $r_0 = 5$, $a = 1$, $d = 0.2$, $p = 0.5$, $c = 0.5$, $m_1 = 0.3\, m_2 = 1$, $M = 10, d_u = 1$, $d_v = 2$, $k_0 = 1$.

5.4.2 The Holling-type II functional response

Now we analyze possible pattern formation of system (5.9) with the Holling type II functional response ([14, 15]) i.e.,

$$p(u, v) = \frac{p}{1 + q\, u}. \tag{5.56}$$

For general death function of predators defined in (5.6), a trivial equilibrium $E_0(0, 0)$ always exists and a semi-trivial equilibrium $E_1((r_0 - d)/a, 0)$ exists if $r_0 > d$ holds. If the death function

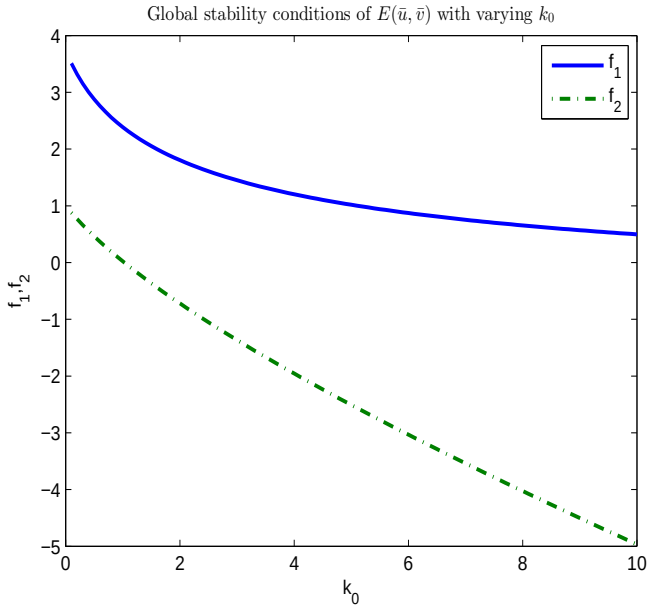

Figure 5.2: Conditions of global stability of $E(\bar{u},\bar{v})$ when k_0 varies with $m(v) = m_1 + m_2\, v$ and $p(u,v) = p$. Parameters are: $r_0 = 5$, $a = 1$, $d = 0.2$, $p = 0.5$, $c = 0.5$, $m_1 = 0.3\, m_2 = 1$, $M = 10, d_u = 1$, $d_v = 2$, $\alpha = 0.5$.

of predators is density-independent, i.e. $m(v) = m_1$, a unique positive equilibrium $E(\bar{u},\bar{v})$ exists if

$$c\,p > m_1\,q \qquad \text{and} \qquad r_0 - d > \frac{a\,m_1}{c\,p - m_1\,q} \tag{5.57}$$

hold, where

$$\begin{aligned}
&\bar{u} = \frac{m_1}{c\,p - m_1\,q},\ \bar{v} = \frac{-a_2 - \sqrt{a_2^2 - 4\,a_1\,a_3}}{2\,a_1},\\
&a_1 = -k_0\,\alpha\,(c\,p - m_1\,q)^2,\\
&a_2 = -\alpha\,c^2\,d\,k_0\,p + \alpha\,c\,d\,k_0\,m_1\,q - a\,\alpha\,c\,k_0\,m_1 - c^2\,p^2 + 2\,c\,m_1\,p\,q - m_1^2\,q^2,\\
&a_3 = -c\,(c\,d\,p - c\,p\,r_0 - d\,m_1\,q + m_1\,q\,r_0 + a\,m_1).
\end{aligned} \tag{5.58}$$

Calculations indicate that pattern formation can not occur around any of these steady states E_0, E_1, and $E(\bar{u},\bar{v})$ if $m(v) = m_1$, which is shown in the following proposition.

Proposition 5.4.5 *Choose the functional response in* (5.56) *for* (5.9). *If the death function of predators is density-independent, then pattern formation can not occur around all the steady states* E_0, E_1, *and* $E(\bar{u},\bar{v})$ *of system* (5.9).

Proof Here we only show the proof for the unique positive equilibrium $E(\bar{u}, \bar{v})$ because the proofs for E_0, E_1 are similar and are thus omitted. Direct calculations lead to

$$\begin{aligned} &f_u = \bar{u}\left(\frac{p\,q\,\bar{v}}{(1+q\,\bar{u})^2} - a\right),\ f_v = -\frac{r_0\,k_0\,\alpha\,\bar{u}}{(1+k_0\,\alpha\,\bar{v})^2} - \frac{p\,\bar{u}}{1+q\,\bar{u}}, \\ &g_u = \frac{c\,p\,\bar{v}}{(1+q\,\bar{u})^2},\ g_v = -m_1 + \frac{c\,p\,\bar{u}}{1+q\,\bar{u}}. \end{aligned} \tag{5.59}$$

By substituting $\bar{u}, \bar{v}$ in (5.58) into (5.59), we obtain that $f_v < 0$, $g_u > 0$, $g_v = 0$. Then (5.33) can be simplified to $f_u < 0$, and hence, (5.37) holds and therefore, pattern formation is impossible to occur around $E(\bar{u}, \bar{v})$.

Now we proceed to analyze the case where the death function of predators is the density-dependent one in (5.6). Similar analyses to that in Proposition 5.4.5 show that there is no pattern formation around E_0 and E_1. For the positive equilibrium $E(\bar{u}, \bar{v})$ when $m(v) = m_1 + m_2\,v$, explicit formula of $E(\bar{u}, \bar{v})$ can not be obtained due to the complexity. However, under the extra conditions in (5.57), the existence of at least one positive equilibrium $E(\bar{u}, \bar{v})$ of (5.9) is guaranteed, as stated in the following lemma.

Lemma 5.4.6 *If $m(v) = m_1 + m_2\,v$, then there exists at least one positive equilibrium $E(\bar{u}, \bar{v})$ for* (5.9) *if* (5.57) *holds.*

Proof From (5.9), the positive equilibrium $E(\bar{u}, \bar{v})$ satisfies

$$\bar{u} = \frac{m_1 + m_2\,\bar{v}}{(c\,p - m_1\,q) - m_2\,q\,\bar{v}}. \tag{5.60}$$

By (5.60), the positivity of $\bar{u}$ requires that $\bar{v} < \bar{v}_{\max}$, where $\bar{v}_{\max}$ is defined by

$$\bar{v}_{\max} = \frac{(c\,p - m_1\,q)}{m_2\,q}. \tag{5.61}$$

In addition, $\bar{v}$ is determined by

$$L(\bar{v}) := a_1\,\bar{v}^4 + a_2\,\bar{v}^3 + a_3\,\bar{v}^2 + a_4\,\bar{v} + a_5 = 0, \tag{5.62}$$

where

$$\begin{aligned} &a_1 = -\alpha\,k_0\,m_2^2\,q^2,\ a_2 = m_2\,q\,(2\,\alpha\,c\,k_0\,p - 2\,\alpha\,k_0\,m_1\,q - m_2\,q), \\ &a_3 = -(c^2\,p^2 + ((-d\,m_2 - 2\,m_1\,p)\,q + a\,m_2)\,c + q^2\,m_1^2)\,k_0\,\alpha + 2\,q\,m_2\,(c\,p - m_1\,q), \\ &a_4 = (-\alpha\,d\,k_0\,p - p^2)\,c^2 + (((\alpha\,d\,k_0 + 2\,p)\,m_1 + m_2\,(d - r_0))\,q - a\,(\alpha\,k_0\,m_1 + m_2))\,c - q^2\,m_1^2, \\ &a_5 = -c\,((-d\,q + q\,r_0 + a)\,m_1 + c\,p\,(d - r_0)). \end{aligned} \tag{5.63}$$

By substituting $\bar{v} = 0$ into (5.62), we obtain

$$L(\bar{v} = 0) = a_5 > 0 \Leftrightarrow (c\,p - m_1\,q)(r_0 - d) > a\,m_1, \tag{5.64}$$

which is equivalent to (5.57). Moreover, substituting $\bar{v} = \bar{v}_{\max}$ into (5.62) gives

$$L(\bar{v} = \bar{v}_{\max}) = -\frac{a\,c^2\,p\,(\alpha\,c\,k_0\,p - \alpha\,k_0\,m_1\,q + m_2\,q)}{m_2\,q^2} < 0 \tag{5.65}$$

if (5.57) holds. Therefore, by the intermediate value theorem, there exists at least one $\bar{v} \in [0,\ \bar{v}_{\max}]$ such that $L(\bar{v}) = 0$. Hence, the existence of at least one positive equilibrium $E(\bar{u}, \bar{v})$ is guaranteed if (5.57) holds.

When $E(\bar{u}, \bar{v})$ exists under $m(v) = m_1 + m_2\,v$, we employ numerical simulations to examine how α would change the stability of $E(\bar{u}, \bar{v})$ when spatial effects exist and generate possible spatial heterogenous patterns. Figure 5.3 indicates that if α is large, the population of both prey and predators tend to a spatial homogeneous steady state. However, if α is small, spatial heterogenous pattern appears, as indicated in Figure 5.4. Biologically, weak prey sensitivity to predation risk is an underlying mechanism for generating spatial patterns in the predator-prey system. Notice that anti-predator behaviors of prey also lead to a cost on the local reproduction of prey. However, the magnitudes of impact that anti-predator behaviors exert on the dispersal of prey and on the local reproduction of prey may be different. Therefore, we also test the role that k_0 plays in predator-prey system. By increasing the value of k_0 to $k_0 = 20$ while holding other parameters in Figure 5.4 unchanged, we obtain a figure similar to Figure 5.3 (omitted). Further check by substituting parameters into (5.35) and (5.36) gives a contradiction, which confirms the non-existence of pattern formation. Therefore, we conclude that large cost of anti-predator response of prey in its reproduction has a stabilizing effect by excluding the appearance of pattern formation and ensures the stability of the positive spatial homogeneous steady state.

5.4.3 Ratio-dependent functional response

In this section, we analyze (5.9) with the ratio-dependent functional response, i.e.

$$p(u, v) = \frac{b_1}{b_2\,v + u} \tag{5.66}$$

again with the predator death rate functions given in (5.6). For either death function of predators, system (5.9) with (5.66) admits a spatial homogeneous semi-trivial equilibrium $E_1\,((r_0 - d)/a, 0)$, which exists if $r_0 > d$. Direct calculations show that pattern formation can not occur around E_1. The proof is similar to the proof in Proposition 5.4.5 and is omitted here.

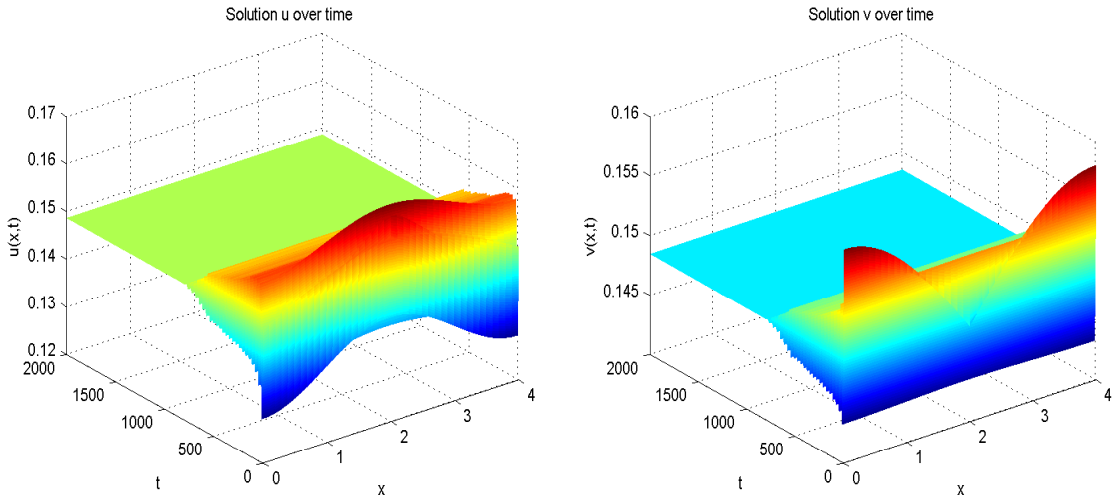

(a) $u(x,t)$ (b) $v(x,t)$

Figure 5.3: Spatial homogeneous steady states of u, v with the Holling type II functional response and density-dependent death function of predators when α is large. Parameters are: $r_0 = .8696$, $d = .1827$, $a = .6338$, $p = 6.395$, $q = 4.333$, $m_1 = 0.72e-2$, $m_2 = .9816$, $c = .2645$, $d_u = 0.2119e-1$, $d_v = 1.531$, $\alpha = 12$, $k_0 = 0.1e-1$, $M = 10$, $L = 4$.

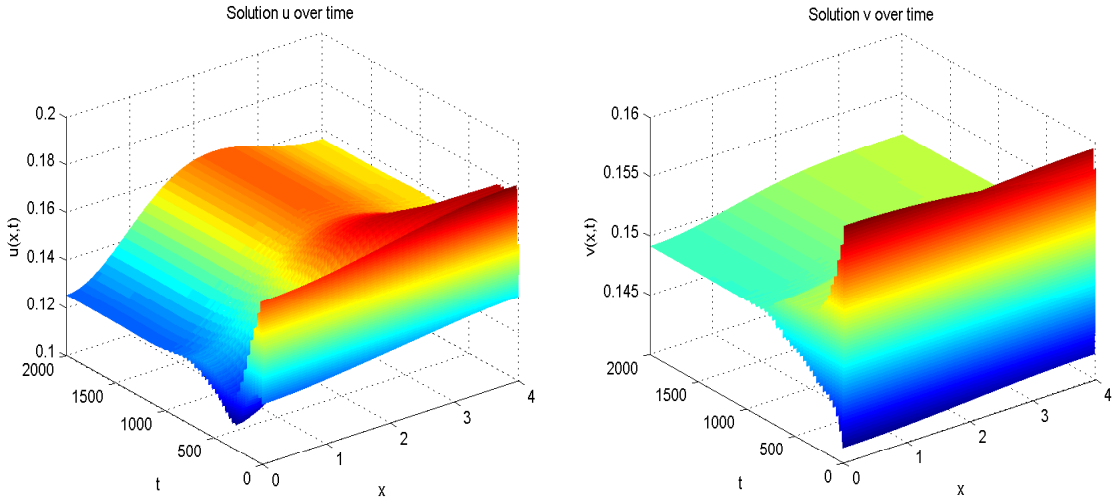

(a) $u(x,t)$ (b) $v(x,t)$

Figure 5.4: Spatial heterogeneous steady states of u, v with the Holling type II functional response and density-dependent death function of predators when α is small. Parameters are: $r_0 = .8696$, $d = .1827$, $a = .6338$, $p = 6.395$, $q = 4.333$, $m_1 = 0.72e-2$, $m_2 = .9816$, $c = .2645$, $d_u = 0.2119e-1$, $d_v = 1.531$, $\alpha = 8$, $k_0 = 0.1e-1$, $M = 10$, $L = 4$.

5.4.3.1 With density independent death rate for the predator

Consider the case with $m(v) = m_1$ first for simplicity. A unique positive equilibrium $E(\bar{u}, \bar{v})$ exists when $m(v) = m_1$ if

$$c\,b_1 > m_1 \qquad \text{and} \qquad r_0 - d > \frac{c\,b_1 - m_1}{c\,b_2}, \tag{5.67}$$

where

$$\begin{cases} \bar{u} = \dfrac{m_1\,b_2\,\bar{v}}{c\,b_1 - m_1},\ \bar{v} = \dfrac{-a_2 - \sqrt{a_2^2 - 4\,a_1\,a_3}}{2\,a_1}, \\ a_1 = -k_0\,\alpha\,a\,m_1\,b_2^2\,c,\ a_2 = -k_0\,\alpha\,(m_1 - c\,b_1)^2 - c\,b_2\,\left(a\,m_1\,b_2 + k_0\,\alpha\,d\,(c\,b_1 - m_1)\right), \\ a_3 = -(c\,b_1 - m_1)\left((c\,b_1 - m_1) + c\,b_2\,(d - r_0)\right). \end{cases} \tag{5.68}$$

Assume $E(\bar{u}, \bar{v})$ exists and we analyze necessary conditions for pattern formation around $E(\bar{u}, \bar{v})$. First consider a special case where prey avoid predation towards lower gradient of predator density but there is no cost on the reproduction success of prey (i.e. $k_0 = 0$ in (5.9)). When $k_0 = 0$, $\bar{u}, \bar{v}$ are simplified to

$$\bar{u} = \frac{c\,b_2\,(r_0 - d) - (c\,b_1 - m_1)}{b_2\,a\,c},\ \bar{v} = \frac{(c\,b_1 - m_1)\,(c\,b_2\,(r_0 - d) - (c\,b_1 - m_1))}{a\,m_1\,c\,b_2^2}, \tag{5.69}$$

which do not involve α. In this case, substituting (5.69) into (5.35) and (5.36) gives the following proposition.

Proposition 5.4.7 *When* (5.67) *holds and* $k_0 = 0$, *pattern formation around* $E(\bar{u}, \bar{v})$ *may occur if*

$$r_0 - d > \frac{(c\,b_1 - m_1)(c\,b_1 + m_1 - c\,b_2\,m_1)}{b_1\,b_2\,c^2}, \tag{5.70}$$

$$\alpha < \frac{f_u\,d_v + g_v\,d_u - 2\,\sqrt{d_u\,d_v\,(f_u\,g_v - f_v\,g_u)}}{g_u\,\beta(\bar{u})\,\bar{u}} \tag{5.71}$$

hold.

Proof Direct calculations show that at $E(\bar{u}, \bar{v})$, we have

$$\begin{aligned} &f_u = \bar{u}\left(-a + \frac{b_1\,\bar{v}}{(b_2\,\bar{v} + \bar{u})^2}\right),\ f_v = \bar{u}\left(-\frac{b_1}{b_2\,\bar{v} + \bar{u}} + \frac{b_1\,b_2\,\bar{v}}{(b_2\,\bar{v} + \bar{u})^2}\right), \\ &g_u = \frac{c\,b_1\,b_2\,\bar{v}^2}{(b_2\,\bar{v} + \bar{u})^2},\ g_v = -\frac{c\,b_1\,b_2\,\bar{u}\,\bar{v}}{(b_2\,\bar{v} + \bar{u})^2}. \end{aligned} \tag{5.72}$$

Substituting (5.72) into (5.35) and (5.36) gives

$$\begin{cases} \alpha < \dfrac{f_u\,d_v + g_v\,d_u}{g_u\,\beta(\bar{u})\bar{u}}, \\ \alpha < \dfrac{f_u\,d_v + g_v\,d_u - 2\,\sqrt{d_u\,d_v\,(f_u\,g_v - f_v\,g_u)}}{g_u\,\beta(\bar{u})\,\bar{u}}, \end{cases} \tag{5.73}$$

which leads to (5.71). Moreover, (5.33) needs to be satisfied to guarantee the local stability of $E(\bar{u}, \bar{v})$ without spatial effect. From (5.72), it is clear that $\lambda_1^0 \lambda_2^0 > 0$ is always satisfied if $E(\bar{u}, \bar{v})$ exists and $\lambda_1^0 + \lambda_2^0 < 0$ gives (5.70).

Proposition 5.4.7 implies that when there is no cost of anti-predator defense on the reproduction success of prey, small predator-taxis sensitivity α may lead to pattern formation around $E(\bar{u}, \bar{v})$. Taking α as a bifurcation parameter, then bifurcation from the spatial homogeneous steady state $E(\bar{u}, \bar{v})$ to a spatial heterogeneous steady state occurs at

$$\alpha_c = \frac{f_u\, d_v + g_v\, d_u - 2\,\sqrt{d_u\, d_v\,(f_u\, g_v - f_v\, g_u)}}{g_u\, \beta(\bar{u})\, \bar{u}}. \tag{5.74}$$

By choosing parameter values as shown in Figure 5.5 and substituting them into (5.74), we obtain the critical value of bifurcation $\alpha_c = 9.874$. Figure 5.5 shows that if $\alpha > \alpha_c$, local stability of $\bar{u}, \bar{v}$ remains even if spatial effects exist. Notice that for model (5.9), a bounded domain Ω is considered. Therefore, conditions (5.70) and (5.71) only give necessary conditions of pattern formation around $E(\bar{u}, \bar{v})$. To proceed with more detailed analysis, consider a one-dimensional domain $[0,\ L]$ with no-flux boundary condition, where the wave number k can be expressed explicitly as $k = (n\,\pi)/L$ with $n = 0,\ \pm 1,\ \pm 2\ \cdots$. From (5.31), the instability of $E(\bar{u}, \bar{v})$ may only occur if $b(k^2)$ changes from positive to negative for some $k > 0$ such that

$$k_1^2 < k^2 < k_2^2 \tag{5.75}$$

where

$$\begin{aligned} k_1^2 &= \frac{-\,(g_u\,\alpha\,\beta(\bar{u})\bar{u} - f_u\, d_v - g_v\, d_u) - \sqrt{\Delta}}{2\, d_u\, d_v}, \\ k_2^2 &= \frac{-\,(g_u\,\alpha\,\beta(\bar{u})\bar{u} - f_u\, d_v - g_v\, d_u) + \sqrt{\Delta}}{2\, d_u\, d_v}, \\ \Delta &= (g_u\,\alpha\,\beta(\bar{u})\,\bar{u} - f_u\, d_v - g_v\, d_u)^2 - 4\, d_u\, d_v\,(f_u\, g_v - f_v\, g_u)\,. \end{aligned} \tag{5.76}$$

Equivalently, (5.75) in terms of modes n becomes

$$n_1^2 < n^2 < n_2^2, \tag{5.77}$$

where $n_1 = (k_1\, L)/\pi,\ n_2 = (k_2\, L)/\pi$. For a bounded domain, the wave number is discrete ([21]). Therefore, the critical value of bifurcation $\alpha_c = 9.874$ we obtained above may not be the actual bifurcation value because an integer n satisfying (5.77) may not exist. However, by choosing parameters in Figure 5.6, we obtain that $n_1 = 0.6177, n_2 = 8.0317$, which admits at least one integer n such that (5.77) is satisfied. Hence, for this parameter set, conditions (5.70) and (5.71) are in fact *sufficient and necessary* conditions for pattern formation. With parameters in Figure

5.6, positive equilibrium $E(\bar{u}, \bar{v})$ loses stability for some spatial modes and heterogeneous spatial patterns emerge.

Now we analyze the case where $k_0 \neq 0$, i.e. there exists cost on the reproduction rate of prey due to anti-predator behaviors of prey. Noticing from (5.68) that $\bar{u}$ and $\bar{v}$ contain α if $k_0 \neq 0$. Still regarding α as a bifurcation parameter in the following analysis but with $k_0 \neq 0$, an explicit formula of α can not be obtained due to the complexity of (5.68). Therefore, we employ numerical simulations to explore the role that α plays in pattern formation when $k_0 \neq 0$. By choosing parameters in Figure 5.7, conditions in (5.33) are satisfied. Furthermore, the solid line in Figure 5.7 corresponds to (5.35) and the dashed line in Figure 5.7 represents (5.36). It is clear that α should satisfy

$$\begin{cases} \alpha > \alpha_1 = 0.2979, \\ \alpha > \alpha_2 = 0.5277 \text{ or } \alpha < \alpha_3 = 0.1833 \end{cases} \tag{5.78}$$

to ensure the pattern formation of $E(\bar{u}, \bar{v})$. Hence, we obtain that $\alpha > \alpha_2$ is a necessary condition for diffusion-taxis-driven instability of $E(\bar{u}, \bar{v})$ by (5.78). We conjecture that $\alpha > \alpha_2$ is also a sufficient condition. Indeed, numerical simulations support this conjecture, implying that $\alpha = \alpha_2$ is the bifurcation value for pattern formation. Figure 5.8 confirms that if α is relatively small, the density of prey and predators tend to a spatial homogeneous steady state eventually. However, if we increase the value of α until it passes the critical bifurcation value $\alpha = \alpha_2$, then spatial heterogeneous steady state emerge, as shown in Figure 5.9.

By comparing the two cases where $k_0 = 0$ and $k_0 \neq 0$, we find some interesting distinctions between the two cases. If $k_0 = 0$, then prey avoid predators by moving towards lower predator density locations but there is no cost of anti-predator behaviors on the local reproduction success of prey. In this circumstance, small predator-taxis leads to instability of spatial homogeneous steady state of predator-prey system, which eventually form spatial heterogeneous patterns. Similar results have been obtained in [16], in which the opposite scenario where prey move randomly but predators chase prey by moving towards higher prey density gradient in addition to random diffusion was studied. In [16], by considering the same ratio dependent functional response between prey and predators, the authors concluded that spatial pattern formation may occur if the prey-taxis was small. However, in contrast to the case where $k_0 = 0$ or the similar conclusion in [16], if $k_0 \neq 0$, (i.e. the cost of anti-predator response is incorporated), analyses above show that *large* predator-taxis may result in spatial pattern formation. Biologically, when the cost of anti-predator behaviors exists, strong anti-predator behaviors of prey have a destabilizing effect by destroying the stability of the uniformly distributed equilibrium, and giving rise to spatial non-homogeneous patterns. On the other hand, weak anti-predator behaviors of prey have a stabilizing effect in predator-prey system by excluding the emergence of spatial pattern

formation. Notice that stronger anti-predator behaviors of prey also carry larger cost on the reproduction success of prey. In order to examine the impact that the cost of avoidance behaviors of prey exerts on spatial distribution of prey and predators, we also conduct simulations by varying the value of k_0. Decreasing the value of k_0 while holding other parameters in Figure 5.9 unchanged gives Figure 5.10, which shows that solutions tend to a homogeneous steady state. Further computation confirms that small k_0 leads to the violation of conditions (5.35) and (5.36), which excludes the possibility of pattern formation. In biological interpretation, *small* cost of anti-predator behaviors has a stabilizing effect by converting a spatial heterogeneous steady state into a spatial homogeneous one if the functional response between predators and prey is ratio dependent.

We also point out here that in [3], the authors analyzed pattern formation of a predator-prey system where both prey and predators disperse randomly. By using numerical simulations, and considering the same ratio-dependent functional response, the authors concluded that the most possible Turing pattern occurred at places where the growth rate of prey and the death rate of predators were similar ([3]). As a special case of (5.9), we also analyze the model

$$\begin{aligned} \frac{\partial u}{\partial t} &= d_u \Delta u + \frac{r_0\, u}{1 + k_0\, \alpha\, v} - d\, u - a\, u^2 - \frac{b_1\, u\, v}{b_2\, v + u}, \\ \frac{\partial v}{\partial t} &= d_v \Delta v + v\left(-m_1 + \frac{c\, b_1\, u}{b_2\, v + u}\right). \end{aligned} \tag{5.79}$$

As shown in (5.79), different from model (5.9), prey have no directed movement but disperse randomly in the habitat. However, in local reaction between prey and predators, the cost of anti-predator behaviors still exists and the reproduction success of prey is reduced as a result. For notational convenience, let $k_1 = k_0\, \alpha$, which represents the level of anti-predator behaviors. Higher level of anti-predator defense of prey (i.e. larger value of k_1) leads to lower reproduction rate of prey. Again similar to the analysis above when $k_0 \neq 0$, we conduct numerical simulations to analyze the role that k_1 exerts in pattern formation. By plotting (5.35) and (5.36) with respect to varying k_1, a figure which is very similar to Figure 5.7 is obtained, indicating that large k_1 may lead to pattern formation. Further numerical simulations of $(u(x,t), v(x,t))$ over time and space confirm that spatial heterogeneous patterns are formed if k_1 is large, which are similar to Figures 5.6(a) and 5.6(b) respectively and are thus omitted. The above analyses of (5.79) indicate that small cost of anti-predator behaviors has a stabilizing effect on predator-prey system by excluding the possibility of Turing bifurcation when both prey and predators move randomly. Different from [3], by incorporating the cost of fear into modelling, Turing instability may or may not occur when birth rate of prey r_0 and death rate of predators m_1 are similar, depending on the value of k_1 indeed.

5.4.3.2 With density dependent death rate for the predator

Now we proceed to the case where the death function of predators is density dependent, where $m(v) = m_1 + m_2\, v$. The existence of positive equilibrium is shown in the following lemma.

Lemma 5.4.8 *If $m(v) = m_1 + m_2\, v$, then at least one positive equilibrium $E(\bar{u}, \bar{v})$ exists if* (5.67) *holds.*

Proof From (5.9), it is obvious that $\bar{u}$ satisfies

$$\bar{u} = \frac{b_2\, \bar{v}\, (m_2\, \bar{v} + m_1)}{(b_1\, c - m_1) - m_2\, \bar{v}}. \tag{5.80}$$

Obviously, the existence of $\bar{u}$ requires that

$$\bar{v} < \frac{b_1\, c - m_1}{m_2} := \bar{v}_{\max}, \tag{5.81}$$

where $b_1\, c > m_1$ holds by (5.67). Moreover, $\bar{v}$ is determined by

$$F(\bar{v}) := a_1\, \bar{v}^3 + a_2\, \bar{v}^2 + a_3\, \bar{v} + a_4 = 0, \tag{5.82}$$

where

$$\begin{aligned}
a_1 &= -\alpha\, k_0\, m_2\, (a\, b_2^2\, c + m_2),\\
a_2 &= -m_2^2 + (((b_2\, d + 2\, b_1)\, c - 2\, m_1)\, k_0\, \alpha - a\, b_2^2\, c)\, m_2 - a\, \alpha\, b_2^2\, c\, k_0\, m_1,\\
a_3 &= -\alpha\, b_1\, k_0\, (b_2\, d + b_1)\, c^2 + (k_0\, m_1\, (b_2\, d + 2\, b_1)\, \alpha - a\, b_2^2\, m_1 + m_2\, (d - r_0)\, b_2 + 2\, b_1\, m_2)\, c\\
&\quad - \alpha\, k_0\, m_1^2 - 2\, m_1\, m_2,\\
a_4 &= -(b_1\, c - m_1)\, (b_2\, c\, d - b_2\, c\, r_0 + b_1\, c - m_1).
\end{aligned} \tag{5.83}$$

From (5.83), $a_4 > 0$ is equivalent to

$$(r_0 - d)\, b_2\, c > b_1\, c - m_1, \tag{5.84}$$

which is implied by (5.67). Furthermore, substituting $\bar{v} = \bar{v}_{\max}$ into (5.82) gives

$$F(\bar{v}_{\max}) = -\frac{a\, b_1\, b_2^2\, c^2\, (b_1\, c - m_1)\, (\alpha\, b_1\, c\, k_0 - \alpha\, k_0\, m_1 + m_2)}{m_2^2} < 0 \tag{5.85}$$

if $b_1\, c > m_1$ is satisfied. Therefore, by the intermediate value theorem, there exists at least one positive equilibrium $E(\bar{u}, \bar{v})$ if (5.67) holds.

When $E(\bar{u}, \bar{v})$ exists with $m(v) = m_1 + m_2\, v$, we analyze possible pattern formation and conduct numerical simulations, following the same procedures as in the previous case where $m(v) = m_1$.

Both theoretical and numerical results are similar to the previous case, in which strong anti-predator behaviors (i.e. large α) induces a spatial heterogeneous steady state, while weak anti-predators behaviors stabilize the system by converting solutions to spatial homogeneous ones. Moreover, small cost of anti-predator behaviors on prey reproduction (i.e. small k_0) may also exclude the occurrence of pattern formation. The difference between the two cases where $m(v) = m_1$ and $m(v) = m_1 + m_2\, v$ lies in that for $m(v) = m_1 + m_2\, v$, large k_0 induces spatial homogeneous but time-periodic solutions (Hopf bifurcation), as shown in Figure 5.11. However, if $m(v) = m_1$, increasing the value of k_0 can not give time-periodically solutions but remain spatial heterogeneous solutions. By further substituting parameters in Figure 5.11 into (5.33), we find that large k_0 leads to $f_u + g_v > 0$, which implies that time-periodic solutions emerge due to Hopf bifurcation.

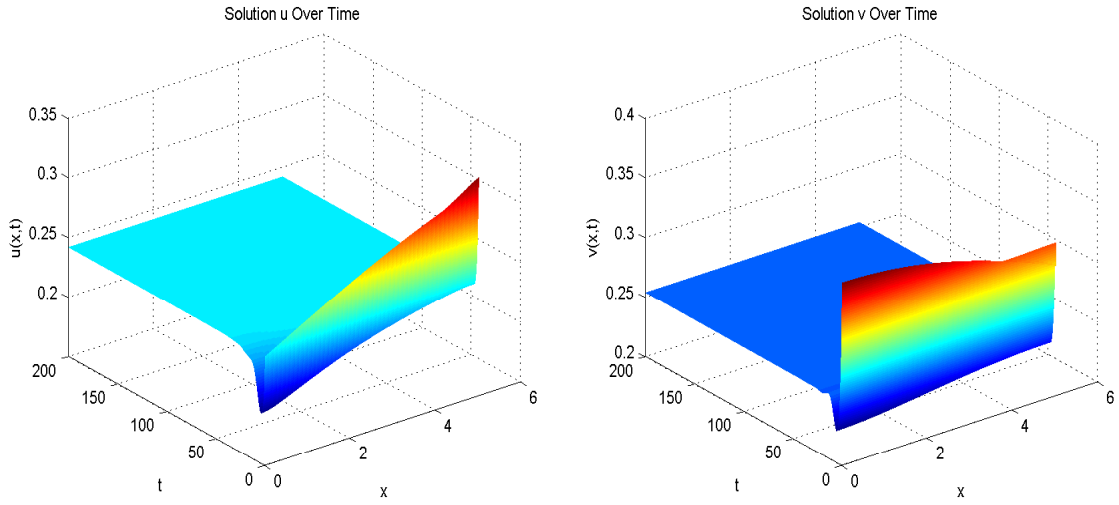

(a) $u(x,t)$ (b) $v(x,t)$

Figure 5.5: Spatial homogeneous steady states of u, v when $k_0 = 0$, α is large, $m(v) = m_1$, and $p(u,v) = b_1/(b_2\, v + u)$. Parameters are: $r_0 = 6.1885$, $d = 4.0730$, $a = 0.8481$, $b_1 = 4.5677$, $b_2 = 1.4380$, $m_1 = 1.6615$, $c = 0.9130$, $\alpha = 12$, $d_u = 0.0113$, $d_v = 4.7804$, $M = 10$, $k_0 = 0$, $L = 5.0212$.

5.4.4 Beddington-DeAngelis functional response

In this section, we analyze possible pattern formation when $p(u,v)$ in (5.9) is chosen as the Beddington-DeAngelis functional response ([7, 11]), i.e.,

$$p(u,v) = \frac{p}{1 + q_1\, u + q_2\, v}. \tag{5.86}$$

For either death function $m(v)$ of predators in (5.6), a trivial equilibrium $E_0(0,0)$ always exists and a semi-trivial equilibrium $E_1((r_0 - d)/a, 0)$ exists if $r_0 > d$. Mathematical analyses show

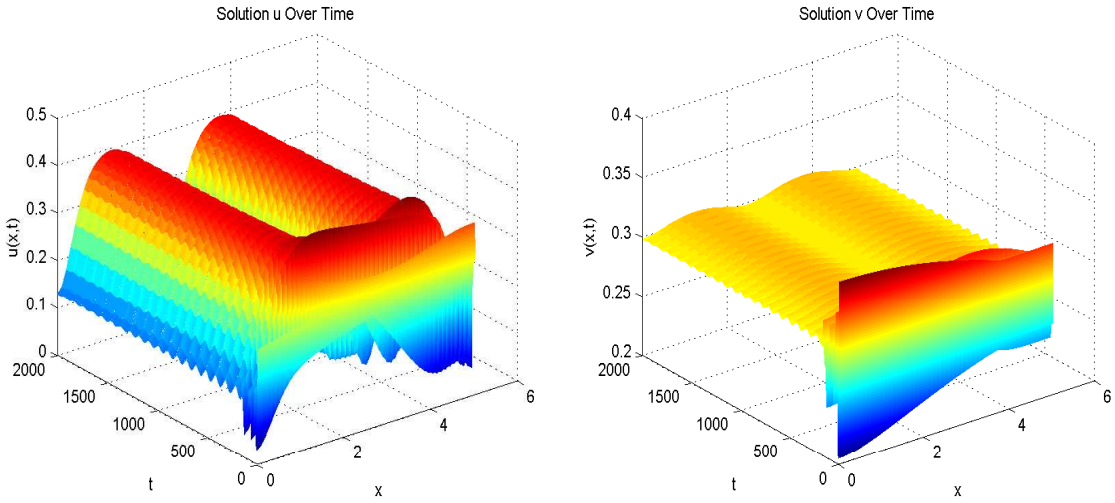

(a) $u(x,t)$ (b) $v(x,t)$

Figure 5.6: Spatial heterogenous steady states of u, v when $k_0 = 0$, α is small, $m(v) = m_1$, and $p(u,v) = b_1/(b_2\, v + u)$. Parameters are: $r_0 = 6.1885$, $d = 4.0730$, $a = 0.8481$, $b_1 = 4.5677$, $b_2 = 1.4380$, $m_1 = 1.6615$, $c = 0.9130$, $\alpha = 5.1571$, $d_u = 0.0113$, $d_v = 4.7804$, $M = 10$, $k_0 = 0$, $L = 5.0212$.

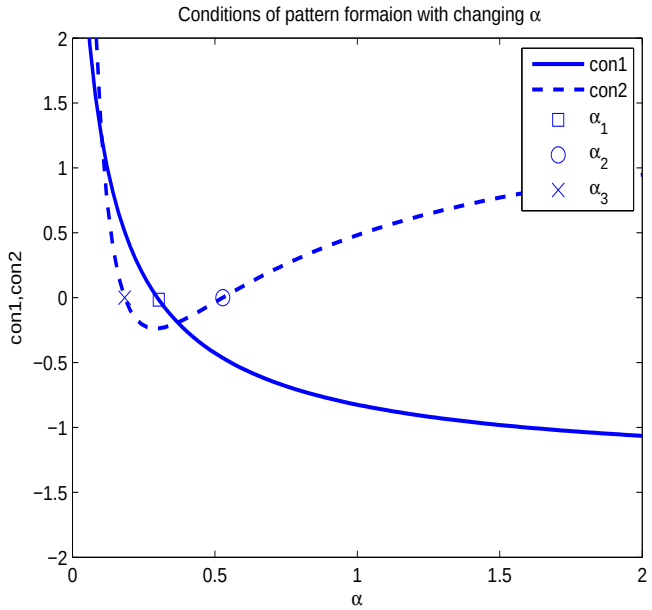

Figure 5.7: Conditions of diffusion-taxis-driven instability of $E(\bar{u}, \bar{v})$ with changing α when $k_0 \neq 0$, $m(v) = m_1$, and $p(u,v) = b_1/(b_2\, v + u)$. Parameters are: $r_0 = 1.7939$, $d = 0.2842$, $a = 0.4373$, $b_1 = 2.9354$, $b_2 = 3.2998$, $m_1 = 0.5614$, $c = 0.6010$, $d_u = 0.0344$, $d_v = 7.2808$, $k_0 = 8.0318$, $M = 10$.

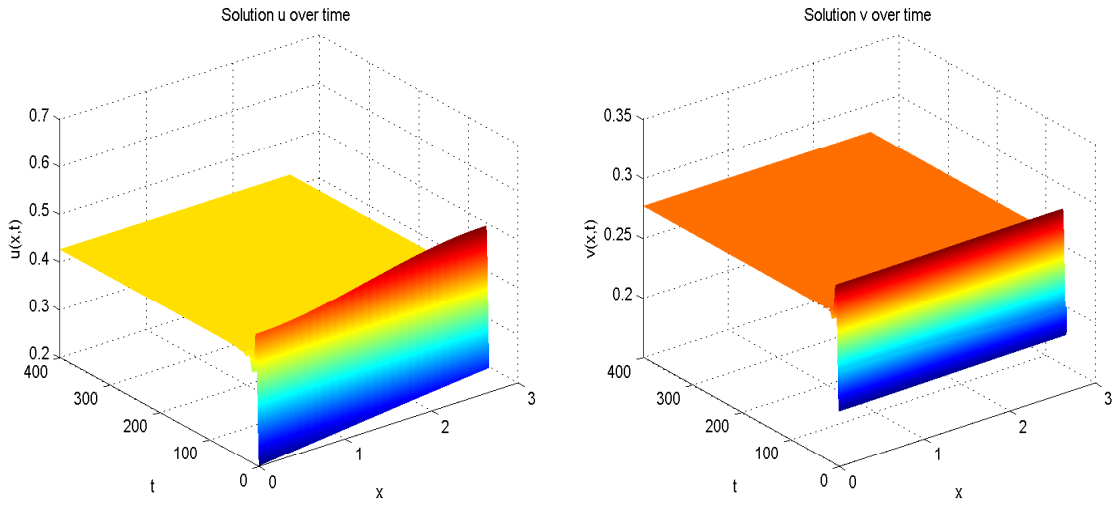

(a) $u(x,t)$ (b) $v(x,t)$

Figure 5.8: Spatial homogeneous steady states of u, v when $k_0 \neq 0$, α is small, $m(v) = m_1$, and $p(u,v) = b_1/(b_2\, v + u)$. Parameters are: $r_0 = 1.7939$, $d = 0.2842$, $a = 0.4373$, $b_1 = 2.9354$, $b_2 = 3.2998$, $m_1 = 0.5614$, $c = 0.6010$, $d_u = 0.0344$, $d_v = 7.2808$, $k_0 = 8.0318$, $M = 10$, $\alpha = 0.3$, $L = 2.6602$.

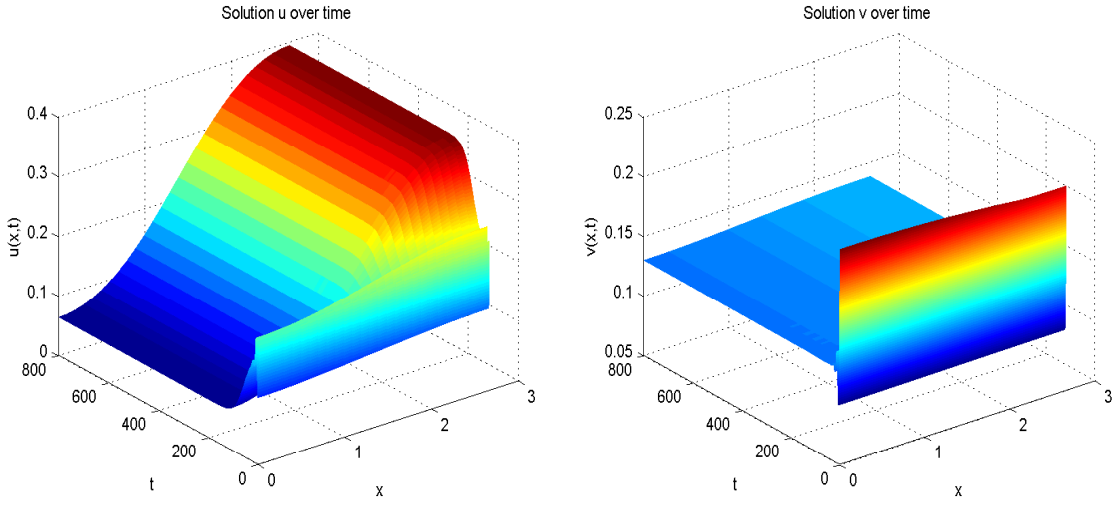

(a) $u(x,t)$ (b) $v(x,t)$

Figure 5.9: Spatial heterogenous steady states of u, v when $k_0 \neq 0$, α is large, $m(v) = m_1$, and $p(u,v) = b_1/(b_2\, v + u)$. Parameters are: $r_0 = 1.7939$, $d = 0.2842$, $a = 0.4373$, $b_1 = 2.9354$, $b_2 = 3.2998$, $m_1 = 0.5614$, $c = 0.6010$, $d_u = 0.0344$, $d_v = 7.2808$, $k_0 = 8.0318$, $M = 10$, $\alpha = 0.7957$, $L = 2.6602$.

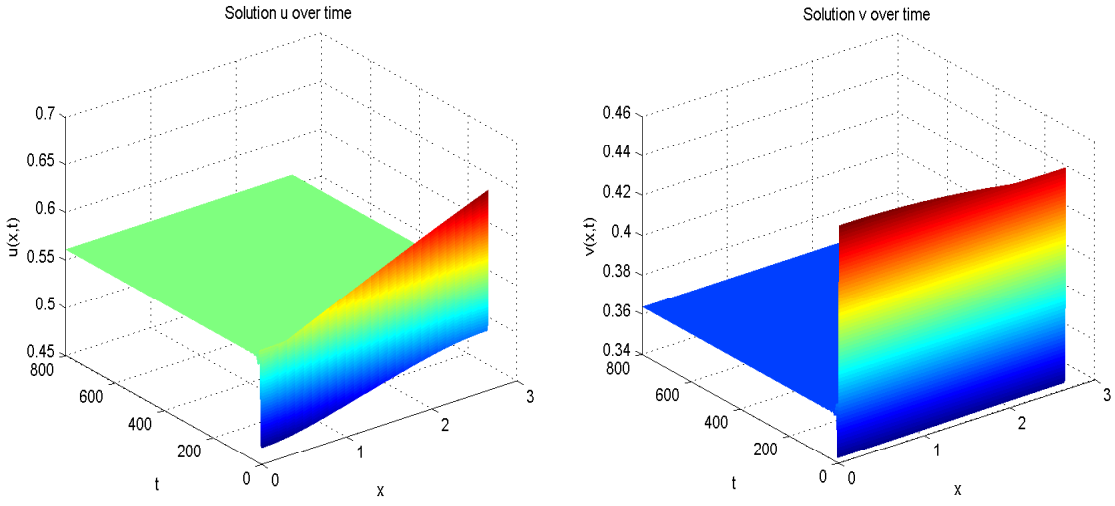

(a) $u(x,t)$ (b) $v(x,t)$

Figure 5.10: Spatial homogeneous steady states of u, v when k_0 is small, $\alpha \neq 0$, $m(v) = m_1$, and $p(u,v) = b_1/(b_2\, v + u)$. Parameters are: $r_0 = 1.7939$, $d = 0.2842$, $a = 0.4373$, $b_1 = 2.9354$, $b_2 = 3.2998$, $m_1 = 0.5614$, $c = 0.6010$, $d_u = 0.0344$, $d_v = 7.2808$, $k_0 = 2$, $M = 10$, $\alpha = 0.7957$, $L = 2.6602$.

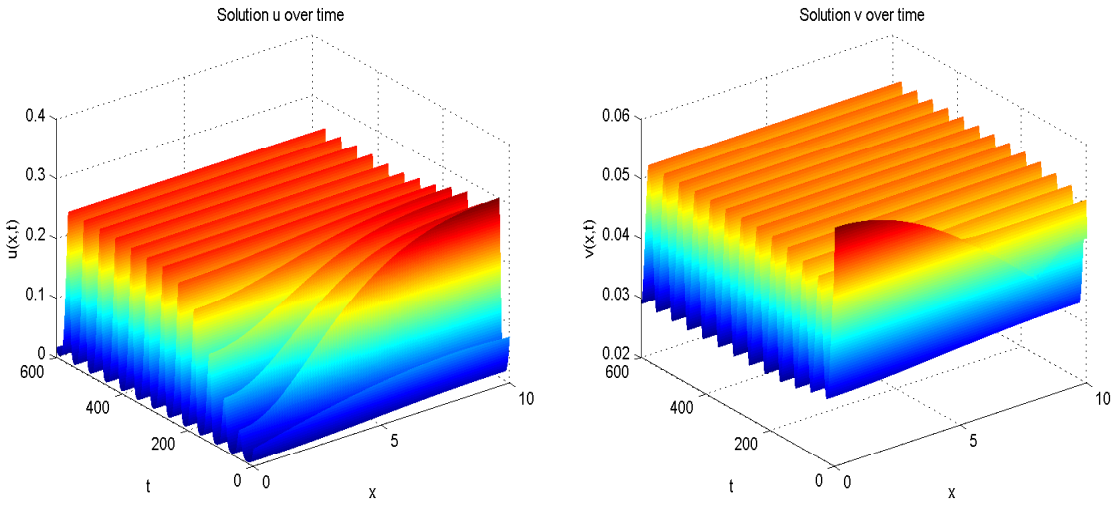

(a) $u(x,t)$ (b) $v(x,t)$

Figure 5.11: Spatial homogeneous but temporal periodic solution u, v over time when $m(v) = m_1 + m_2\, v$, k_0 is large, and $p(u,v) = b_1/(b_2\, v + u)$. Parameters are: $r_0 = 4.8712$, $d = .9235$, $a = .9508$, $b_1 = .3433$, $b_2 = .6731$, $m_1 = 0.228e - 1$, $m_2 = .7908$, $c = .2959$, $d_u = .1516$, $d_v = 8.5545$, $k_0 = 10$, $\alpha = 7.4798$, $M = 10$, $L = 10$.

that pattern formation can not occur around E_0 or E_1. Because the result is similar to the results in previous sections and the analyses follow standard procedures, we omit the proof here. Due to the complexity of the Beddington-DeAngelis functional response (5.86), pattern formation around positive equilibrium is explored by numerical simulations. As shown in Figure 5.12 and Figure 5.13 respectively, for the case where $m(v) = m_1$, small α may induce pattern formation but large α inhibits the emergence of spatial heterogeneous patterns. The simulation results hold for either $k_0 = 0$ or $k_0 \neq 0$. Also, we obtain a figure which is very similar to Figure 5.12 by increasing the value of k_0 to $k_0 = 10$ while holding other parameters in Figure 5.13 unchanged. Biologically, it indicates that large cost of anti-predator behaviors on the reproduction of prey has a stabilizing effect by converting a spatially heterogeneous steady-state to spatially homogeneous one. The same conclusions hold for the case where $m(v) = m_1 + m_2\, v$, for which we conduct simulations and do not observe difference from the previous density-independent case.

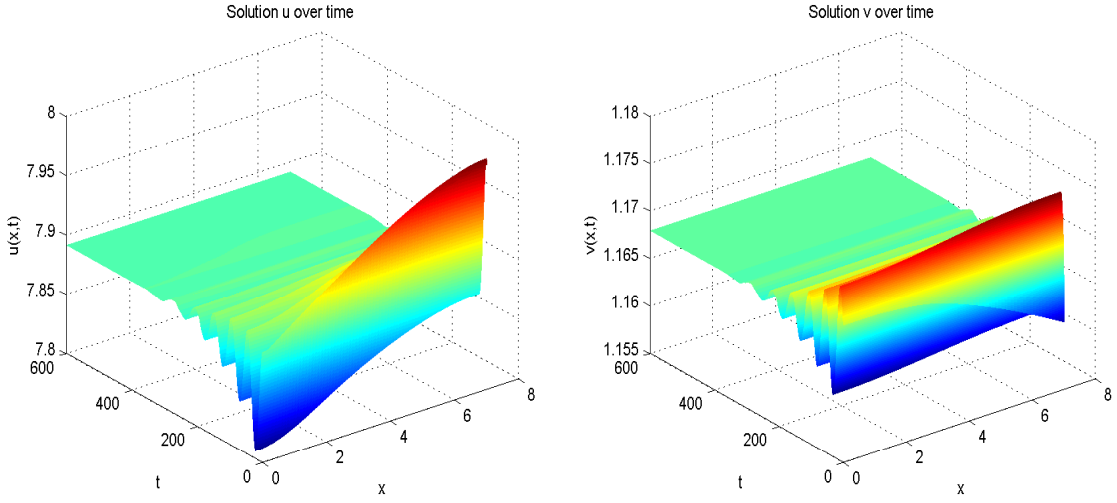

(a) $u(x,t)$ (b) $v(x,t)$

Figure 5.12: Spatial homogeneous steady states of u, v when $m(v) = m_1, k_0 \neq 0$, α is large, and $p(u,v) = p/(1 + q_1\, u + q_2\, v)$. Parameters are: $r_0 = .3558$, $d = 0.832e - 1$, $a = 0.106e - 1$, $p = .6313$, $q_1 = .4418$, $q_2 = .3188$, $m_1 = .4901$, $c = .4780$, $d_u = 0.324e - 1$, $d_v = 3.7446$, $M = 100$, $\alpha = 0.1$, $k_0 = 1, L = 7$.

5.5 Conclusions and Discussions

In this paper, we proposed a spatial predator-prey model with avoidance behaviors of prey and the corresponding cost of anti-predator responses on the reproduction success of prey. The focus is on the formation of spatial patterns. Various functional responses and both density-independent and density-dependent death rates of predators were considered in the model

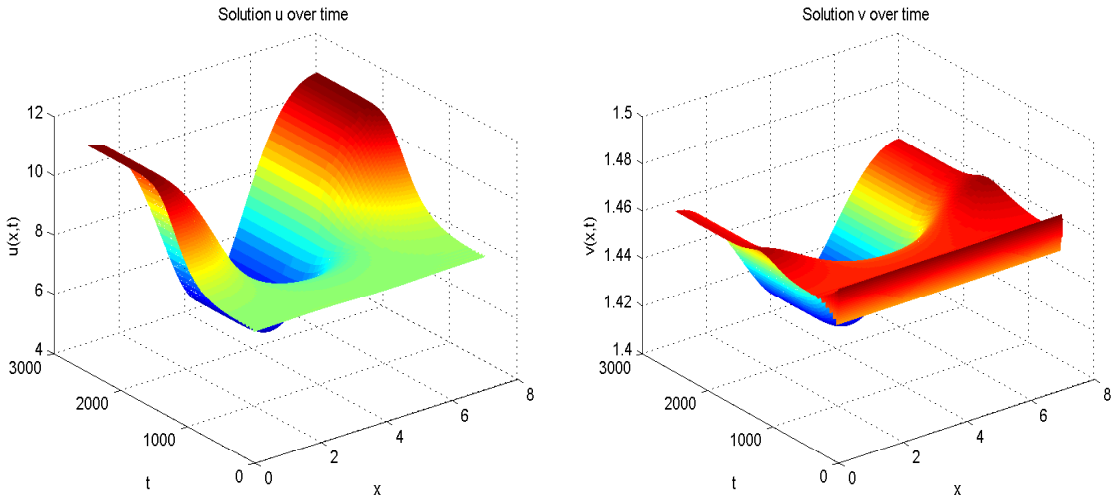

(a) $u(x,t)$ (b) $v(x,t)$

Figure 5.13: Spatial heterogeneous steady states of u, v when $m(v) = m_1, k_0 \neq 0$, α is small, and $p(u,v) = p/(1 + q_1\, u + q_2\, v)$. Parameters are: $r_0 = .3558$, $d = 0.832e-1$, $a = 0.106e-1$, $p = .6313$, $q_1 = .4418$, $q_2 = .3188$, $m_1 = .4901$, $c = .4780$, $d_u = 0.324e-1$, $d_v = 3.7446$, $M = 100$, $\alpha = 0.01$, $k_0 = 1, L = 7$.

for analysis. Mathematical analyses show that pattern formation can't occur if the functional response is linear or if it is the Holling type II functional response with density-independent death of predators. However, pattern formation may occur if the death rate of predators is density-dependent with the Holling type II functional response. Moreover, functional responses other than prey-dependent only ones, including ratio-dependent functional response and the Beddington-DeAngelis functional response, may allow the emergence of spatial heterogeneous patterns as well. Under conditions for pattern formation, the common point for the case with the Holling type II functional response and the case where the functional response is chosen as the Beddington-DeAngelis type is that small prey sensitivity to predation risk (i.e. small α) induces spatial heterogeneous steady states while large α excludes pattern formation. In addition, large cost of anti-predator behaviors on the reproduction rate of prey (i.e. large k_0) has a stabilizing effect by transferring spatial heterogeneous steady states into homogeneous ones. The case where the functional response is a ratio-dependent one exhibits different mechanisms for pattern formation, compared with other cases. For a special case where the prey avoid predation by moving to habitats with lower predator density but the cost of such anti-predator behaviors is ignored (i.e. $k_0 = 0$), we obtain similar conclusions. However, if the cost of anti-predator responses is incorporated, mathematical analyses give an opposite result. To elaborate, large prey sensitivity to predation risk (i.e. large α) may lead to a spatially heterogeneous steady state by destroying the local stability of a positive constant equilibrium while small α excludes the

possibility of pattern formation. Moreover, different from other cases where large k_0 stabilizes system, in the case of ratio dependent functional response, small k_0 inhibits the emergence of pattern formation and stabilize a homogeneous equilibrium as well. Via both mathematical analyses and numerical simulations, we may conclude that anti-predator behaviors of prey and the cost on prey's reproduction success have important impacts in pattern formation in spatial predator-prey systems. Avoidance behaviors of prey and the cost of fear may have either stabilizing effect or destabilizing effect, when they interplay with different functional responses.

In this paper, we mainly focused on modelling avoidance behaviors and the cost of anti-predator behaviors on the reproduction of prey in a spatial predator-prey system. Therefore, predators are assumed to move randomly in their habitats. For future extensions, it is possible to incorporate a prey-taxis term, which describes a biased movement of predators to forage prey. It is interesting to see how the repulsion and attraction effects work together and even more interestingly, how they interplay with the cost of anti-predator behaviors. We leave these as future work.

Bibliography

[1] B. E. Ainseba, M. Bendahmane, and A. Noussair. A reaction-diffusion system modeling predator-prey with prey-taxis. *Nonlinear Analysis: Real World Applications*, 9:2086–2105, 2008.

[2] N. D. Alikakos. An application of the invariance principle to reaction-diffusion equations. *Journal of Differential Equations*, 33:201–225, 1979.

[3] D. Alonso, F. Bartumeus, and J. Catalan. Mutual interference between predators can give rise to Turing spatial patterns. *Ecology*, 83:28–34, 2002.

[4] H. Amann. Dynamic theory of quasilinear parabolic systems iii: Global existence. *Mathematische Zeitschrift*, 202:219–250, 1989.

[5] H. Amann. Dynamic theory of quasilinear parabolic equations ii: Reaction-diffusion systems. *Differential Integral Equations*, 3:13–75, 1990.

[6] H. Amann. Nonhomogeneous linear and quasilinear elliptic and parabolic boundary value problems. In *Function spaces, differential operators and nonlinear analysis*, pages 9–126. Springer, 1993.

[7] J. R. Beddington. Mutual interference between parasites or predators and its effect on searching efficiency. *Journal of Animal Ecology*, 44:331–340, 1975.

[8] V. N. Biktashev, J. Brindley, A. V. Holden, and M. A. Tsyganov. Pursuit-evasion predator-prey waves in two spatial dimensions. *Chaos: An Interdisciplinary Journal of Nonlinear Science*, 14:988–994, 2004.

[9] S. Creel and D. Christianson. Relationships between direct predation and risk effects. *Trends in Ecology & Evolution*, 23:194–201, 2008.

[10] W. Cresswell. Predation in bird populations. *Journal of Ornithology*, 152:251–263, 2011.

[11] D. L. DeAngelis, R. A. Goldstein, and R. V. O'neill. A model for tropic interaction. *Ecology*, 56:881–892, 1975.

[12] T. Hillen and K. J. Painter. Global existence for a parabolic chemotaxis model with prevention of overcrowding. *Advances in Applied Mathematics*, 26:280–301, 2001.

[13] T. Hillen and K. J. Painter. A user's guide to PDE models for chemotaxis. *Journal of Mathematical Biology*, 58:183–217, 2009.

[14] C. S. Holling. The components of predation as revealed by a study of small-mammal predation of the European pine sawfly. *The Canadian Entomologist*, 91:293–320, 1959.

[15] C. S. Holling. Some characteristics of simple types of predation and parasitism. *The Canadian Entomologist*, 91:385–398, 1959.

[16] J. M. Lee, T. Hillen, and M. A. Lewis. Pattern formation in prey-taxis systems. *Journal of Biological Dynamics*, 3:551–573, 2009.

[17] S. A. Levin. The problem of pattern and scale in ecology. *Ecology*, 73:1943–1967, 1992.

[18] J. D. Meiss. *Differential dynamical systems*, volume 14. SIAM, 2007.

[19] M. Mimura. Asymptotic behavior of a parabolic system related to a planktonic prey and predator system. *SIAM Journal on Applied Mathematics*, 37:499–512, 1979.

[20] M. Mimura and J. D. Murray. On a diffusive prey-predator model which exhibits patchiness. *Journal of Theoretical Biology*, 75:249–262, 1978.

[21] J. D. Murray. *Mathematical Biology II: Spatial Models and Biomedical Applications*, volume 18. Springer-Verlag New York Incorporated, 2001.

[22] K. J. Painter and T. Hillen. Volume-filling and quorum-sensing in models for chemosensitive movement. *Can. Appl. Math. Quart*, 10:501–543, 2002.

[23] D. Ryan and R. S. Cantrell. Avoidance behavior in intraguild predation communities: a cross-diffusion model. *Discrete and Continuous Dynamical Systems*, 35:1641–1663, 2015.

[24] H. Shi and S. Ruan. Spatial, temporal and spatiotemporal patterns of diffusive predator-prey models with mutual interference. *IMA Journal of Applied Mathematics,*, 80:1534–1568, 2015.

[25] H. L. Smith. *Monotone Dynamical Systems: An Introduction to the Theory of Competitive and Cooperative Systems*, volume 41. American Mathematical Society, 2008.

[26] Y. Song and X. Zou. Spatiotemporal dynamics in a diffusive ratio-dependent predator-prey model near a Hopf-Turing bifurcation point. *Computers & Mathematics with Applications*, 67:1978–1997, 2014.

[27] J. H. Steele. *Spatial pattern in plankton communities*, volume 3. Springer Science & Business Media, 1978.

[28] Y. Tao. Global existence of classical solutions to a predator-prey model with nolinear prey-taxis. *Nonlinear Analysis: Real World Applications*, 11:2056–2064, 2010.

[29] X. Wang, W. Wang, and G. Zhang. Global bifurcation of solutions for a predator-prey model with prey-taxis. *Mathematical Methods in the Applied Sciences*, 38:431–443, 2015.

[30] X. Wang, L. Y. Zanette, and X. Zou. Modelling the fear effect in predatorprey interactions. *Journal of Mathematical Biology*, 2016. doi: 10.1007/s00285-016-0989-1.

[31] Z. Wang and T. Hillen. Classical solutions and pattern formation for a volume filling chemotaxis model. *Chaos: An Interdisciplinary Journal of Nonlinear Science*, 17:037108, 2007.

[32] S. Wu, J. Shi, and B. Wu. Global existence of solutions and uniform persistence of a diffusive predator-prey model with prey-taxis. *Journal of Differential Equations*, 260: 5847–5874, 2016.

[33] L. Y. Zanette, A. F. White, M. C. Allen, and M. Clinchy. Perceived predation risk reduces the number of offspring songbirds produce per year. *Science*, 334:1398–1401, 2011.

Chapter 6

Conclusions and discussions

In this thesis, we studied two different effects between predator-prey interaction: direct effect and indirect effect. To study direct effect, we proposed a two-patch model where prey are sessile in each isolated patch but predators move between patches to forage prey. The dispersal strategy of predators is assumed to be adaptive to maximize individual fitness. Explicit conditions for predator persistence or extinction were obtained through persistence theory ([7, 19]). Numerical simulations were conducted to explore the role that adaptive dispersal of predators plays in predator-prey system. By numerical simulation, we observed that either weak or strong adaptation of predators stabilizes the system if the population of prey and predators tend to a steady state in one patch but tend to a limit cycle in the other patch. Moreover, torus bifurcation was identified by numerical simulations when the population of prey and predators tend to limit cycles in both patches. Via studying the model which incorporates the population dynamics and adaptive dynamics together, we gained more insights of effects that adaptive strategy has on the system.

To study the indirect effects in predator-prey interactions, we proposed three models, including an ODE model, a DDE model and then a PDE model. As discussed in Chapter **1**, indirect effects have been experimentally observed in multiple field experiments ([1, 2, 3, 4, 5, 10, 11, 12, 14, 18, 20, 21]) and play an even more important role in determining the demography of prey or predators but has been largely ignored in mathematical modelling. Therefore, we proposed models to explore the role that the cost of avoidance behaviors plays in predator-prey interaction.

In Chapter **3**, as a first attempt of modelling the cost of fear, we proposed an ODE model, which incorporates the cost of anti-predator behaviors in the birth rate of prey. It is well-known that when the functional response between predators and prey is chosen as the Holling type II functional response ([8, 9]), the positive equilibrium may lose stability and give rise to periodic oscillations if the carrying capacity of prey increases to pass a critical value. However, the phase

plane analysis shows that the limit cycle stays very close to the boundary such that a small perturbation may lead to species extinction. This is referred to as the 'paradox of enrichment' ([6, 13, 15, 16]). Mathematical analyses of our model showed that high levels of anti-predator response inhibit the appearance of limit cycle and thus eliminate the 'paradox of enrichment'. However, if the level of anti-predator behaviors is relatively low, periodic oscillations may still occur due to Hopf bifurcation. Analysis showed that Hopf bifurcation in our model can be both supercritical and subcritical, which is different from the model without fear effect where Hopf bifurcation is typically supercritical. The existence of subcritical Hopf bifurcation implies the bi-stability in predator-prey system.

As an extension of the model in Chapter **3**, we proposed a DDE model which divides prey into two different stages and includes adult prey's adaptive avoidance of predators. Mathematical analyses showed that the positive equilibrium may lose stability if the maturation delay between juvenile and adult prey increases but regain stability if the delay becomes very large. Numerical simulations showed that either strong adaptation of adult prey or the large cost of anti-predator behaviors destabilizes predator-prey interaction by giving rise to periodic oscillations. However, large population of predators stabilizes the system by excluding periodic solutions. By numerical simulations, we also observed that adult prey avoid predation more sensitively if population of predators is larger and demonstrate weaker anti-predator behaviors if the cost of fear is larger.

In order to explore how the cost of anti-predator behaviors affects the spatial distribution of prey and predators, we studied a spatial model with avoidance behaviors of prey and the cost of fear in Chapter **5**. For the spatial model, we considered a homogeneous environment and studied the mechanisms that can give rise to spatial heterogeneous distributions. Both mathematical and numerical analyses indicate that either small or large prey's sensitivity to predation risk may lead to pattern formation. Similarly, either small or large cost of anti-predator behaviors stabilizes predator-prey system by inhibiting the appearance of pattern formation, depending on the particular form of functional response.

In summary, by incorporating the avoidance behaviors of prey and the accompanying cost of anti-predator behaviors into modelling, we obtained some interesting results that differ from models ignoring the cost of fear. Mathematical and numerical simulations demonstrate the effects that anti-predator behaviors have in predator-prey interactions, which give a more thorough understanding of predator-prey systems.

For possible future research projects, we may consider a more complicated situation where the predator population varies with time, in contrast to regarding the predator population as a constant, which is an extension of the work in Chapter **4**. Also, we noticed that ecological systems in nature are very complicated and a single species may play both roles as prey and predators in a food web. For example, an intraguild community was studied where prey and

predator consume a common resource ([17]). It is interesting to examine how the cost of anti-predator behaviors affects the food web, including the interaction among three species or more. These remain as future topics and need further detailed examination.

Bibliography

[1] S. Creel, D. Christianson, S. Liley, and J. A. Winnie. Predation risk affects reproductive physiology and demography of elk. *Science*, 315:960–960, 2007.

[2] S. Eggers, M. Griesser, and J. Ekman. Predator-induced plasticity in nest visitation rates in the Siberian jay (*perisoreus infaustus)*. *Behavioral Ecology*, 16:309–315, 2005.

[3] S. Eggers, M. Griesser, M. Nystrand, and J. Ekman. Predation risk induces changes in nest-site selection and clutch size in the siberian jay. *Proceedings of the Royal Society of London B: Biological Sciences*, 273:701–706, 2006.

[4] J. J. Fontaine and T. E. Martin. Parent birds assess nest predation risk and adjust their reproductive strategies. *Ecology letters*, 9:428–434, 2006.

[5] C. K. Ghalambor, S. I. Peluc, and T. E. Martin. Plasticity of parental care under the risk of predation: how much should parents reduce care? *Biology Letters*, 9:20130154, 2013.

[6] M. E. Gilpin and M. L. Rosenzweig. Enriched predator-prey systems: theoretical stability. *Science*, 177:902–904, 1972.

[7] J. K. Hale and P. Waltman. Persistence in infinite-dimensional systems. *SIAM Journal on Mathematical Analysis*, 20:388–395, 1989.

[8] C. S. Holling. The components of predation as revealed by a study of small-mammal predation of the European pine sawfly. *The Canadian Entomologist*, 91:293–320, 1959.

[9] C. S. Holling. Some characteristics of simple types of predation and parasitism. *The Canadian Entomologist*, 91:385–398, 1959.

[10] F. Hua, R. J. Fletcher, K. E. Sieving, and R. M. Dorazio. Too risky to settle: avian community structure changes in response to perceived predation risk on adults and offspring. *Proceedings of the Royal Society of London B: Biological Sciences*, 280:20130762, 2013.

[11] F. Hua, K. E. Sieving, R. J. Fletcher, and C. A. Wright. Increased perception of predation risk to adults and offspring alters avian reproductive strategy and performance. *Behavioral Ecology*, 25:509–519, 2014.

[12] J. D. Ibáñez-Álamo and M. Soler. Predator-induced female behavior in the absence of male incubation feeding: an experimental study. *Behavioral Ecology and Sociobiology*, 66:1067–1073, 2012.

[13] C. D. McAllister, R. J. LeBrasseur, T. R. Parsons, and M. L. Rosenzweig. Stability of enriched aquatic ecosystems. *Science*, 175:562–565, 1972.

[14] J. L. Orrock and R. J. Fletcher. An island-wide predator manipulation reveals immediate and long-lasting matching of risk by prey. *Proceedings of the Royal Society of London B: Biological Sciences*, 281:20140391, 2014.

[15] J. F. Riebesell. Paradox of enrichment in competitive systems. *Ecology*, 55:183–187, 1974.

[16] M. L. Rosenzweig. Paradox of enrichment: destabilization of exploitation ecosystems in ecological time. *Science*, 171:385–387, 1971.

[17] D. Ryan and R. S. Cantrell. Avoidance behavior in intraguild predation communities: a cross-diffusion model. *Discrete and Continuous Dynamical Systems*, 35:1641–1663, 2015.

[18] M. J. Sheriff, C. J. Krebs, and R. Boonstra. The sensitive hare: sublethal effects of predator stress on reproduction in snowshoe hares. *Journal of Animal Ecology*, 78:1249–1258, 2009.

[19] H. R. Thieme. Persistence under relaxed point-dissipativity (with application to an endemic model). *SIAM Journal on Mathematical Analysis*, 24:407–435, 1993.

[20] A. J. Wirsing and W. J. Ripple. A comparison of shark and wolf research reveals similar behavioral responses by prey. *Frontiers in Ecology and the Environment*, 9:335–341, 2011.

[21] L. Y. Zanette, A. F. White, M. C. Allen, and M. Clinchy. Perceived predation risk reduces the number of offspring songbirds produce per year. *Science*, 334:1398–1401, 2011.

Curriculum Vitae

Name:	Xiaoying Wang
Post-Secondary Education and Degrees:	University of Western Ontario London, ON, Canada 2011 - current Ph.D Candidate Capital Normal University Beijing, P. R. China 2007 - 2011 B.Sc
Honours and Awards:	Western Graduate Research Scholarships 2012-2016 Excellent Undergraduate Student Scholarship 2008-2011
Related Work Experience:	Teaching Assistant University of Western Ontario 2011 - 2016

Publications:

1. **X. Wang** and X. Zou (2016), On a two-patch predator-prey model with adaptive habitancy of predators, *Discrete and Continuous Dynamical Systems-Series B*, 21(2), 677-697.

2. **X. Wang**, L. Zanette and X. Zou, Modelling the fear effect in predator-prey interactions, Journal of Mathematical Biology, DOI 10.1007/s00285-016-0989-1, in press.

3. **X. Wang** and X. Zou, Modelling the fear effect in predator-prey interactions with adaptive avoidance of predators, in preparation.

4. **X. Wang** and X. Zou, Pattern formation of a predator-prey model with the cost of anti-predator behaviors, in preparation.